

RSC Pharmaceutics

Accepted Manuscript

This article can be cited before page numbers have been issued, to do this please use: M. K. Goshisht, A. Goshisht, A. Bajpai and A. Bajpai, *RSC Pharm.*, 2025, DOI: 10.1039/D5PM00137D.



This is an Accepted Manuscript, which has been through the Royal Society of Chemistry peer review process and has been accepted for publication.

Accepted Manuscripts are published online shortly after acceptance, before technical editing, formatting and proof reading. Using this free service, authors can make their results available to the community, in citable form, before we publish the edited article. We will replace this Accepted Manuscript with the edited and formatted Advance Article as soon as it is available.

You can find more information about Accepted Manuscripts in the [Information for Authors](#).

Please note that technical editing may introduce minor changes to the text and/or graphics, which may alter content. The journal's standard [Terms & Conditions](#) and the [Ethical guidelines](#) still apply. In no event shall the Royal Society of Chemistry be held responsible for any errors or omissions in this Accepted Manuscript or any consequences arising from the use of any information it contains.

ARTICLE

Recent advances in biomedical applications of smart nanomaterials: A comprehensive review

Manoj Kumar Goshisht,^{*a,b} Ashu Goshisht,^{*c} Animesh Bajpai,^d and Abhishek Bajpai^eReceived 00th January 20xx,
Accepted 00th January 20xx

DOI: 10.1039/x0xx00000x

Smart nanomaterials (NMs) have emerged as a transformative tool in biomedical field owing to their distinct physicochemical possessions and multifunctional abilities. In this comprehensive review, we have featured the current advancements in utilization of smart NMs in four critical domains of biomedical science: (i) wound healing, (ii) cancer theranostic, (iii) tissue engineering and regeneration, and (iv) nanotoxicity assessment. In the first section, we have discussed the wound healing applications of metallic and non-metallic smart NMs in controlled drug delivery, rapid tissue repair/regeneration, and antimicrobial properties in synergism with photodynamic and photothermal therapy. The second section encompasses recent breakthroughs in cancer theranostic that leverages the dual functionality of smart NMs for simultaneous diagnosis and therapy. Nanocarriers designed with imaging agents and therapeutic payloads enable targeted drug delivery along with reduction in side effects and improvement in treatment efficacy. The integration of stimuli-responsive mechanisms, such as pH and temperature sensitivity, further enhances their theranostic potential. The third section underscores NMs based efficient scaffolds and 3-dimensional (3D) bioprinting strategies to boost tissue engineering and regeneration by delivering growth factors, genetic materials, and bioactive chemicals. The fourth section encompasses recent breakthroughs in nanotoxicity assessment through *in vitro*, *in vivo*, and *in silico* approaches. The section also includes key toxicity mechanisms and challenges of smart nanomaterials in clinical translation.

1. Introduction

Nanoscale materials with unique features allowing them to respond dynamically to different extraneous stimuli like pH/light/temperature, chemical signals,

and magnetic or electric fields are called smart nanomaterials.¹ Stimuli responsive quantum dots, polymers, metal-organic frameworks (MOFs), metal oxide nanoparticles (NPs) (e.g., iron/zinc/copper/titanium oxide), Au/Ag NPs, carbon NPs (e.g., fullerenes and carbon nanotubes), and nanocomposites are generally used as smart nanomaterials.² Their dynamic responsiveness makes them supreme candidates in wound healing treatments, cancer theranostic, drug release, environmental monitoring, sensing, and various other fields requiring materials with "intelligent" behaviour.

^a Department of Chemistry, Shaheed Mahendra Karma Vishwavidyalaya, Jagdalpur, Bastar, Chhattisgarh 494001, India

^b Department of Chemistry, Government Naveen College Tokapal, Bastar, Chhattisgarh 494442, India

^c Department of History, Indira Gandhi National Open University, Maidan Garhi, New Delhi, 110068, India

^d Department of Chemistry, University of Delhi, Delhi 110007, India

^e Department of Physics, Government Kaktiya Post Graduate College, Jagdalpur 494001, India

† Footnotes relating to the title and/or authors should appear here.

Supplementary Information available: [details of any supplementary information available should be included here]. See DOI: 10.1039/x0xx00000x



The skin, as the body's largest organ, is essential for overall health, functioning both as a protective barrier and an active participant in physiological processes. It helps maintain homeostasis by detecting environmental changes, regulating the temperature of body, and preserving humoral balance.^{3,4} Wounds occur when the skin's structure as well as integrity are disrupted by various interior and exterior factors. Quotidian causes include burns, trauma, and/or diabetes.⁵ Once the skin is compromised, the body becomes more vulnerable to microbial infections. Although the natural wound healing process is initiated to restore skin wholeness,⁶ certain conditions-including infections and uncontrolled inflammations however can hinder recovery, leading to chronic wounds.^{7,8} In the United States, approximately 6.5 million patients suffer from chronic wounds each year.⁹

Nanotechnology has made significant strides in the field of wound repair over the past few decades.¹⁰ The distinct properties of NMs, like their quantum size effects and surface chemistry, have led to innovative strategies in wound healing. These properties of NMs play a crucial role in regulating the wound microenvironment, controlling infections, promoting angiogenesis, and enhancing reepithelialization.¹¹ Moreover, the high surface area of NMs makes them an outstanding candidate for target specific drug release owing to their capability to encapsulate the therapeutic drugs, thereby regulating wound healing processes. Moreover, NMs based composite scaffolds, hybrid bioinks, and 3D bioprinting strategies have advanced the tissue engineering and regeneration (TER) field.¹²

Cancer represents a serious public health challenge, with mortality rates rising expeditiously worldwide,¹³ resulting in approximately 10 million deaths each year.¹⁴ Chemotherapy remains the most prevalent anticancer drug owing to its high effectiveness.¹⁵ However, chemotherapy's effectiveness is often hindered by its poor selectivity

toward tumour cells as well as difficulties in releasing medicines to the site of tumour efficiently^[16]. In addition, the emergence of multi-drug resistance (MDR) further poses obstacles in the successful outcomes of chemotherapy. The intricate nature of microenvironment of tumours¹⁶ as well as variation in nature of all patients also add to the challenges of development of worthwhile therapeutic agent options.

Smart NMs represent a remarkable progress in cancer therapy, offering a promising alternate to conventional therapeutics. These NMs are designed to respond to different biomolecules, pH, and stimuli, leading to their aggregation at tumour site and subsequent release of therapeutic payloads.^{17,18} This targeted and triggered drug delivery mechanism establishes a smart treatment mode, allowing for enhanced efficacy and reduced off-target effects.¹⁸⁻²¹ Moreover, smart NMs have the capability to co-deliver therapeutics and diagnostic reagents simultaneously. This aspect has greatly contributed to the development of theranostics, which combine therapy and diagnostics in a single platform. By integrating therapeutic and diagnostic functionalities, smart NMs hold immense potential for personalized cancer treatment strategies.²²

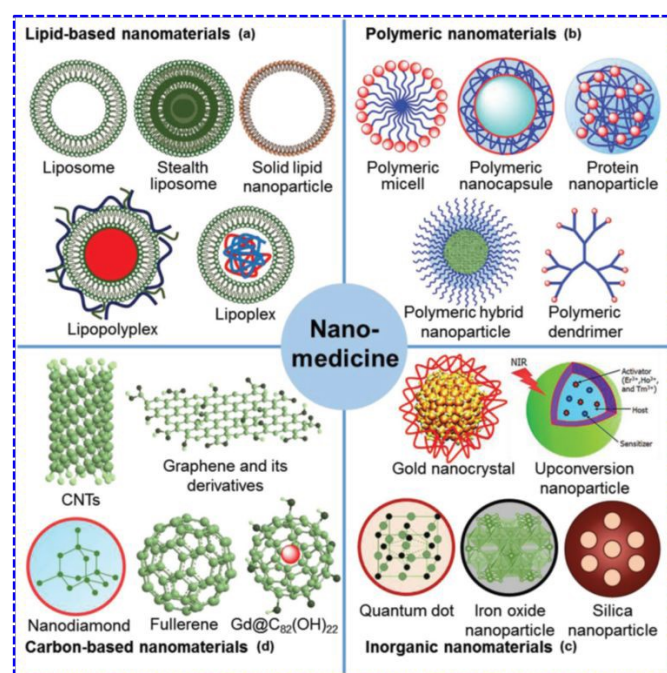


Fig. 1. Schematic representation of different smart nanomaterials employed in wound healing, tissue engineering/regeneration, and cancer therapy. Reprinted with permission from the ref. 23. Copyright 2019, WILEY-VCH Verlag GmbH & Co. KGaA, Weinheim.

Different types of smart nanomaterials with distinct morphology and properties used in biomedical applications are presented in Figure.1.²³

Although smart NMs offer significant benefits in healthcare and other fields, their potential menace to environment and health cannot be ignored.²⁴⁻²⁶ In the last decade, worthy attention has been given towards the nanotoxicity assessment. Nanotoxicity is influenced by various factors related to both the NMs themselves (e.g., their chemical composition, shape, size, and coating) and the biological systems they interact with.²⁷ Exposure of cells/tissues to NMs can affect them through multiple mechanisms, each contributing to potential health risks. NMs can reduce the ability of cells to survive and proliferate, hinder tissue growth and repair processes, generation of reactive oxygen species (ROS)/cytokines, damage of cell membrane/DNA/mitochondria, apoptosis, lipid peroxidation, cell cycle dysregulation, genotoxicity, necrosis, and metabolic/cell morphology changes.²⁷⁻³²

In this review, applications of smart NMs based on wound healing, cancer theranostic, and tissue engineering and regeneration have been discussed comprehensively. Different type of nanocarriers, such as metallic, non-metallic, and polymeric or biomimetic used for delivery of drugs, bioactive chemicals, and genetic materials in wound healing, cancer therapy and tissue engineering and regeneration have been highlighted throughout the article. But the applications of smart NMs are not without concern. That is why in the last section, we have discussed the *in vivo*, *in silico*, and *in vitro* toxicity of NMs and summarized them in table format (Table 6 and Table 7).

2. General description of smart NMs

View Article Online

DOI: 10.1039/D5PM00137D

NMs own notable properties and characteristics owing to nanoscale facets, which usually range between 1 and 100 nm. This size range gives nanomaterials a high surface area and results in quantum effects, which significantly alter their physical/chemical/biological effects than their bulk analogues.³³

Smart/responsive/intelligent nanomaterials are fabricated to respond to various environmental and biological stimuli in a controlled manner. Thermo-responsive NMs change their properties countering temperature. For instance, poly(N-isopropylacrylamide) exhibits a phase transition near human body temperature, making it useful in drug delivery and tissue engineering.³⁴ pH responsive NMs respond to changes in pH and are useful for delivering drug to specific parts of the body (such as infection/tumour sites that have typically lower pH).³⁵ Photo-responsive NMs change their chemical or physical properties in response to light.³⁶ These NMs are employed in targeted drug delivery, optical devices, and sensors. Smart magnetic NMs can be manipulated by external magnetic fields, allowing precise control for applications like hyperthermia and targeted drug delivery therapy. Conductive NMs can respond to electrical stimuli, making them useful in electronics and wearable devices.³⁷

In biomedical applications, Smart NMs are usually engineered to be biocompatible as well as biodegradable, reducing the menace of adverse reactions. For instance, smart NMs in medicine delivery systems are fabricated to degrade harmlessly after releasing their cargo.³⁸ Some smart NMs, such as silver and zinc oxide NPs, exhibit inherent antibacterial properties.^{39,40} They are commonly employed in medical coatings, textiles, and food packaging. Hydrogels, especially those integrated with NPs, can swell as well as contract because of pH, temperature, or even magnetic field changes. They are promising for tissue engineering and drug release vehicles that release drugs



following specific body conditions.⁴¹ Smart textiles and wearable electronics utilize NMs to add flexibility, durability, and responsiveness to devices.

NMs are constantly utilized to improve performance, reduce costs, and enhance compatibility with existing systems.

2.1. Surface chemistry and conjugation of nanomaterials

Surface chemistry and conjugation strategies play a vital role in designing smart or stimuli-responsive nanomaterials. The surface chemistry governs the interaction of nanomaterials with their surrounding environment, affecting key characteristics such as stability, solubility, and biocompatibility.^{42,43}

Covalent bonding provides a strong and stable connection between different functional groups and nanomaterial surfaces, helping to maintain the integrity and activity of duo in aqueous and biological conditions. Covalent strategies like amide bond formation, thioether and disulfide linkages, gold-thiol (Au-S) interactions, Schiff base chemistry, and click reactions are frequently utilized in the development of durable nanomedicine systems.⁴⁴

Noncovalent attachment of different functional groups/biomolecules to nanomaterials is driven by fundamental molecular interactions, including electrostatic forces, hydrogen bonds, π - π stacking, and hydrophobic effects.⁴⁵ The inherent sequence tunability and structural adaptability of biomolecules like nucleic acids, lipids, and proteins facilitate these interactions. This approach is economical and maintains the native functionality of attached biomolecules without the need for chemical alterations. However, compared to covalent strategies, noncovalent methods offer lower stability and are more susceptible to variations in environmental conditions such as pH and ionic strength. Conjugation techniques like covalent and non-covalent which involve attaching functional

These effects can be tuned by altering material composition, proportion, size, and functional groups attached to the NPs. Now a days, smart

molecules to the nanomaterial surface, impart responsiveness to endogenous (pH, enzyme, hypoxia, glutathione, etc.) and exogenous (temperature, light, magnet, etc.) stimuli.⁴⁶ This enables controlled and adaptive behaviour of the nanomaterials under varying conditions (Figure 2).

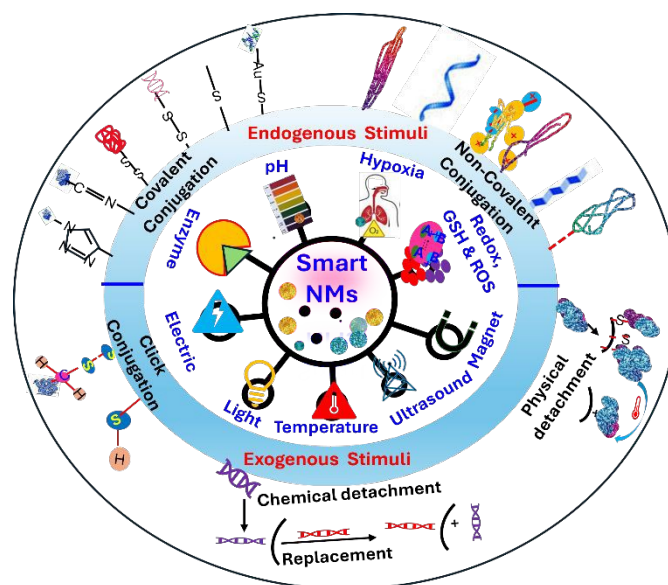


Fig. 2. Schematic representation of conjugation and detachment strategies along with endogenous and exogenous stimuli. Responsible for targeted and controlled therapeutic action of smart nanomaterials.

2.2. Stability and degradation kinetics of smart nanomaterials

Stability governs the circulation time, shelf-life, and targeting precision of smart nanomaterials. Degradation kinetics involve the timing and location of therapeutic release and clearance from the body. Guo *et al.*⁴⁷ synthesized triblock polymer functionalized superparamagnetic Fe_3O_4 nanomaterials with pH responsive properties. In addition, synergistic effect between ionic bonding and hydrophobic interactions increased the loading efficiency of drug at 7.4 pH. However, at endosomal or lysosomal acidic pH (< 5.5) ionic bonding breaks and drug is released showing target specific release of drug. In other study, Fuoco *et al.*⁴⁸



prepared redox-responsive PEG-SS-PLA based nanomaterials where PEG stands for poly(ethylene glycol) and PLA stands for poly(lactide). The nanomaterials were stable extracellularly but degrade in high glutathione (GSH) environments due to disulphide bond cleavage showing tumour specific targeting ability of nanomaterials.

2.3. Drug loading and release efficiency

The drug loading and release efficiency of smart nanomaterials depends on encapsulation technique, material matrix, and intermolecular interactions (hydrophobic, electrostatic, H-bonding, etc.).⁴⁹ The drug loading and release efficiency of different types of smart nanomaterials has been discussed in the Table 1.

3. Wound healing applications of smart nanomaterials

Wounds are injuries to the skin and underlying tissues that disrupt normal anatomical structure and function.⁵⁰ The wound healing process involves four coordinated stages: hemostasis, inflammation, proliferation, and remodeling.⁵¹ Smart nanomaterials can sense and respond to biochemical or biophysical cues at the wound site. Smart nanomaterials enhance each phase by delivering bioactive agents or modulating cellular responses in a stimulus-responsive manner (Table 2). These materials exhibit adaptive, targeted, and controlled

therapeutic functionalities, enabling them to address the dynamic and complex nature of acute and chronic wounds.⁵²

The mechanism of smart nanomaterials is inherently adaptive, targeted, and intelligent, tailored to wound microenvironment dynamics.⁵³ They surpass conventional nanomaterials, which offer static and non-selective functions. By combining real-time sensing with precise therapeutic delivery, smart nanomaterials represent a next-generation platform in advanced wound healing technologies. Mechanistic advancement of smart nanomaterials over conventional nanomaterials for wound healing and cancer therapy applications is presented in Table 3 and Table 5, respectively.

Despite their promising applications, clinical translation faces obstacles of (i) toxicity and biocompatibility of certain nanomaterials; (ii) scale-up and reproducibility in manufacturing; (iii) long-term safety and regulatory approval; (iv) cost-effectiveness in healthcare settings.⁵⁴ Advancements in biodegradable smart polymers, personalized wound care, and real-time biosensing will guide the next generation of smart nanomaterial-based wound treatments.

Table 1. Summary of drug loading efficiency of smart nanomaterials.

| S. No. | Smart nanomaterial type | Drug loading (%) | Method | Ref. |
|--------|-------------------------|------------------|----------------------------------------|------|
| 1. | Liposomes | 5–15% | Passive loading, remote loading | 49 |
| 2. | Polymeric micelles | 10–20% | Self-assembly of amphiphilic polymers | 55 |
| 3. | Dendrimers | >20% | Covalent or electrostatic conjugation | 56 |
| 4. | Mesoporous silica NPs | >30% | Pore loading, pH-labile caps | 57 |
| 5. | Nanogels | ~10–30% | Swelling in drug solution and trapping | 58 |



Table 2. Stimuli responsive behaviour of smart nanomaterials in wound healing.View Article Online
DOI: 10.1039/D5PM00137D

| S. No. | Stimulus | Typical wound condition | Smart nanomaterial response |
|--------|----------------------------------------------|----------------------------------------|----------------------------------------------------|
| 1. | pH | Acidic pH in chronic/infected wounds | Trigger drug/gene release |
| 2. | Enzymes like matrix metalloproteinase (MMPs) | Overexpressed in chronic wounds | Enzyme-triggered therapeutic release |
| 3. | Temperature | Elevated in inflamed/infected tissue | Thermosensitive drug release |
| 4. | ROS | Excess ROS during chronic inflammation | Scavenge ROS, release antioxidants |
| 5. | Bacterial toxins | Infection | Smart antimicrobial release or membrane disruption |

Table 3. Comparative mechanistic insights of smart nanomaterials over conventional nanomaterials in wound healing applications.

| S. No. | Aspect | Conventional nanomaterials | Smart nanomaterials |
|--------|-----------------------------|-------------------------------------------------------------------------------------|---------------------------------------------------------------------------------------------------------------------|
| 1. | Design | Passive delivery systems with fixed properties | Engineered to respond to specific stimuli (e.g., ROS, pH, temperature, enzymes, etc.) in the wound microenvironment |
| 2. | Stimulus response | None/minimal | Responsive to internal (e.g., infection, ROS, pH, etc.) or external (e.g., light, magnetic field, etc.) cues. |
| 3. | Drug release | Continuous/burst release, often non-specific | Controlled and on demand release of therapeutics in response to wound-specific stimuli |
| 4. | Targeting capability | Non-targeted accumulation at wound site | Localized and targeted delivery based on microenvironmental characteristics |
| 5. | Healing modulation | May offer antimicrobial/antioxidant support | Multifunctional: antibacterial, anti-inflammatory, haemostatic, pro-angiogenic, and even immune-modulatory |
| 6. | Biocompatibility and safety | Biocompatible but potential risk of overdose/toxicity owing to uncontrolled release | Reduced /minimal side effects through spatial and temporal control of therapeutic action |

3.1. Wound healing applications of metal-based smart NMs

Metal-based NMs, such as metal NPs (MNPs), metal oxide NPs (MONPs), and metal nanoclusters (MNCs) exhibit significant antimicrobial properties

against a wide range of bacteria.^{59,60} The antibacterial mechanistic of these NMs usually involve the destruction of the bacterial cell membrane, interference with cytoplasmic enzyme activities, and oxidative stress-induced damage to DNA and plasmids.⁶¹ Among these, MNPs and



MONPs are particularly noteworthy for their potent antibacterial activity, in context of wound healing.

Silver NPs are extensively employed in wound dressings and coatings due to their broad-spectrum antibacterial affairs and ability to advance wound

healing.⁶² They are often incorporated into ointments, hydrogels, and bandages. The antibacterial action of AgNPs involves multiple pathways, including the silver ions release, which

can derange the bacterial cell wall and membrane, leading to cell lysis. Silver ions also interact with thiol groups in proteins, disrupting bacterial enzymes and metabolic processes.⁶³ Additionally, AgNPs engender oxidative stress by creating ROS, causing damage to bacterial DNA and other cellular components.

Gold nanoparticles (AuNPs) are employed in wound healing primarily for their anti-inflammatory properties and ability to enhance the healing process.⁶⁴ They are often combined with other therapeutic agents to improve their efficacy.^{65,66} While AuNPs are less toxic to bacteria compared to silver and zinc oxide nanoparticles (ZnO-NPs), they

can still exert antibacterial effects. These mechanisms include disrupting bacterial cell membranes, binding to bacterial DNA and proteins, and inducing oxidative stress.^{67,68} Moreover, AuNPs can enhance the efficacy of antibiotics by facilitating their entry into bacteria.⁶⁹ Recently, Singh *et al.*⁷⁰ developed a smart drug delivery system (DDS) employing core-shell nanofibers fabricated via coaxial electrospinning. The system was engineered to achieve sequential drug release, which is vital for treating complex wounds that require stage-specific therapeutic interventions. The shell is composed of poly-L-lactic acid loaded with lidocaine drug enabling immediate release at room temperature.



The core contains poly(N-isopropylacrylamide) polymer infused with gold nanorods (GNRs) and levofloxacin. GNRs enable near-infrared (NIR) light-triggered heating which induces swelling and shrinking of the core polymer to enable on-demand, sustained release of levofloxacin. In the absence of smart nanomaterials, it is not possible to deliver on-demand and sustained release of drugs effectively.

ZnO-NPs are commonly employed in wound dressings and topical applications owing to their antimicrobial virtues, biocompatibility, and capability to promote wound healing.^{71,72} These NPs provide UV protection, which is beneficial for skin applications. ZnO-NPs also cause antibacterial activity by releasing zinc ions (Zn^{2+}), ultimately disrupting bacterial cell membrane and interfering with enzyme activities.⁷³ Additionally, ZnO-NPs generate ROS, resulting in oxidative destruction of bacterial proteins, lipids, and DNA. The targeted antimicrobial treatments, contributing to better clinical outcomes and improved patient care. photocatalytic potential of ZnO-NPs in presence of

UV light further intensifies their antibacterial effects.⁷⁴

DOI: 10.1039/D5PM00137D

Smart metal-based nanomaterials outperform conventional ones by offering controlled, targeted, and multifunctional wound healing support i.e., antibacterial, antioxidant, angiogenic, and pro-regenerative actions tailored to wound microenvironments.⁷⁵ While they reduce toxicity risks through precision delivery, the long-term safety of the nanocarriers (polymers, ligands, composites, etc.) and metal ion release profiles still require extensive *in vivo* and clinical validation. The clinical and translational studies of metal nanomaterials have been presented in Table 4.

Moreover, scale-up production with reproducibility, regulatory hurdles for complex nanostructures, and comprehensive toxicity and pharmacokinetic profiles are some of the challenges that need to be addressed.

Table 4. Clinical and translational studies on metal-based nanomaterials in wound healing

| Material /Product | Nanomaterial and formulation | Study Type | Model / Population | Key Findings | Ref. |
|---------------------------------|------------------------------|-------------------------------------------------------------------|------------------------------------------|-----------------------------------------------------------------------------------------------------------------------------------------------------------------------------------------------------------------------------------------------------------------------------------------------------------------------|------|
| Silver colloid dressing | Ionic silver colloid | Randomized Controlled Trials (RCT) (n=25 silver vs n=25 standard) | Diabetic foot ulcers (Wagner grade I-II) | 85.7% healed in silver group versus 41.7% in control at 12 weeks; mean wound reduction 85.6% versus 68.6%, $p < 0.05$ | 76 |
| Silver based dressing materials | | Observational study included 50 diabetic foot ulcer cases. | Diabetic foot ulcers | 3 cases (6%) showed purulent discharge from the wound, absence of granulation tissue, presence of microorganisms and hence poor healing rate. Whereas remaining 47 cases (94%) showed minimal/serous discharge, presence of healthy granulation tissue, no microorganism on culture report and thus good healing rate | 77 |
| Silver colloid dressing | Ionic silver colloid | Double-blind experiment included 50 patients | Non-ischemic DFUs | 67.77 \pm 17.82% reduction in ulcer area in silver group compared to 21.70 \pm 23.52% in conventional saline group. Silver group (23.15 \pm 8.15 days) required fewer days to reach the endpoint compared to saline group (48.35 \pm 18.07 days). | 78 |



| | | | | |
|--------------------------------------|------------------------------------|-------------------------------------|----------------------------|------------------------------------------------------------------------------------------------------------------------------------------------------|
| Silver colloid nanoparticle dressing | Nanoparticulate silver hydrogel | Prospective observational (n=800) | Acute diabetic foot ulcers | Complete healing at 4 wk in $\leq 10\text{ cm}^2$ ulcers: 100% silver vs 68.4% control, faster rate overall |
| Copper dressing | Copper oxide microparticles | In Vitro study | --- | The dressing showed microbial titer reductions (4-logs) within 3 h of exposure at 37 °C ($p < 0.001$). |
| Copper dressing | Copper oxide impregnated dressings | Randomized controlled (n=23) trials | Diabetic foot wounds | 47.83% (11/23) and 34.78% (8/23) wounds closed in the copper dressings and NPWT (negative pressure wound therapy) arms, respectively ($p > 0.05$). |

3.2. Wound healing applications of non-metallic NMs

The integration of non-metallic NMs in biomedical applications, particularly in wound healing, has shown promising results due to their broad-spectrum antimicrobial properties. Their ability to be functionalized and incorporated into various forms such as dressings, hydrogels, and coatings makes them versatile tools in the fight against bacterial infections and in enhancing wound healing processes.⁸²

3.2.1. Wound healing applications of graphene together with its derivatives

Graphene, GO (graphene oxide), and rGO (reduced graphene oxide) hold significant promise in antimicrobial applications and wound healing. Their ability to damage the membrane of microbes (by their sharp edges) and induce oxidative stress, combined with their potential for functionalization and photothermal therapy, makes them versatile and powerful tools in the fight against bacterial infections.⁸³ These properties facilitate the development of advanced wound dressings and

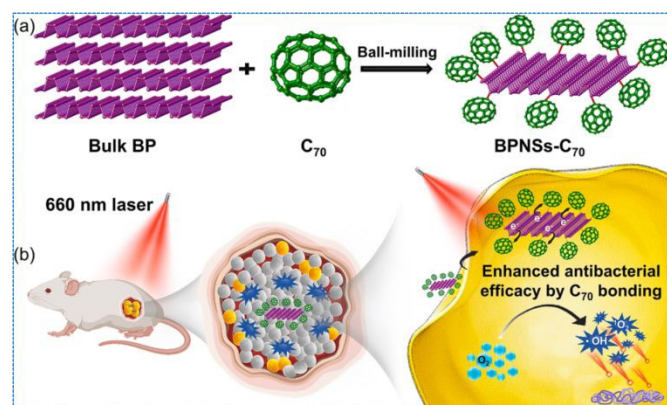


Fig. 3. (a) Schematic representation of synthesis of BPNSs- C_{70} hybrid; (b) Antibacterial efficacy of the hybrid (BPNSs- C_{70}) under 600 nm irradiation. Reprinted with permission from ref. 84. Copyright 2023, Elsevier.

Xie *et al.*⁸⁴ developed an edge-selectively passivated black phosphorus (BP) nanosheet (BPNS) hybrid by covalently fixing fullerene C_{70} at the edges, resulting in BPNSs- C_{70} , aiming to create a novel hybrid antibacterial agent with outstanding antibacterial potency. (Fig. 3). The synthesis of BPNSs- C_{70} was obtained via a sustainable and straightforward one step mechanochemical process. BPNSs- C_{70} hybrid demonstrated superior hydroxyl radical ($\bullet\text{OH}$) and singlet oxygen ($^1\text{O}_2$) production capabilities compared to pristine BPNSs and BP- C_{70} , under light irradiation. This resulted in improved antibacterial performance (99.97%) against MRSA (methicillin-resistant *Staphylococcus aureus*) after irradiation for just 5 minutes. *In vivo* examination confirmed the superior antibacterial capability of the synthesized hybrid, showcasing faster disinfection and recovery of abscesses. The escalated antibacterial efficacy of



BPNSs- C_{70} was ascribed to the synergistically revamped $\bullet OH$ and singlet oxygen production owing to intramolecular transfer from BPNSs to C_{70} . This innovative approach opens new routes for the antibacterial applications of BPNSs, leveraging the improved stability and ROS generation capabilities imparted by the fullerene modification.

3.2.2. Wound healing applications of black phosphorus

BP, first synthesized in 1914, has achieved remarkable recognition owing to its distinctive properties and potential biomedical applications.⁸⁵ High-energy mechanical milling is a favoured technique to fabricate BP NPs because it produces NPs with excellent biocompatibility and biodegradability, making them promising wound healers.⁸⁶ For instance, Huang *et al.*⁸⁷ reported a wound dressing laden with silk fibroin-functionalized BPNSs, demonstrating excellent photothermal effects that accelerated wound healing by eliminating bacterial infections.

Recently, Huang *et al.*⁸⁸ presented BP quantum dots lodged nanohydrogel (BPQDs@NH) for photodynamic and photothermal elimination of MDR bacterial infections on diabetic wounds (Fig. 4). *In vitro* investigations showed around 90 % MRSA destruction due to BPQDs and increased temperature of the hydrogel due to NIR irradiations (808 nm), suggesting potential improvements in diabetic wound healing. The strong bactericidal potential of BPQDs was preferentially ascribed to several mechanisms: (i) the destruction of cell integrity, (ii) ROS production, (iii) the induction of lipid peroxidation, and (iv) the disruption of bacterial metabolism. Additionally, *in-vivo* animal model experiments revealed that treatment with BPQDs lodged nanohydrogel under NIR irradiation attained the highest rates of healing of MRSA-infected diabetic wounds. This treatment also resulted in the highest expression of vascular

endothelial growth factor (VEGF), indicating enhanced wound healing.

DOI: 10.1039/D5PM00137D

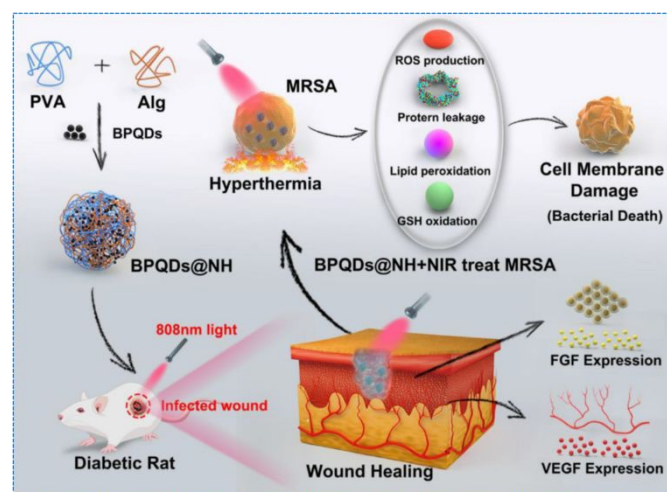


Fig. 4. Schematic illustration of preparation of black phosphorus quantum dots lodged nanohydrogel (BPQDs@NH) and its synergistic antibacterial efficacy in presence of NIR irradiations against MRSA infected wound treatment. Reprinted with permission from ref. 88. Copyright 2022, Elsevier.

3.2.3. Wound healing applications of MXenes

MXenes are innovative 2D NMs characterized by $M_{n+1}X_nT_x$ formula, where M, X, n, and T represent an early transition element (V, Cr, Zn, Ti, etc.), carbon and/or nitrogen, 1-3, and surface terminating groups (e.g., $-F$, $-O$, $-OH$)⁶⁶, respectively. Here, M is an early transition metal (e.g., V, Ti, Cr, Zr, and Nb), X can be either carbon(c)/nitrogen(n), n ranges from 1 to 3, and T denotes surface-terminating functional groups (e.g., $-F$, $-O$, $-OH$).⁸⁹ To date, approximately 70 different MXenes have been discovered, with $Ti_3C_2T_x$ being the first and most extensively studied member of this family.⁹⁰ $Ti_3C_2T_x$ MXene nanosheets have demonstrated sturdy antibacterial efficacy, particularly toward *B. subtilis* and *E. coli*. bacteria. Studies have shown that $Ti_3C_2T_x$ exhibits significantly stronger antibacterial activity compared to graphene oxide (GO) nanosheets at equivalent concentrations.⁹¹ The mechanism of antibacterial activity of MXene nanosheets is primarily attributed to the combination of mechanical damage to cell membranes of microbes by the nanosheet's sharp edges together with oxidative stress induced by electron transfer.⁹²



Furthermore, photothermally active MXenes possess strong antibacterial efficacy. Gao *et al.*⁹³ indicated that the antibacterial efficacy of $\text{Ti}_3\text{C}_2\text{T}_x$ MXenes correlates inversely with size of nanosheet in the presence of light. Due to their notable antibacterial properties and photothermal conversion efficiency, MXene nanosheets can be combined with other compounds to create composite antibacterial NMs. For instance, Yu *et al.*⁹⁴ fabricated indocyanine green (ICG)-laden $\text{Ti}_3\text{C}_2\text{T}_x$ nanosheets to establish dual effect of PDT and PTT for treating bacterial infections. The biocompatibility as well as cytotoxicity of MXenes are influenced by several factors, including dosage, lateral size, and surface modifications.⁹⁵ It's important to note that MXenes are prone to oxidation, which can compromise the integrity and functionality of the nanosheets. Therefore, chemical modifications are necessary to prevent oxidation and preserve their properties.⁹⁶

Park *et al.*⁹⁷ developed ciprofloxacin and MXene based hydrogel (CIP@MX@Gel) groups for *in vivo* treatment of skin wounds of mice (Fig. 5). The CIP@MX@Gel with NIR group exhibited the outstanding wound relieving at all time points (Fig. 5A and B). It showed 61.03% ($\pm 5.60\%$) and 90.14% ($\pm 2.31\%$) wound closure on day 7 and 14, respectively. This was notably faster than the other groups, where the sham set attained 77.41% and the 0 $\mu\text{g/mL}$ set attained 75.15%. The groups with 100 $\mu\text{g/mL}$ and 100 $\mu\text{g/mL}$ with NIR had even slower healing rates of 53.07% ($\pm 7.80\%$) and 50.93% ($\pm 10.73\%$), respectively. In absence of light, the CIP-MX@Gel set indicated 85.74% ($\pm 5.71\%$) closure of wound by day 14. Hematoxylin-Eosin staining on seventh and fourteenth days revealed that the CIP-MX@Gel with NIR had little panniculus gap and the highest granulation threshold, indicating superior tissue regeneration (Fig. 5C-G). These trends were consistent over time, with the CIP-MX@Gel with light showing the best results. Masson's trichrome staining showed that the

CIP-MX@Gel with NIR group had the highest collagen fibre abundance on days seventh and fourteenth, indicating that the regenerated tissue in this group was most similar to normal, uninjured skin.

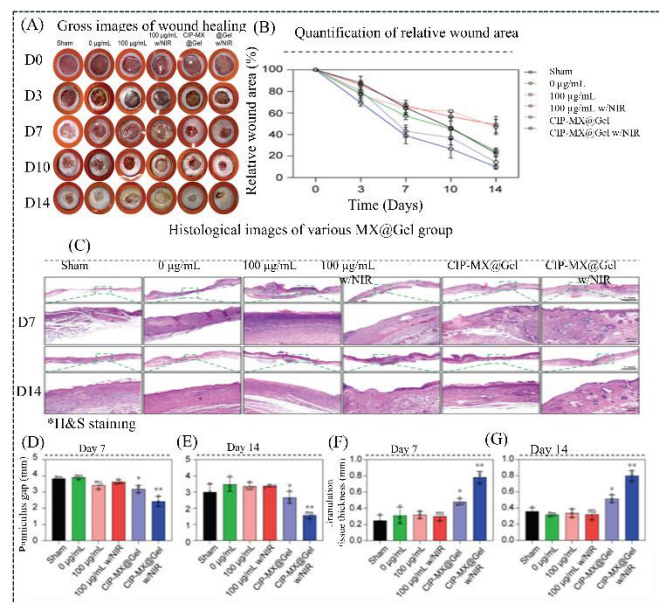


Fig. 5. Evaluation of *in vivo* healing of wound by CIP-MX@Gel. (A) Wound images during the treatment period of 14 days. (B) Quantification of wound area. (C) H&E staining pictures of treated wound tissues on day seventh and . (D, E) Panniculus gap quantification of the treated wound tissues on 7th and 14th day. (F, G) Granulation tissue thickness quantification of the treated wound tissues on seventh and fourteenth day. Reproduced with permission from ref. 97. Copyright 2023, Elsevier.

3.2.4. Wound healing applications of molybdenum disulphide

MoS_2 , as a member of the TMDs (transition metal dichalcogenides) family, offers a range of beneficial properties that make it worthy for various advanced applications, distinctly in the biomedical field.^{98,99} MoS_2 -based NMs (e.g., MoS_2 nanosheets, MoS_2 quantum dots, and MoS_2 nanoflowers) offer promising solutions for antibacterial applications, particularly in treating infected wounds. Their ability to generate ROS, induce physical damage to bacterial membranes, and convert NIR light into heat makes them effective in combating resistant bacterial infections.¹⁰⁰ The high biocompatibility and low cytotoxicity of MoS_2 further enhance its potential for clinical applications. Yin *et al.*¹⁰¹



demonstrated enhancement of healing of wounds by PEG modified MoS₂ nanoflowers (NFs). They converted H₂O₂ into hydroxyl radicals (\cdot OH) and utilized NIR irradiation for synergistic antibacterial action toward *Bacillus subtilis* and ampicillin-resistant *E. coli* *in vitro* and acceleration of infected wound relieving *in vivo*. In another study, Cao *et al.*¹⁰² loaded Ag⁺ ions into MoS₂ nanosheets for enhancing infected wound healing. This nanocomposite combined the antibacterial properties of both MoS₂ and silver ions. When applied to MRSA-infected wounds, the nanocomposite promoted faster wound healing.

3.3. NMs-based drug delivery systems for the treatment of wounds

NMs have shown great promise not only as direct therapeutic agents for promoting wound alleviating but also as effective DDSs (drug delivery systems).¹⁰³ NMs enhance the wound alleviating process by ensuring the sustained release of drugs at the affected site. This approach ensures a consistent therapeutic effect and minimizes the need for frequent application. Vascular dysfunction at the wound site can impair the delivery and effectiveness of therapeutic agents. Strategies need to be developed to enhance drug penetration and retention in such environments. The wound environment contains various detrimental factors which can degrade and dismantle the delivered drugs. Protective and stabilizing mechanisms should be incorporated into the DDSs. Therapeutic agents must be delivered in a controlled manner to avoid various astray due to excessive dosages. This includes precise timing and localization of drug release to match the wound healing stages.^{104,105}

Recently, Mao *et al.*¹⁰⁶ developed antibiotic-free remarkable nanocomposite hydrogels possessing impressive antioxidant and antimicrobial virtues, utilizing gelatine (Gel), bacterial cellulose (BC) as well as selenium NPs for wound alleviating applications (Fig. 6). The BC@Gel@SeNPs

hydrogel displayed notable mechanical strength, swelling capability, biodegradability, and flexibility, together with a controlled release of selenium NPs. The SeNPs decoration endured the hydrogels with outstanding antioxidant and anti-inflammatory capacities. The BC/Gel/SeNPs hydrogel demonstrated remarkable wound healing capabilities owing to the collaborative upshot of Gel and SeNPs. It accelerated the *in vivo* wound healing process by lessening inflammatory responses, increasing wound closure, promoting granulation tissue formation, encouraging collagen deposition, stimulating angiogenesis, and activating and differentiating fibroblasts into myofibroblasts (Fig. 6).

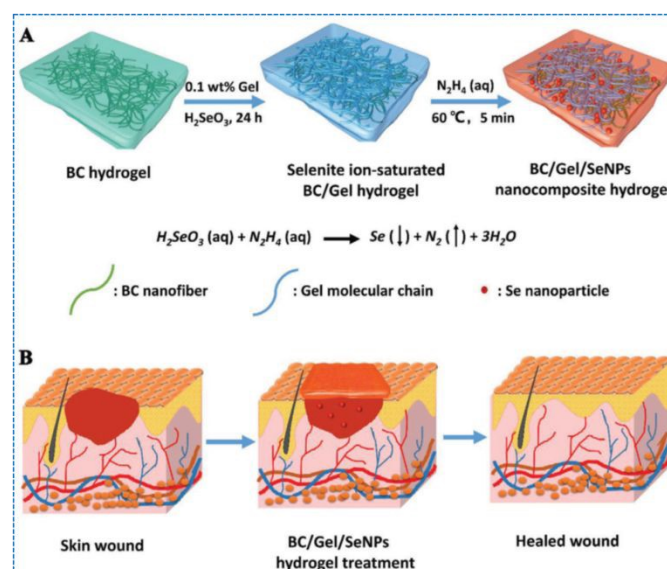


Fig. 6. Schematic representation (A) of BC/Gel/SeNPs nanocomposite hydrogel synthesis; (B) applicability of the synthesized hydrogel in alleviating wound. Reprinted with permission from ref. 106. Copyright 2021, Wiley-VCH GmbH.

Wang *et al.*¹⁰⁷ developed a novel approach to wound healing by incorporating antimicrobial peptides (AMPs) and collagen III (Col III) into microneedle (MN) patches. These patches were designed to release AMPs and Col III slowly and in a controlled manner, targeting deep wound tissues. By encapsulating AMPs in a chitosan (CS) and gum arabic (GA) based nanogel and embedding them within microneedle patches, the researchers improved the stability and biocompatibility of the



AMPs. Once the MN patches penetrated the biofilm formed by *Staphylococcus aureus*, they dissolved and released CGA-NPs. These nanoparticles then responded to the infected sites, efficiently killing the bacteria. Simultaneously, Col III facilitated wound healing, making this dual-action delivery system a promising solution for treating infected wounds. The study observed wound healing in mice over a period of 10 days following six different treatments (see Fig. 7 A and B). The treatments worked efficiently against *S. aureus*. The other treatments lacking antimicrobial potential toward *S. aureus*, had the largest scar areas and showed a significant presence of *S. aureus* in skin tissue. In contrast, NPs based treatments were reported potent bactericidal agents. Moreover, the sustained release of CGA-NPs from the microneedles further contributed to preventing the recurrence of *S. aureus* infections. This prolonged release ensured that the bacteria were not only killed initially but that any remaining bacteria were also continuously targeted, reducing the likelihood of reinfection and promoting more effective wound healing.

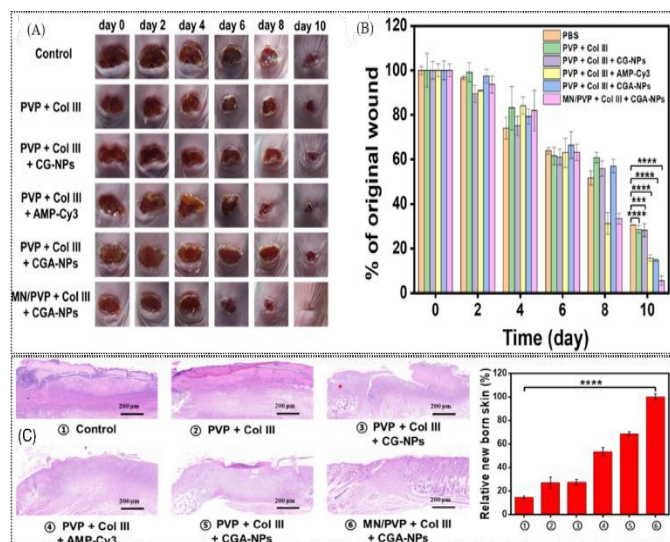


Fig 7. Healing of wound of mice over a period of ten days. (A) Wound pictures (B) wound area quantification of infected mice with divergent treatment groups over a period of 10 days. (C) Pictures with H&E staining and quantification of data of the newborn skin of the wounded tissue of infected mice with divergent treatment groups on the 10th day. Reprinted with permission from ref 107. Copyright 2023, American Chemical Society.

Hematoxylin and eosin staining of the affected tissue was conducted to further assess the wound alleviating effects across different treatment groups (Fig. 7 C). In the synthesized nanocomposite, the H&E staining results confirmed the superior healing outcomes, indicating successful re-epithelialization. Additionally, the formation of hair follicles and blood vessels was observed, suggesting that the underlying tissue structures were being effectively restored. These findings reinforced that the MN/PVP + Col III + CGA-NP treatment provided the best overall wound-healing effect among the groups studied.

4. Cancer treatment using smart nanomaterials

Cancer cells have quite a survival toolkit. Their ability to adjust and thrive under harsh conditions like low oxygen or limited nutrients is one reason why treating cancer can be so challenging.^{108,109} The classification of cancer into solid and liquid tumours is indeed important, as it affects how they're diagnosed and treated. Traditional therapies like surgery, chemotherapy, and radiation therapy have been the mainstays for a long time, but they do come with limitations and potential side effects.¹¹⁰ Theranostic nanomedicines, however, show great promise in cancer treatment. Their ability to detect specific cancer biomarkers and simultaneously deliver therapeutic agents can lead to more targeted and effective treatments. Nanotheranostic can combine multiple functionalities in a single nanosystem, such as drug delivery, imaging, and targeting, thus streamlining the treatment process, and reducing the need for multiple interventions.¹¹¹ This can be particularly beneficial for early-stage cancers or localized tumours where precise and localized treatment is crucial.

4.1. Advantage of smart nanomaterials over conventional nanomaterials in cancer therapeutic



Tumours often have an acidic microenvironment (pH ~ 6.5-6.8). Smart nanomaterials utilize acid-labile linkers (e.g., hydrazone, imine, etc.) that break at tumour pH to release the encapsulated/tethered drug.¹¹² Intracellular GSH levels are 100-1000 times higher than extracellular. Smart nanomaterials with disulfide and diselenide linkers degrade in high-GSH environments, promoting intracellular drug release.

Overexpressed enzymes like (MMP-2), and cathepsin B in tumours can cleave peptide and polymeric shells of smart nanomaterials, exposing the active core.¹¹³ Photothermal agents (e.g., GNRs, carbon nanodots, etc.) convert NIR light to heat, causing local hyperthermia for tumour ablation or drug release. Key advantages of smart nanomaterials over conventional nanomaterials utilized in cancer theranostics have been summarized in Table 5.

Table 5. Summary of advantages of smart nanomaterials over conventional nanomaterials utilized in cancer therapy

| S. No. | Feature | Conventional nanomaterials | Smart nanomaterials |
|--------|-----------------------------------|--------------------------------------------------------------------------------------------------------------------------------------------|-------------------------------------------------------------------------------------------------------------------------------------------------------------------------------------------|
| 1. | Design philosophy | These are inert or passive carriers of therapeutic agents, generally lacking stimuli-responsive features. | These are engineered with stimuli-responsive and multifunctional components that actively respond to tumour microenvironment (TME) or external signals. |
| 2. | Targeting mechanism | These generally rely on passive targeting via the enhanced permeability and retention (EPR) effect. | These use active targeting through ligand-receptor interactions (e.g., folate), combined with stimuli-triggered release (e.g., ROS, pH, enzymes, temperature, etc.). |
| 3. | Drug release kinetics | Uncontrolled release may result in premature drug leakage and systemic toxicity. | Controlled and on-demand release triggered by tumour-specific stimuli, minimizing off-target effects. |
| 4. | TME responsiveness | These lack sensitivity to tumour-specific features (e.g., hypoxia, acidic pH, high GSH, MMPs, etc.). | These incorporate smart moieties (e.g., redox-cleavable linkers, pH-sensitive bonds, enzyme-sensitive shells, etc.) to exploit TME characteristics for site-specific activation. |
| 5. | Therapeutic modalities | These are primarily responsible for chemotherapeutic drug delivery. These have limited potential for combinatorial or synergistic effects. | These are enabled with multimodal therapy (e.g., chemotherapeutic-photothermal, chemotherapeutic-immunotherapeutic, PDT/PTT + gene therapy), boosting efficacy and overcoming resistance. |
| 6. | Tumour penetration | Often limited due to size, lack of dynamic size/charge modulation. | Smart systems can shrink, swell, and switch charge for deep tumour penetration and intracellular delivery. |
| 7. | Biodistribution and clearance | Due to limited biodegradability there is a risk of accumulation in in reticuloendothelial system. | Surface functionalization (e.g., PEGylation) and biodegradable cores improve circulation, clearance, and reduce accumulation in reticuloendothelial system. |
| 8. | Therapeutic resistance management | Less capable of addressing MDR mechanisms. | These can bypass MDR by targeting specific pathways (e.g., endosomal escape, mitochondrial targeting, efflux pump inhibition, etc.). |
| 9. | Diagnostic integration | Rarely include imaging agents or real-time tracking capability. | These are designed as theranostic platforms integrating imaging (e.g., magnetic resonance imaging, computed tomography, fluorescence, etc.) for precision medicine. |
| 10. | Clinical translation potential | These are easier to scale and standardize; several approved for clinical use (e.g., Doxil). | These are more complex in design and regulation, but offer superior specificity, lower toxicity, and higher therapeutic index in preclinical models. |



ARTICLE

4.2. Cancer treatment using smart inorganic nanomaterials

Inorganic NMs, particularly metal (gold, iron, zinc, silver, etc.) and rare-earth metal NPs (e.g., lanthanum oxide and ytterbium oxide), have garnered remarkable interest in biomedical applications owing to their distinct physical and chemical virtues at the nanoscale. Silica NPs are also widely used due to their biocompatibility, ease of functionalization, and low toxicity.

4.2.1. Cancer treatment using gold nanoparticles

Simple production, large surface area, high stability, surface plasmon resonance (SPR), multi-functionalization, and customizable surface chemistry of gold nanoparticles (AuNPs) makes them tremendously useful in diagnostic of several malignancies and delivery of medications. The exceptional optical and physical properties of GNRs, nanocubes, nanostars, nanospheres, and nanocages appeal them for targeted delivery of drugs, photodynamic therapy (PDT), photothermal therapy (PTT), photoimaging, and biosensors to diagnosis and treat tumours.^{114,115}

Xu *et al.*¹¹⁶ developed a sophisticated nanoplatform for targeted and combination therapy for breast cancer, incorporating GSH, hyaluronidase (HAase), and pH sensitivity. GNRs were initially encased with hydrazide and thiol di-functionalized hyaluronic acid (HA) via Au-S linkages. Cy7.5 imaging agent and 5-aminolevulinic acid (ALA) photosensitizer were then covalently conjugated onto HA for fluorescence imaging and PDT, respectively. Anti-HER2 antibodies, being highly specific for HER2 receptors, were fixed onto HA to get the multifunctional nanomaterial (Fig. 8). The

NM is designed to exploit the dual receptor-mediated endocytosis of CD44 and HER2, leading to high tumour accumulation.

As all know, cancer cells typically exhibit a more acidic microenvironment and higher concentrations of HAase and GSH. This triggers the liberation of ALA and Cy7.5 within tumour cells. Intracellularly, the HA coating is degraded by enzyme Haase and GSH, further enabling the release of Cy7.5 and ALA. Upon near-infrared (NIR) irradiation guided by fluorescence imaging, the dual-targeting and triple-responsive nanoframework (GNR-HA-ALA/Cy7.5-HER2) achieves superb remedial efficacy. The combination of PDT and PTT in a targeted manner enhanced treatment effects and minimized detrimental effects.

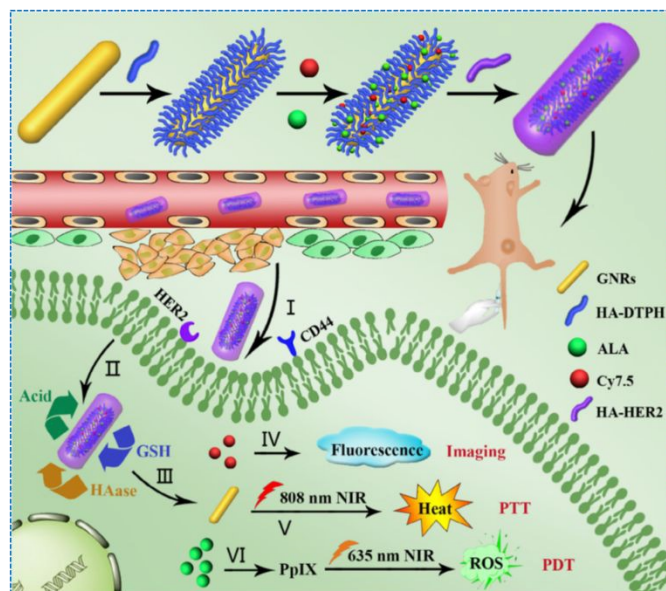


Fig. 8. Schematic depiction of GNRs and combination therapy for treating breast cancer. (I) The nanoplatform accumulates at the tumour area via EPR (enhanced permeability and retention) effect, taking advantage of the leaky vasculature found in tumours. (II) The nanoplatform is identified by HER2 and CD44 receptors present on tumour surface. Subsequently, it undergoes internalization into the tumour cells. (III) The acidic microenvironment of tumour triggers the liberation of 5-aminolevulinic acid (ALA), a photosensitizer utilized



in PDT. Hyaluronic acid (HA) coating on the nanoplatform is deteriorated by GSH and enzyme hyaluronidase, further smoothing the liberation of Cy7.5 and ALA. Reprinted with permission from ref. 116. Copyright 2019, Elsevier.

Recently, Liu *et al.*¹¹⁷ presented an intriguing study that investigates how the surface chemistry of NPs can influence their behaviour in biological systems, particularly focusing on blood circulation time and targeting efficiency. The study involves AuNPs, a tumour targeting peptide (Pep2), a zwitterionic peptide (for instance, EK), and fat (for instance, stearine) separately or in combination. The study presents a model system using Pep2-functionalized gold NPs (AuNPs-Pep2) that are designed to be similar in physical properties (size, shape, elasticity, etc.) but contradict in surface compositions. The study further employs engineering strategies, such as modification of EK and EK-fat for modifying the surface of AuNPs-Pep2 nanoparticles. These modifications are designed to enhance the binding efficacy of the nanoparticles to tumorous cells and improve their targeting efficiency (Fig. 9). Preliminary results from *in vitro* experiments demonstrate that the modified nanoparticles exhibit higher binding affinity to tumour cells compared to unmodified AuNPs-Pep2 nanoparticles. Additionally, *in-vivo* experiments show that the engineered AuNPs-Pep2-EK-fat nanoparticles achieve significantly higher rate of accumulation in tumourous areas of mice.

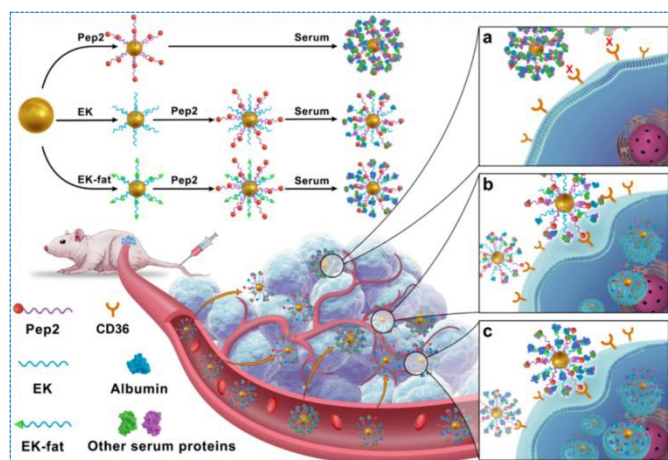


Fig. 9. The pictorial representation of fabrication of Pep2-functionalized gold NPs (AuNPs-Pep2) and their interaction with tumour cells highlights the importance of surface chemical properties

in nanoparticle-cell interactions. (a) The AuNPs-Pep2 encounter a challenge in cell recognition because their surface becomes covered by a protein corona. This corona, composed of plasma proteins, can hinder the direct interaction between the nanoparticles and the CD36-overexpressing tumour cells. (b) To address the recognition blockade caused by the protein corona, EK peptides are added to the nanoparticle surface. These peptides help reduce the adsorption of plasma proteins on the NPs surface. As a result, the nanoparticles become more accessible for correct recognition and internalization by the CD36-overexpressing tumour cells. (c) Further optimization is achieved by adding EK-fat peptides to the nanoparticle surface. These peptides alter the composition of the protein corona, leading to an increase in the amount of albumin while reducing the presence of other proteins. This compositional change in the protein corona facilitates the correct recognition and internalization of the nanoparticles by the tumour cells. Reprinted with permission from ref 117. Copyright 2023, Elsevier.

4.2.2. Cancer treatment using iron oxide nanoparticles

Iron oxide nanoparticles (IONPs) have enormous potential in theranostic due to their distinct characteristics like biocompatibility, magnetic properties, and tunable surface chemistry.^{118,119} They can be coated with drugs and functionalized with targeting molecules (e.g., antibodies, aptamers, etc.) that bind to cancer cells. Upon reaching the tumour site, the drug can be released in a controlled manner, reducing various systemic ramifications and ameliorating the therapeutic index.¹²⁰ They engender heat after exposition to magnetic field.¹²¹ This heat can be used to selectively demolish carcinogenic cells together with not harming close healthy tissues. They are targeted to the tumour site, and when exposed to the magnetic field, they increase the temperature of the tumour cells to a level that induces apoptosis/necrosis. They also possess superparamagnetic properties, making them highly useful in MRI (magnetic resonance imaging) as contrast agents. Their magnetic behaviour can be exploited to guide nanoparticles to specific locations in the body using external magnetic fields, which is particularly useful in target-based drugs.^{122,123} Recent reports have demonstrated that IONPs coated with responsive polymers exhibit different behaviours in response to variations in temperature and pH gradients.^{124,125}



Recently, Li *et al.*¹²⁶ developed an impressive nanodrug called OPPL that combines oleic acid-amended superparamagnetic IONPs (O-SPIONs) with PPL polymer to deliver both a platinum prodrug and lauric acid for treating colorectal cancer (CRC) as shown in Fig. 10. OPPL demonstrates synergistic enhancement of biofilm disruption affairs toward Fn (Fusobacterium nucleatum) when combined with the antimicrobial LA. This synergy is achieved through the production ROS via the nanodrug's peroxidase-like activity. OPPL increases intracellular ROS levels, promotes lipid peroxides, and depletes glutathione, ultimately leading to ferroptosis. This mechanism enhances the cytotoxicity of nanodrug against CRC cells. *In vivo* studies demonstrate several favourable outcomes: (i) OPPL shows increased accumulation at tumour sites, likely due to its design and magnetic properties. (ii) nanodrug enables magnetic resonance imaging, furnishing a minimally intrusive means of monitoring tumour response and drug distribution. (iii) OPPL inhibits tumour growth effectively. (iv) the nanodrug also inhibits the growth of Fn within the tumour environment, which is crucial for CRC infected with this bacterium.

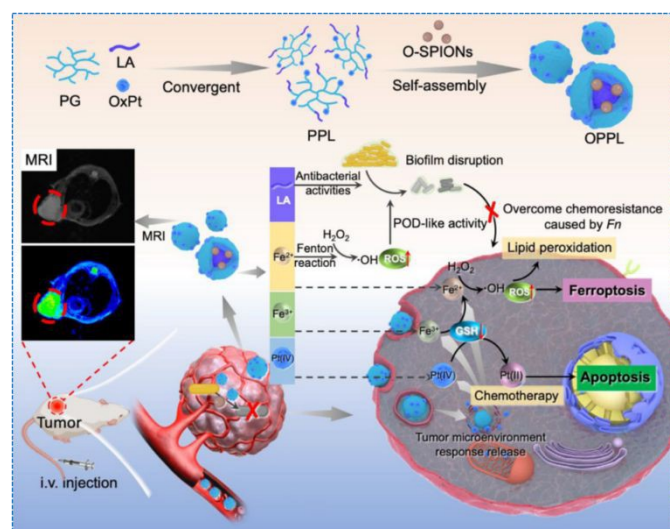


Fig. 10. Schematic illustration of development of the multifunctional nanodrug (OPPL), integration of antimicrobial properties with targeted cancer therapy to address both the bacterial infection and the cancer cells, ultimately improving treatment outcomes for Fn-infected CRC. Reprinted with permission from ref. 126. Copyright 2024, Elsevier.

4.2.3. Cancer treatment using mesoporous silica nanoparticles (MSNs)

DOI: 10.1039/D5PM00137D

According to IUPAC (International Union of Pure and Applied Chemistry), mesoporous materials are characterized by having pores of diameters ranging from 2 to 50 nm.¹²⁷ MSNs have gained extensive interest due to their tunable particle sizes (e.g., 50 to 300 nm), large surface areas, homogeneous as well as adjustable pore sizes (e.g., 2 to 6 nm), high pore volumes, and biocompatibility. MSNs are particularly valuable as smart nanocarriers in drug releasing systems owing to tunable particle size and configurable pore size, allowing the loading of drugs in divergent molecular forms. The high surface areas of both the interior pores and the external surfaces are ideal for grafting various functional groups, enhancing their functionality. MSNs are advantageous for cancer treatment as they can adhere to tumours by the EPR effect.¹²⁸ Their biocompatibility ensures minimal toxicity to healthy cells.

Conventional MSNs face several challenges, such as nonspecific binding to human serum proteins, hemolysis of RBCs, and phagocytosis by macrophages. These issues contribute to short blood circulation half-lives of these conventional MSNs. However, various strategies can be employed to overcome these limitations and enhance their functionality as smart nanocarriers. Polyethylene glycol (PEG) can be grafted onto the surface of MSNs to create a stealth layer, reducing immune recognition and clearance. This modification helps in prolonging the blood circulation time of MSNs by minimizing hemolysis, nonspecific protein binding, and phagocytosis.¹²⁹ Co-polymers can be grafted with MSNs to control the pore openings of MSNs. For example, poly(N-isopropylacrylamide) fastened with hollow MSNs can switch the nanochannels between “open” as well as “closed” states in response to temperature changes, enabling on-demand load and release of small molecules.¹³⁰ The surface of MSNs can be adjusted with targeting



ligands, like folate, peptides, mannose, and transferrin protein. These modifications facilitate active targeting to cells and/or tissues, enhancing the therapeutic productiveness and eliminating off-target effects.^{131,132} Smart MSNs are engineered to release their loaded drugs responding to various stimuli (e.g., pH, redox reaction, magnetic field, temperature, light, etc.), enhancing their functionality and specificity in drug delivery.¹³³

Zhang *et al.*¹³⁴ developed a redox and pH dual-responsive targeted drug release system employing hollow MSNs (HMSNs) grafted with bovine serum albumin-folic acid (BSA-FA), termed as HBF, through imine bonds for responsive and targeted delivery of doxorubicin (DOX) and methylene blue (MB), termed as MD@HBF. The engineered HBF nanoparticle serves as a carrier for the drugs. This targeted delivery enhances the therapeutic effect while minimizing damage to healthy cells. The use of combination therapy is emphasized as an effective approach to address the limitations of monotherapy and enhance therapeutic efficacy. In this case, the combination involves both chemotherapy (DOX) and photodynamic therapy (MB), offering a synergistic effect against cancer cells. *In vitro* experiments, including cell uptake studies and toxicity assays, validate the efficacy and safety of MD@HBF. The *in vivo* study demonstrates induction of apoptosis in cancerous cells (Fig. 11). The combination of chemo-photodynamic therapy employing MD@HBF shows outstanding synergistic killing efficiency against cancer cells, as indicated by a low combination index (CI = 0.325).

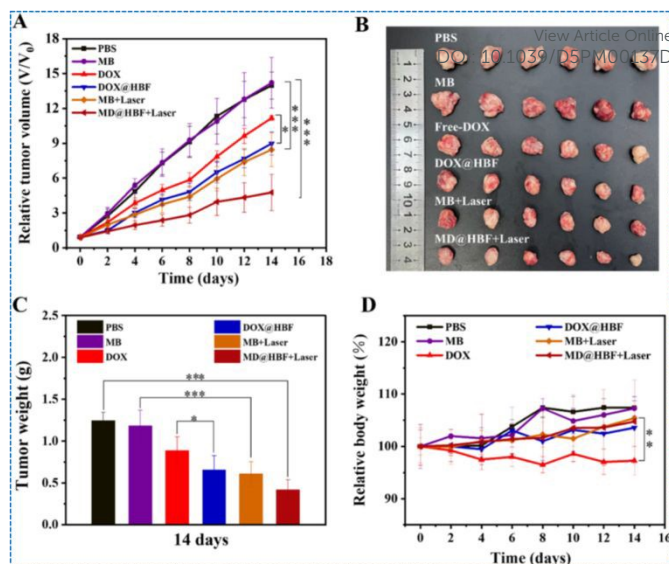


Fig. 11. (A) Variation of tumour volume with time (B) Representative images of tumours of the rat supplied with control (PBS), DOX, MB, MB + Laser, DOX@HBF, and MD@HBF + Laser. (C) tumour weight variation after treatment over the period of 14 days. (D) mice weight variation during treatment period of fourteen days. Reprinted with permission from ref. 134. Copyright 2023, Elsevier.

4.2.4. Cancer treatment using quantum dots

Quantum dots (QDs) are semiconductor NPs that exhibit distinct optical and/or electronic characteristics, making them highly suitable for various biomedical applications, including cancer therapy.¹³⁵ QDs can be synthesized employing a top down/bottom-up scheme, each with its distinct techniques and advantages. Ion implantation, molecular beam epitaxy, and x-ray lithography are common top-down techniques to synthesize QDs.¹³⁶ In contrast, a bottom-up strategy involves the assembly of QDs from atomic or molecular precursors. This approach is often employed to create colloidal QDs. Chemical reduction, self-assembly, and surface passivation are the key steps in the bottom-up synthesis of colloidal QDs.¹³⁷ Due to their tunable fluorescence, high brightness, and stability, QDs have been explored for imaging, diagnosis, and cure of cancer. Commercially available QDs are typically composed of three main components: the core, the shell, and a capping substance. The core of a QD is made from semiconductor materials and is primarily responsible for the QD's optical properties, such as



fluorescence and emission wavelength. The choice of material and the size of the core determine the specific colour of light emitted by the QD when excited. Common semiconductor materials used for the core include cadmium selenide and telluride. The core's size and composition control the quantum confinement effect, which dictates the emission wavelength and brightness.

The shell is constructed around the semiconductor core to enhance the QD's optical properties and stability. The shell material (e.g., zinc sulphide) is typically another semiconductor with a wider bandgap than the core. The shell passivates the core surface, reducing non-radiative recombination sites and thereby increasing the quantum yield (brightness) of the QDs. It protects the core from oxidation and other environmental factors, enhancing the stability and durability of the QDs. The shell can improve the biocompatibility of QDs for biological applications. Organic molecules, polymers, silica, etc. are used for capping. The capping layer stabilizes, solubilizes, and functionalizes the QDs. QDs functionalized by targeting ligands (e.g., antibodies, peptides, proteins, and folate), can bind to cancer cells, enabling precise imaging and localization of tumours.¹³⁸ They can be conjugated with drugs or therapeutic agents for targeted delivery, reducing astray and enhancing therapeutic efficacy. They can also serve as photosensitizers, generating ROS upon light activation to kill cancer cells.

QDs, like many NPs, are taken up non-specifically by the reticuloendothelial system. They accumulate in tumour tissues due to EPR effect. This phenomenon occurs because tumour vasculature is often more permeable than normal blood vessels, allowing nanoparticles to pass through and remain in the tumour environment. The fluorescence properties of QDs make them highly effective for visualizing cancer cells and tissues, providing several advantages over traditional imaging agents. For instance, QDs with a copper indium selenide

(CISE) core and a zinc sulphide (ZnS) shell, doped with manganese (Mn) and functionalized with folic acid were produced which exhibited 31.2% fluorescence efficiency.¹³⁹

4.3. Cancer treatment using polymer-based smart nanocarriers

Polymer-based smart nanocarriers are gaining significant attention for their potential in cancer treatment. These nanocarriers are designed to improve the targeted delivery of anticancer drugs, minimize side effects, and enhance therapeutic efficacy by exploiting the unique properties of polymers.^{140,141}

4.3.1. Cancer treatment using polymeric nanomaterials

Polymeric NPs (PNPs) mark a significant advancement in biomedical applications, fostering collaboration among various disciplines like biology, chemistry, engineering, and medicine. This convergence has spurred a medical revolution, resulting in remarkable progress in medicine delivery, biomaterials, and tissue engineering.^{142,143} The discovery of PNPs has paved the way for more effective treatments utilizing nucleic acids, proteins, and other active molecules.¹⁴⁴ This interdisciplinary approach has greatly enhanced our ability to deliver therapies with precision and efficacy, leading to transformative impacts in healthcare.

PNPs have a variety of advantages over traditional drug formulations in terms of stability, structural decomposition, premature release, and nonspecific release kinetics. Additionally, the ability to combine materials with divergent chemical compositions allows for the fabrication of nanoparticles with synergistic characteristics. The most employed techniques for preparing PNPs include emulsion polymerization, dialysis, solvent evaporation, etc. Incorporating biological response elements into polymer designs is a cutting-edge strategy. By leveraging biological cues or processes, such as



specific enzyme activities or pH levels in different tissues, researchers can attune medicine release profiles for enhanced therapeutic outcomes. Polymers like poly (D, L-lactic-co-glycolic acid) (PLGA) being biodegradable as well as biocompatible can be employed for controlled drug release. Its properties can be manipulated by adjusting factors like drug concentration and lactide to ethyl ester ratio allowing for customized release kinetics. The hydrophobic nature of PLGA, in combination with methyl groups, influences water absorption and degradation rates. Increasing polylactic acid content typically reduces water absorption, slowing down degradation and prolonging the liberation of encased drugs.

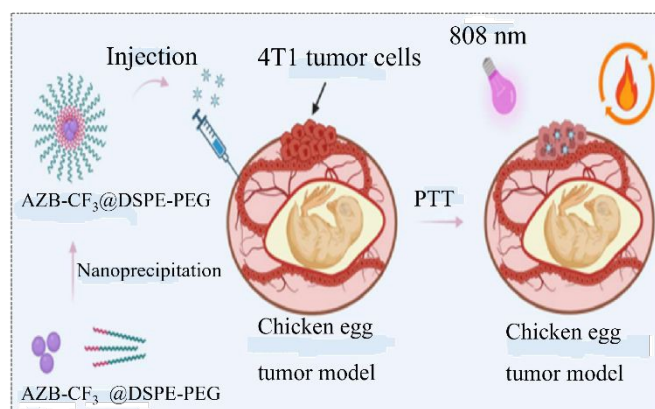


Fig. 12. Schematic representation of the synthesis of polymeric nanoparticles and their usage in the treatment of cancer based on photothermal effect in the chicken egg tumour model. Reproduced with permission from ref. 145. Copyright 2024, Royal Society of Chemistry.

Chansaenpak *et al.*¹⁴⁵ presented aza-BODIPY derivative based nanosystem (AZB-CF₃@DSPE-PEG NPs) for cancer treatment exhibiting outstanding photostability as well as colloidal stability. The nanoparticles exhibited good biocompatibility both *in vitro* (cell cultures) and *in ovo* (chicken egg model). The nanoparticles demonstrated high PTT efficacy, suitable for cancer treatment. When tested on 4T1 breast cancer cells, the NPs (containing 20 μ M AZB-CF₃) combined with 5 minutes of 808 nm laser irradiation resulted in approximately 10% cell viability, indicating significant cancer cell death (Fig. 12). The NPs also

showed properties that inhibit angiogenesis and metastasis. Approximately 40% vascular destruction was observed in the chicken egg tumour model.

4.3.2. Cancer treatment using dendrimers

Dendrimers are nanoscale, spherical, and/or symmetrical make-up characterized by their tree-like branches or arms.¹⁴⁶ The outer layer is made up of functional groups employed for drug/medication conjugation and targeting, enhancing drug encasing efficacy, reducing drug toxicity, and facilitating controlled deliverance mechanisms within the inner layer.¹⁴⁷ Dendrimers can be customized and modified in various ways, leading to the creation of numerous molecules with specified characteristics and functions. In the divergent method, dendrimers grow from the inside out, with layers being added progressively from the core to the periphery. In contrast, the convergent method involves growth from the outside in, where dendritic branches are synthesized separately and then attached to a central core. These methods were originally developed to create dendrite structures.¹⁴⁸ The ability to control the properties of dendrimers during synthesis makes them highly promising for various pharmaceutical applications.¹⁴⁹

Recio-Ruiz *et al.*¹⁵⁰ reported a carbosilane based dendrimer that improves compatibility with lipophilic drugs and enhances nanostructures properties owing to the lipophilic, stable, and inert essence of the carbosilane scaffolds. For instance, delivering drugs to the central nervous system, which is typically hindered by the blood-brain barrier, can be obtained by linking the medication to a polyamidoamine dendrimer, allowing it to overcome this barrier.¹⁵¹ Polylysine dendrimers show potential as biodegradable carriers that can deliver cytotoxic medications to solid tumours.¹⁵²



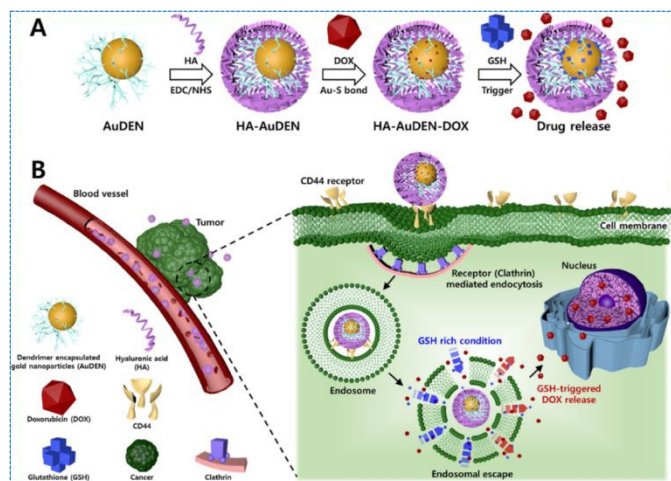


Fig. 13. Schematic representation of (A) the HA-AuDEN-DOX synthesis protocols; and (B) mechanisms of delivery of DOX, HA, and HA-AuDEN-DOX for treating ovarian cancer, facilitating a better understanding of the overall process and its therapeutic potential. Reprinted with permission from ref. 153. Copyright 2022, Elsevier.

Lee *et al.*¹⁵³ integrated active therapeutic agents' delivery system with stimuli-controlled drug in a single nanocarrier, utilizing HA-modified dendrimers encasing gold NPs (AuDEN) for treating ovarian cancer (Fig. 13). HA was utilized due to its ability to target cluster determinant 44 (CD44)-overexpressing cancerous cells. DOX is loaded onto the nanocarriers by self-assembling thiolated DOX on the gold surface, resulting in high drug loading content and chemical stability. The high glutathione concentration and tumour acidic (pH 5.6) microenvironment control the release of medications. In comparison to free DOX, the nanocarrier exhibited more cytotoxicity towards cancer cells.

4.3.3. Cancer treatment using micelles

Polymer micelles are fascinating nanostructures that have gained significant attention in biological applications owing to their distinct properties. Their size normally varies from 10 to 100 nm and composed of two distinct regions: the core part (being colloidally stable) and the outer part, also known as the shell or corona region, which consists of solvated hydrophilic polymer chains. In contrast, reverse micelle features a hydrophobic corona and a hydrophilic core.¹⁵⁴ The unique structure and

properties of micelles, particularly their corona-core arrangement, enhance the solubility of hydrophobic substances in water. Consequently, polymeric micelles can encapsulate amphipathic drugs, making them highly valuable in biomedical applications. Polymeric micelles are highly effective in encapsulating (solubilizing) hydrophobic drugs within their hydrophobic core. This physical encapsulation offers several significant advantages: (i) encapsulating hydrophobic drugs within the core of polymer micelles can help mitigate or eliminate adverse effects of the drugs, as the encapsulation can prevent direct interaction of the drug with healthy tissues; (ii) enhancement of water solubility of hydrophobic and insoluble drugs. This escalated solubility improves the bioavailability and therapeutic efficacy of these drugs; (iii) the tuned structure of polymer micelles control over the drug release rate precisely. This controlled release can be customized to accomplish sustained or targeted delivery, improving the therapeutic outcomes; (iv) by encapsulating drugs within their core, polymer micelles protect drug molecules from degradation caused by ecological factors such as pH changes and temperature variations. This protection enhances the stability as well as shelf life of the drugs. Furthermore, advancements in synthetic chemistry have expanded the functionality of polymer micelles.¹⁵⁵

The employment of long-established polymer micelles for targeting tumours in systemic cancer therapy is an innovative and promising strategy. These nanoscale vesicles, often modified on their surfaces for enhanced functionality, are designed to deliver small anti-tumour molecules, such as paclitaxel, directly to cancer cells. Previous report exhibited preferential accumulation of micelles in leaky vasculature of tumours due to EPR effect.¹⁵⁶ The extracellular microenvironment of tumours was reported to be more acidic than normal tissues and blood due to the high metabolic activity of cancer cells.¹⁵⁷ pH-sensitive micelles can be



designed to disassemble and release their drug payload in reaction to this acidic environment, providing targeted drug delivery to tumour sites. These smart nanoparticles can target transferrin receptors, which are often overexpressed in cancer cells, allowing for more precise drug delivery.¹⁵⁸ Folate-modified micelles target folate receptors, which are frequently overexpressed in various cancers. This system can efficaciously reduce the systemic adverse effects of doxorubicin, particularly its cardiotoxicity and pulmonary toxicity, while enhancing its anti-tumour efficacy.¹⁵⁹ The pH-sensitive together with thermosensitive polymeric micelles can exploit tumour's acidic environment and heat produced by PTT. This dual-responsive approach allows for controlled drug release, making it suitable for combined chemo-photothermal cancer treatments.¹⁶⁰

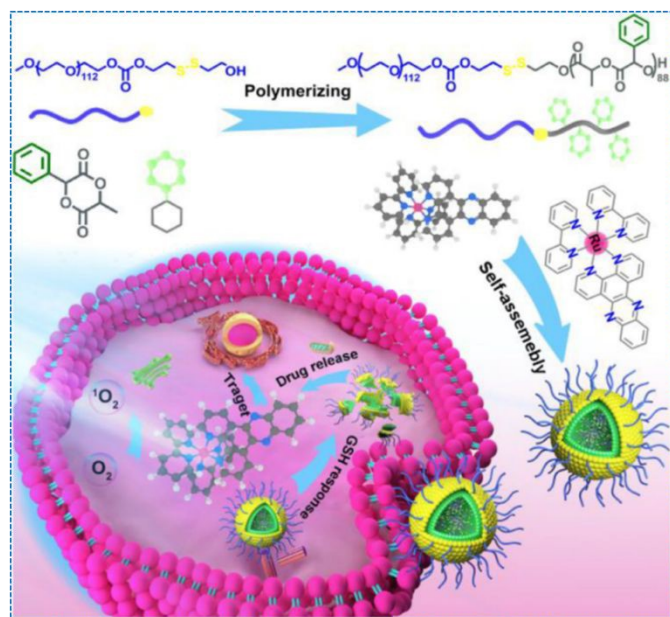


Fig. 14. Pictorial representation of biodegradable Ru-accommodating poly(lactide) MPEG-SS-PMLA@Ru micelles for increased delivery of Ru (II) polypyridyl complexes and cancer phototherapy. The disulfide bonds in the micelles are sensitive to the reductive environment found in tumours, where the GSH concentration is significantly higher than in normal tissues. Reprinted with permission from ref. 161. Copyright, 2023, Elsevier.

PLA-based micelles, particularly those composed of diblock copolymers, MPEG-SS-PMLA, represent a propitious technique for

enhancing cancer therapy through the effective delivery and controlled release of ruthenium complexes.¹⁶¹ Their high drug loading capacity, sensitivity to the tumour microenvironment, and ability to induce targeted apoptosis via PDT highlight their potential in advancing cancer treatment strategies (Fig. 14). These micelles exemplify the integration of nanotechnology and smart drug delivery systems to improve the precision and efficacy of cancer therapies.

4.4. Cancer treatment using biomimetic smart nanocarriers

Biomimetic nanocarriers are designed to mimic natural biological structures and processes, enhancing their ability to specifically target cancer cells and deliver therapeutic agents effectively.¹⁶²

4.4.1. Cancer treatment using liposomes

Liposomes are a type of amphipathic NPs characterized by a membrane-like structure composed primarily of phospholipids. These phospholipids are made up of a phosphatic hydrophilic (water-attracting) head and a fatty acidic hydrophobic (water-repelling) tail. Liposomes have a fascinating cell-like structure that makes them versatile carriers for various types of drugs, both lipid-soluble and water-soluble. This dual compatibility allows liposomes to carry a wide range of drugs. Multi-lamellar vesicles (MLVs) contain multiple lipid bilayers and are larger in size. They can carry a higher payload but may have slower release kinetics. Uni-lamellar vesicles (ULVs) have a single lipid bilayer and come in different sizes.¹⁶³ Liposomes can fuse with cell membranes, facilitating the delivery of encapsulated drugs directly into cells. This mechanism of cellular uptake is advantageous for targeted drug delivery and improving therapeutic efficacy.

While conventional techniques for liposome preparation have been widely used, they come with limitations such as solvent residues, heterogeneous



size distribution, and scalability issues. Innovative technologies leveraging supercritical fluids offer potential solutions by providing more environmentally friendly, efficient, and scalable methods for liposome production.¹⁶⁴ By incorporating PEGylation, stimuli-responsiveness, and radiolabelling, the smart liposomes provide improved stability, targeted delivery, and multifunctional capabilities, enhancing their potential for effective drug delivery, diagnostics, and therapeutic applications.¹⁶⁵⁻¹⁶⁷

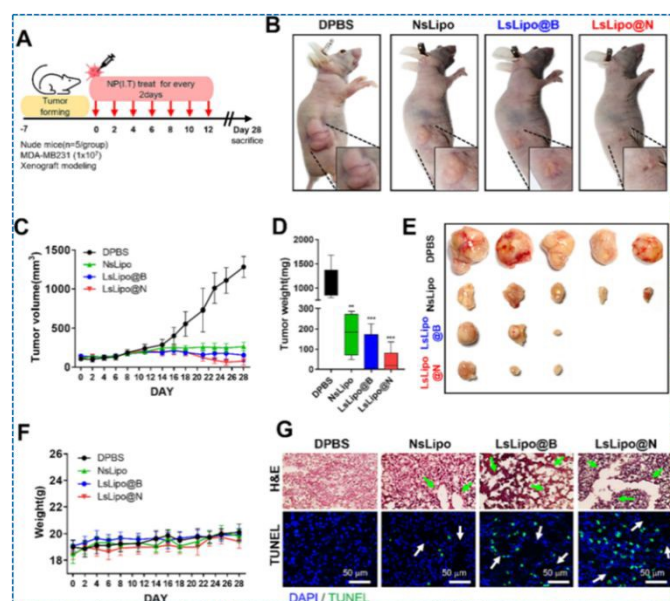


Fig. 15. (A) injection of LsLipo and NsLipo into the nude mice tumours; (B) LsLipo treated tumours were reported smaller than the NsLipo treated tumours; (C) As compared to conventional liposomes, LsLipo treatment caused a huge decrease in growth rate of tumours; (D-E) LsLipo@N holding more amount of PTX and DOX, led to more *in vivo* anticancer effect and smaller tumour growth compared to NsLipo and LsLipo@B; (F) Very less body weight differences between the different groups show non-toxic nature of liposomes which cause no side effect in the mice; (G) Tumour tissue analysis results showed high porous appearance of liposome treated tumour tissues due to increased tumour cell death compared to dense tumour tissues of control mice. Reprinted with permission from ref. 168. Copyright 2024, Elsevier.

Lee *et al.*¹⁶⁸ generated liposomes by combining DSPE and DSPE-PEG-2k lipids, loaded them with DOX and PTX (commonly used chemotherapeutic agents), and explored the effects of LED (light emitting diode) irradiation on their structure and drug loading capability. LsLipo (LED-irradiated liposomes) displayed rougher and

irregular surfaces than the NsLipo (non-irradiated liposomes). LED irradiation increased the loading efficiency of PTX and DOX in liposomes. The structural changes, for instance reduced membrane rigidity, likely facilitated better encapsulation of the drugs. Additionally, in a breast cancer mouse model, these LED-irradiated liposomes demonstrated a therapeutic effect by effectively reducing the size and weight of tumours (Fig. 15 B-G). Fig. 15A shows injection of LsLipo and NsLipo into nude mice tumours. The tumours treated with LsLipo were smaller as compared to bigger NsLipo treated tumours. (Fig. 15B). As compared to conventional liposomes, LsLipo treatment caused a huge decrease in growth rate of tumours (Fig. 15C). LsLipo@N holding more amount of PTX and DOX, led to more *in vivo* anticancer effect and smaller tumour growth compared to NsLipo and LsLipo@B (Fig. 14 D-E). Very few body weight differences between the different groups show the non-toxic nature of liposomes which cause no side effect in the mice (Fig. 15F). Tumour tissue analysis results showed high porous appearance of liposome treated tumour tissues due to increased tumour cell death compared to dense tumour tissues of control mice (Fig. 15G).

4.4.2. Cancer treatment using protein nanoparticles

Protein NPs have transpired as a propitious strategy for cancer treatment, offering targeted delivery, controlled release, and reduced side effects compared to conventional treatments. They are simple to synthesize, non-immunogenic, non-toxic, biodegradable, biocompatible, and have high binding potential with various drugs/medications.¹⁶⁹ The presence of functional groups on protein surfaces allows for easy modification with targeting polymers, ligands, and other molecules, enabling the creation of smart nanoparticles for targeted drug delivery.¹⁷⁰ Albumin, one of the most abundant proteins in plasma, has been widely employed to create NPs for therapeutic system due to its biocompatibility, non-immunogenicity, and ability



to bind various drugs. Doxorubicin-loaded HAS (human serum albumin) NPs have shown more advancements in *in-vitro* anticancer potential toward neuroblastoma cell lines compared to the pure drug.¹⁷¹ PTX-loaded BSA (bovine serum albumin) NPs decorated with folic acid have demonstrated great potential in targeting prostate cancer.¹⁷²⁽¹⁴⁷⁾ This targeted approach increases the uptake of the NPs by cancer cells, enhancing the therapeutic effect of paclitaxel.¹⁷³ Abraxane, with a diameter of approximately 130 nm, is the first commercially available nanoparticle drug approved by the FDA. It has shown remarkable effectuality in treating breast cancer and represents a significant advancement in nanoparticle-based drug delivery systems.^{174,175}

Recently, Meng *et al.*¹⁷⁶ hypothesized an innovative and promising approach to target tumour cells by leveraging the natural properties of active HSA to deliver the PTEN (phosphate and tensin homology) protein. Leveraging active HSA can facilitate the delivery of PTEN protein into tumour cells via Gp60 (albondin)- and SPARC (osteonectin/BM40)-mediated pathways, thereby restoring the tumour suppressor function of PTEN and offering a novel anti-tumour strategy (Fig. 16). Gp60-mediated pathway leverages the high expression of Gp60 in endothelial cells to facilitate transcytosis and tumour cell targeting. SPARC-mediated pathway exploits SPARC's overexpression in tumour cells for enhanced albumin binding and internalization.

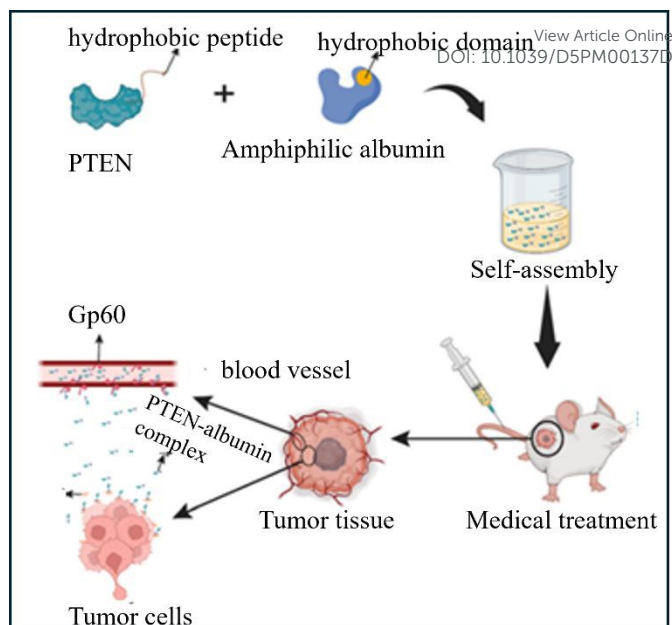
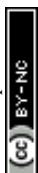


Fig. 16. Schematic illustration of the hypothesis from the formation of PTEN-albumin complexes to their targeted delivery to tumour cells via the Gp60 and SPARC pathways, ultimately aiming to restore the tumour-suppressing functions of PTEN within the tumour environment. Reprinted with permission from ref 176. Copyright 2024, Elsevier.

4.4.3. Cancer treatment using cell membrane nanomaterials

Conventional NPs for cancer therapy face significant challenges, including rapid clearance from the bloodstream, easy recognition and neutralization by immune system, and insufficient accumulation at target site.¹⁷⁷ Cell membrane coated NPs (CMCNPs) are potent bio-inspired NMs to address these issues. The presence of numerous proteins on cell membranes allows CMCNPs to dodge the immune system and enhance circulation period and target specificity.¹⁷⁷⁻¹⁷⁹ The preparation of CMCNPs involves isolation of cell membranes from the chosen cell source (e.g., cancer cells, platelets, etc.) and encapsulation of core nanoparticles within the isolated membrane vesicles, forming CMCNPs.

Liu *et al.*¹⁸⁰ developed core-shell NPs, comprising upconversion NPs (UCNPs) as core and $\text{Zn}_x\text{Mn}_{1-x}\text{S}$ (ZMS) as shell, coated with BxPC-3 pancreatic cancer cell membranes, abbreviated as BUC@ZMS to enhance homologous targeting and



provide a synergistic treatment approach combining CDT and PDT for pancreatic ductal adenocarcinoma (PDAC) (Fig. 17). In the presence of NIR, UCNPs cause ROS generation. Mn ions in ZMS catalyze the Fenton-like reaction, converting hydrogen peroxide (H_2O_2) into hydroxyl radicals ($\bullet OH$), further increasing ROS levels and enhancing the sensitivity of tumour cells to oxidative stress. *In vitro* study confirmed high levels of ROS production in pancreatic cancer cells treated with BUC@ZMS nanoparticles as well as significant reduction in intracellular GSH levels. *In vivo* study showed that BUC@ZMS nanoparticles accumulate in tumour sites and suppress growth of PDAC, with minimal observed toxicity to healthy tissues.

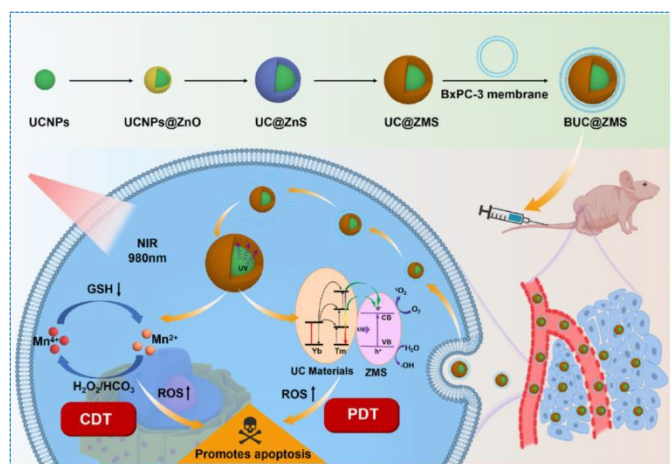


Fig. 17. Schematic representation of the design and functionality of BUC@ZMS core-shell nanoparticles, highlighting their components, mechanisms of action, and therapeutic potential for pancreatic cancer treatment. Reprinted with permission from ref. 180. Copyright 2023, Elsevier.

4.5. Cancer treatment using carbon-based nanomaterials

Carbon-based NMs have garnered significant attention in cancer treatment owing to their distinct characteristics, like high surface area, chemical versatility, and functionalization with targeting ligands for targeted therapy.^{181,182} Graphene's excellent photothermal conversion efficiency makes it suitable for PTT. Upon exposure to near-infrared (NIR) light, graphene can generate localized heat to kill cancer cells. Graphene-based materials can also

generate ROS under light irradiation, contributing to PDT. This section provides an overview of the essence of divergent carbon NMs, together with graphene, graphdiyne, fullerenes, carbon nanotubes (CNTs), and carbon quantum dots (CQDs), to anticancer strategies.¹⁸¹⁻¹⁸³

Being inherently hydrophobic, these carbon NMs are suitable for loading drugs via π - π bonding or hydrophobic interactions.¹⁸⁴ Due to their versatile functionalization possibilities, these NMs can be amended with divergent biomolecules covalently as well as non-covalently, which enhances their biocompatibility, water, and biosafety.¹⁸⁵ Moreover, various targeting ligands or functional molecules can be encased into carbon NMs to escalate their targetability.¹⁸⁶ This approach can significantly alter the electronic, mechanical, and chemical properties of NMs. Covalent functionalization involves oxidation, halogenation, amination, click chemistry, nitrene addition, Bingel reaction, addition reactions, cyclopropanations, etc. Non-covalent functionalization involves weaker interactions inclusive of van der Waals interactions, π - π stacking interactions, hydrogen bonding, host-guest chemistry, and electrostatic interactions (Fig. 18).¹⁸⁷

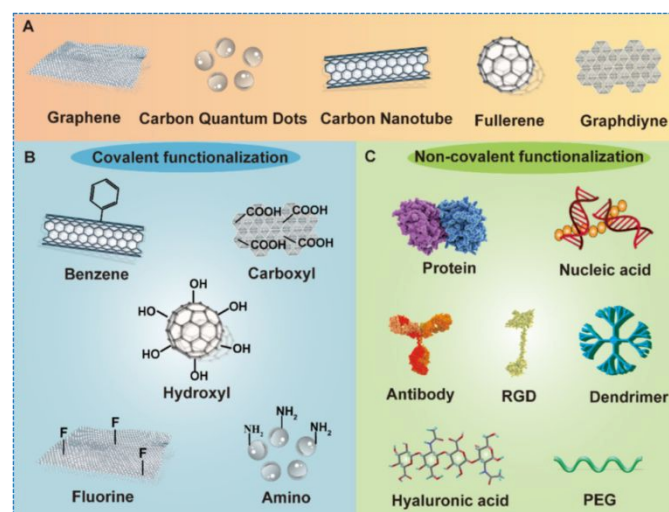


Fig. 18. Schematic showing divergent carbon NMs and strategies of functionalization. Carbon NMs can be functionalized with both covalent and non-covalent methods employing different biomolecules and chemical groups. The functionalized carbon NMs play an exuberant role in targeted drug delivery in cancer treatment. Reprinted from ref. 187. Copyright 2022, The Author(s). This is an open access



ARTICLE

Journal Name

article distributed under the terms of the Creative Commons Attribution License (<https://creativecommons.org/licenses/by/4.0/>).

Wu *et al.*¹⁸⁸ developed a nanohybrid drug delivery system sensitive to redox conditions, pH, and enzymatic activity. This system was fabricated via assembling GSH sensitive BSA encased DOX and MMP-2 sensitive gelatine onto graphene oxide (GO) nanosheets for attaining controlled drug release (Fig. 19). In the TME, which has high levels of proteases, the nanosystem released 5 nm nano-units enveloping DOX. Upon reaching the reductive, acidic, and enzymatic conditions of the tumour tissue, the system enables a synergistic therapeutic effect. This is achieved through the switchable release of DOX, which can be controlled by irradiating NIR laser. *In vitro* observations showed that the nanosystem could heat up to 45.6°C after 5 minutes of NIR laser irradiation, ablating MCF-7 cancer cells.

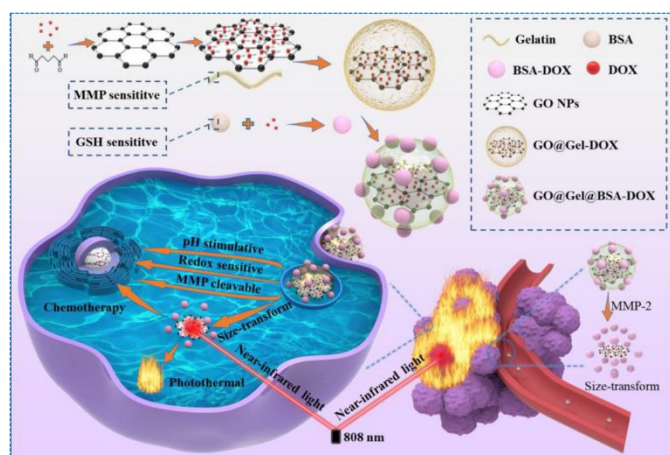


Fig. 19. Schematic illustration of construction and functional mechanism of GO@Gel@BSA-DOX nanohybrids designed for TME-responsive drug release and cancer treatment. Reprinted with permission from ref. 188. Copyright 2021, Royal Society of Chemistry.

Recently, Zhao *et al.*¹⁸⁹ demonstrated the potential of carbon nanoparticle suspension injection (CNSI) in cancer treatment through the photothermal effect under NIR irradiation. This method effectively eliminates primary tumours and induces immunogenic cell death (ICD). Additionally, when combined with anti-programmed cell death protein 1 (aPD-1) therapy,

CNSI under irradiation spurs an immune response that inhibits the growth of distal tumours. The study also explored the use of phototherapy to treat metastatic lymph nodes. NIR irradiation of CNSI in these nodes eradicates cancer cells and activates the immune response within the lymphatic system. The synergy between CNSI-mediated PTT and aPD-1 therapy significantly boosts the overall anti-tumour effect (Fig. 20), demonstrating the potential to control and eliminate metastatic disease.

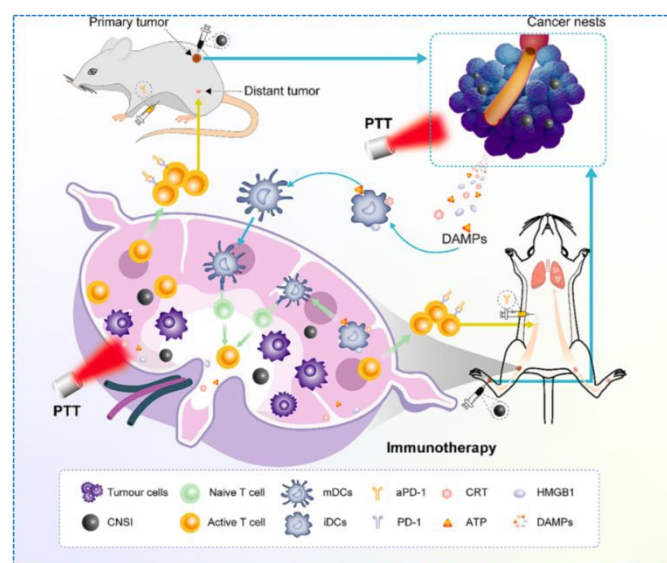


Fig. 20. Schematic representation of carbon nanoparticle suspension injection (CNSI)-mediated PTT and immunotherapy toward cancer metastasis. Reprinted with permission from ref. 189. Copyright 2024, Elsevier.

4.6. Cancer treatment using advanced nanomaterials

BP and MOF both represent the forefront of advanced NMs, each offering unique properties and vast potential across various applications.¹⁹⁰ In this section, I have discussed the anticancer applications of BP and MOF.

4.6.1. Cancer treatment using black phosphorus

BP has emerged as a propitious material in cancer treatment, particularly in drug delivery systems and tumour microenvironment modulators, potentially enhancing the immune response against cancer cells.^{191,192} It can be used in combination with



chemotherapy/radiotherapy to enhance overall treatment efficacy. The PEGylated BP nanoparticles are particularly promising as a novel nanotheranostic agent due to their ability to: (i) generate heat from NIR light, which can be used for photothermal therapy to ablate cancer cells. (ii) provide enhanced contrast for photoacoustic imaging, facilitating better visualization and targeting tumours.¹⁹³

Geng *et al.*¹⁹⁴ reported a significant advancement in the field of pancreatic cancer treatment through the development of an innovative combination chemotherapeutic approach leveraging gemcitabine (GEM) and bioactive black phosphorus. GEM triggers blockage of cell cycle in the G0/G1 phase. The co-loading of iRGD-amended zein NPs with GEM and BP quantum dots (BPQDs) termed BP-GEM@NPs ensured the direct delivery of the chemotherapeutic agents at the tumour site and enhanced their effectiveness. After intravenous injection, BP-GEM@NPs demonstrated marvellous tumour targeting proficiency, allowing for more sustained therapeutic effects, and a higher rate of pancreatic tumour cell apoptosis (Fig. 21).

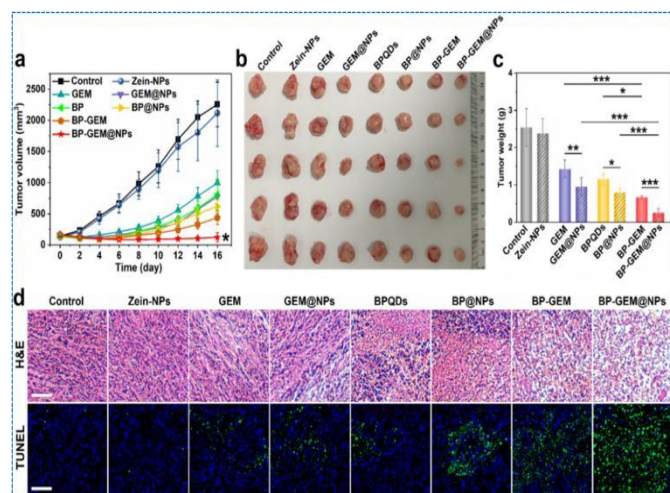


Fig. 21. Synergistic anticancer upshots of BP-GEM@NPs on tumour bearing mice *in vivo*. (a) Profiles of tumour growth. All the treatments show clear inhibition of growth of tumour compared to blank Zein-NPs and control groups, showing chemotherapeutic impacts of GEM and BPQDs toward pancreatic carcinoma. The BP-GEM@NPs averted the tumour growth completely. (b) Photographs showing maximum inhibition of tumour growth by the BP-GEM@NPs (c) The tumour weights of BP-GEM@NPs groups are highly lower due to

prolonged blood circulation and targeted drug delivery effects. (d) Hematoxylin & eosin staining and TUNEL assay show that BP-GEM@NPs cause severe nucleus shrinkage, karyorrhexis, plasmatorrhexis, and larger degree of apoptosis. Reprinted with permission from ref. 194. Copyright 2023, Elsevier.

4.6.2. Cancer treatment using MOF nanomaterials

MOFs are one to three-dimensional porous materials made up of metal ions coordinating to organic ligands.¹⁹⁵ Due to their versatile chemical composition and structure, MOFs have gained significant attention in gas storage, separation, catalysis, and biomedical applications. The prominent types of MOFs include: (i) zeolitic imidazolate frameworks (ZIFs). ZIFs use imidazole or its derivatives as ligands; (ii) materials of institute lavoisier (MIL). For example, MIL-53, MIL-88, and MIL-101; (iii) MOFs with alkaline earth metals (AEPFs). Metal canisters consist of alkaline earth metals such as calcium, strontium, and magnesium; (iv) MOFs with rare earth metals (RPFs). Metal canisters include rare earth elements like lanthanides and benzenecarboxylated acids as ligands; (v) HKUST-1 (Hong Kong university of science and technology). Copper ions coordinated with benzenetricarboxylate (BTC); (vi) UiO series (university of Oslo). These are zirconium-based MOFs. Examples include UiO-66 and UiO-67; (vii) IRMOF (isoreticular MOFs). Composition involves zinc ions with terephthalate linkers. Examples include IRMOF-1 to IRMOF-16; (viii) PCN (porous coordination networks). Composition involves metal ions with various organic linkers; (ix) post-synthetic modified MOFs.¹⁹⁶

MOFs have garnered noteworthy attention as hybrid crystalline porous biomaterials, distinctly in the realm of DDS. Their unique characteristics such as adjustable pore sizes and shapes, ultrahigh surface areas, and versatile functionalities tune for developing advanced drug delivery systems.¹⁹⁷ However, challenges such as physiological instability and cytotoxicity owing to toxic metal ions



have limited their applications. Though, this approach enhances the stability, biocompatibility, and therapeutic efficacy of MOFs.

The multifunctional hybrid systems can be employed to generate ROS upon light irradiation, effectively killing cancer cells. MOFs with photothermal properties can absorb NIR light and convert it into heat, destroying cancer cells with localized hyperthermia. These can encapsulate chemotherapeutic drugs, providing targeted and controlled release, minimizing side effects on healthy tissues. Combining different therapeutic modalities (e.g., PDT, PTT, chemotherapy) within a single MOF platform can produce synergistic effects, improving overall treatment outcomes.¹⁹⁸ A recent study demonstrated the use of an endogenous copper MOF nanozyme therapy for colon cancer treatment. This innovative approach leverages endogenous biomarkers to trigger the "turn-on" production of drugs in situ, simplifying the creation of nanomedicine and enhancing the targeting of cancer treatment.¹⁹⁹

Ji *et al.*²⁰⁰ have developed an innovative multifunctional copper-based MOF (Cu-MOF) nanoparticle, loaded with mitoxantrone (MTO) and azobenzene (AXB) and decorated with a tumour cell membrane (TCM) to form M/A@MOF@CM. This hybrid system is designed for a synergistic anticancer therapy that induces cuproptosis, ferroptosis, and apoptosis (Fig. 22). TCM provides a homologous targeting mechanism, enhancing cellular uptake through membrane-mediated endocytosis. It helps evade immune detection, improving biocompatibility and reducing off-target effects. Mechanism of action involves depletion of GSH through reduction of Cu^{2+} to Cu^+ . Disruption of cellular energy metabolism, increasing cytoplasmic copper concentration, which is conducive to the production of hydroxyl radicals ($\bullet\text{OH}$). High copper ion concentrations cause the loss of ferredoxin 1 (FDX1) and lipoylated proteins

(LIAS), leading to cell death through a process known as cuproptosis. Increased ROS levels cause lipid peroxidation, damaging cell membranes. Glutathione peroxidase 4 (GPX4) deactivation further enhances ferroptosis. MTO directly intercalates DNA, triggering apoptosis through DNA damage and cell cycle arrest. The combination of cuproptosis, ferroptosis, and MTO-induced apoptosis leads to robust and efficient tumour cell elimination. The treatment induces severe ICD, distinguished by the liberation of damage-associated molecular patterns (DAMPs) and tumour-associated antigens (TAAs). The release of DAMPs and TAAs elicits strong systemic immune responses, enhancing the ability to inhibit distant (abscopal) tumours and reduce metastasis, particularly in the lungs. M/A@MOF@CM combines chemotherapy, CDT, and PTT, providing a broad range of therapeutic activities. TCM decoration enhances tumour-specific targeting and uptake, ameliorating remedy proficiency and lessening side effects.

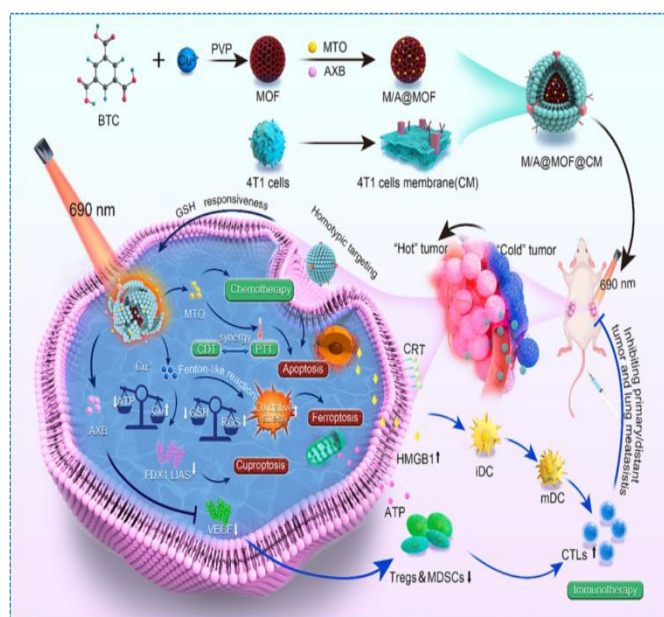


Fig. 22. Schematic showing synthesis and anticancer mechanism of MOF based nanosystem in mice. Reprinted with permission from ref. 200. Copyright 2024, Elsevier.

4.6.3. Cancer treatment using MXenes



The properties of MXenes have been discussed in wound healing section. In this section, applications of MXenes in cancer treatment have been discussed.

Wu *et al.*²⁰¹ reported a smart responsive $\text{Ti}_3\text{C}_2\text{T}_x$ nano-drug delivery system. The exceptional properties of $\text{Ti}_3\text{C}_2\text{T}_x$ MXenes inclusive of functional groups accessibility, negatively charged surface, and photothermal effect played outstanding role in the construction of smart $\text{Ti}_3\text{C}_2\text{T}_x$ -DOX-PMash-Tf nanoplatfrom by assembling positively charged DOX, PMash (sulfhydryl-modified polymethacrylic acid) shell and the Tf protein layer. The carboxyl groups in PMash are protonated in acidic domain, leading to partial cleavage of the shell, while excessive GSH can break the disulfide bonds, resulting in disintegration and controlled release of drug. The addition of a tumour-targeting Tf layer ensures that the smart material is preferentially directed towards tumour cells, enhancing the specificity and reducing off-target effects.

MTT assay was used to evaluate the effectiveness of a nanomedicine release system in killing human hypopharyngeal carcinoma cells (FaDu) *in vitro*. Various treatment groups, including normal saline (NS), $\text{Ti}_3\text{C}_2\text{T}_x$, free DOX, $\text{Ti}_3\text{C}_2\text{T}_x$ -DOX, $\text{Ti}_3\text{C}_2\text{T}_x$ -DOX-PMash, and $\text{Ti}_3\text{C}_2\text{T}_x$ -DOX-PMash-Tf were employed for the purpose. Free DOX exhibited higher cytotoxicity than $\text{Ti}_3\text{C}_2\text{T}_x$ -DOX-PMash-Tf (Fig. 23A). The lower cytotoxicity of $\text{Ti}_3\text{C}_2\text{T}_x$ -DOX-PMash-Tf than free DOX was attributed to incomplete drug release from nanocarrier platform within 24-hour culture period. This suggested lower drug concentration delivered to cells than originally loaded concentration. The survival rate of cells treated with $\text{Ti}_3\text{C}_2\text{T}_x$ alone was 97.9% without NIR irradiation, indicating good biocompatibility of the $\text{Ti}_3\text{C}_2\text{T}_x$ nanomaterial. In the presence of $\text{Ti}_3\text{C}_2\text{T}_x$, laser irradiation reduced the viability of tumour cells, demonstrating the effectiveness of the photothermal effect in inducing cell death. The cytotoxicity of $\text{Ti}_3\text{C}_2\text{T}_x$ -DOX-

PMash and $\text{Ti}_3\text{C}_2\text{T}_x$ -DOX was similar, but both exhibited higher cytotoxicity than that of $\text{Ti}_3\text{C}_2\text{T}_x$ alone. $\text{Ti}_3\text{C}_2\text{T}_x$ -DOX-PMash-Tf had lower cytotoxicity than free DOX but was more cytotoxic than other NM groups. $\text{Ti}_3\text{C}_2\text{T}_x$ -DOX-PMash-Tf was shown to effectively target tumour cells expressing the Tf receptor. Upon entering cancer cells, the GSH cleaved the disulfide bond present in the nanocarrier which led to drug release and subsequent cell death. The IC_{50} (half maximal inhibitory concentration) of $\text{Ti}_3\text{C}_2\text{T}_x$ -DOX-PMash-Tf + NIR, $\text{Ti}_3\text{C}_2\text{T}_x$ -DOX-PMash-Tf, and DOX were reported as 0.22, 1.26, and 0.41 $\mu\text{g/mL}$, respectively (Fig. 23B). The decrease in IC_{50} value under NIR indicates enhanced cytotoxicity and confirms that photothermal therapy can markedly improve therapeutic efficacy.

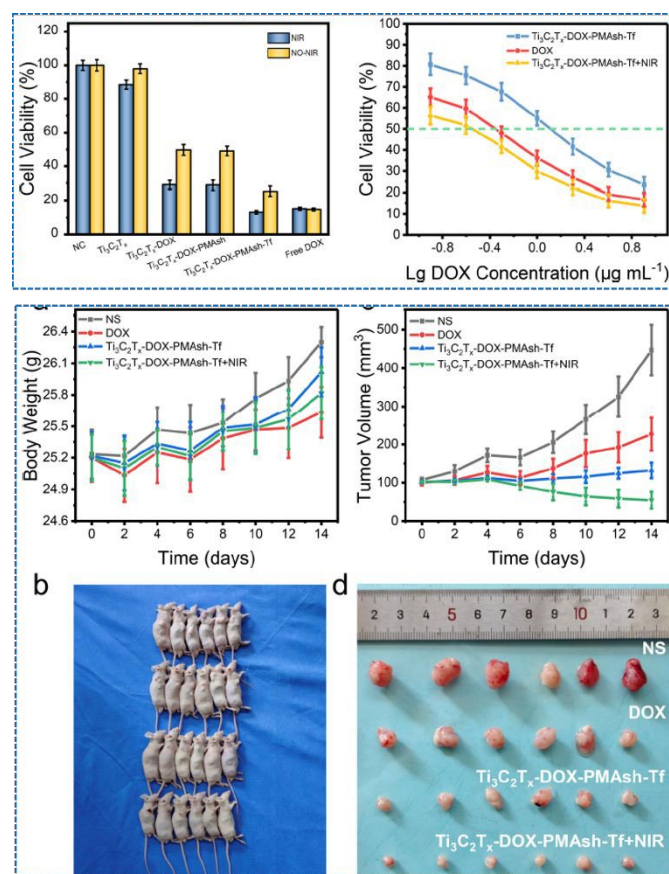


Fig. 23. The MTT assay providing insights into the cytotoxic effects of different treatment groups on FaDu cells, both with and without NIR laser irradiation. Enhanced cytotoxicity was observed due to the photothermal effect of $\text{Ti}_3\text{C}_2\text{T}_x$ MXene, which led to increased cell death, either through enhanced drug release or direct thermal damage. (B) IC_{50} value of different treatment groups. $\text{Ti}_3\text{C}_2\text{T}_x$ -DOX-PMash-



Tf + NIR likely have a lower IC_{50} than without NIR, indicating enhanced cytotoxicity due to the combined chemo-photothermal therapy. (C-F) *In vivo* investigation of anticancer activity in mice with different treatment groups. (C) Changes in the body weight of tumour bearing mice over treatment of fourteen days. (E) Post-treatment digital images of mice. (D) Curve showing change in tumour volume during treatment period of fourteen days. (F) Post-treatment digital images of tumours. Reprinted with permission from ref. 201. Copyright 2023, American Chemical Society.

They further conducted an *in vivo* examination to evaluate the effectiveness of a $Ti_3C_2T_x$ -DOX-PMASH-Tf nanomaterial as a drug release system for treating FaDu tumours in mice. The experiment compared the effects of different treatment groups, including a control group, a group treated with free DOX, a group treated with the nanomaterial ($Ti_3C_2T_x$ -DOX-PMASH-Tf), and a group treated with the nanomaterial plus NIR irradiation. Mice were injected with 5 mg/kg DOX on days 0 and 5. In the case of the NIR group, nine hours after injection, the tumour region was treated with radiations for ten minutes at 1 W/cm². This irradiation raised the tumour area temperature from 30° centigrade to 46.3° centigrade, inducing a photothermal effect. The body weight and survival of all mice was reported stable after treatment for fourteen days (Fig. 23C). Tumour volume measurements and post-treatment tumour extraction indicated that the $Ti_3C_2T_x$ -DOX-PMASH-Tf + NIR group exhibited the most significant inhibition of tumour growth (Fig. 23 D-F). Overall, this study showed significant efficacy of the $Ti_3C_2T_x$ -DOX-PMASH-Tf composite material in killing carcinogenic cells *in vitro* and inhibiting tumour growth *in vivo* when exposed to 808 nm laser irradiation. The combination of targeted drug delivery and photothermal effects resulted in enhanced therapeutic outcomes.

Dai *et al.*²⁰² showcased a significant advancement in the field of cancer nanotheranostic by modifying the surface of Ta_4C_3 MXenes with manganese oxide nanoparticles (MnOx). They combined multiple imaging and therapeutic modalities into a single platform and enhanced both

the diagnostic and treatment capabilities in cancer therapy. The tantalum in Ta_4C_3 MXenes acted as a high-performance contrast agent for contrast-enhanced CT imaging. This made it easier to visualize tumours with greater clarity and detail using CT scans. The manganese oxide nanoparticles incorporated into the MXene structure were responsive to the tumour microenvironment, making them effective contrast agents for T1-weighted MRI. This responsiveness allowed for better imaging of tumours, particularly in distinguishing them from surrounding healthy tissues.

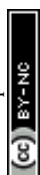
5. Tissue engineering and regeneration applications of smart nanomaterials

NMs-based drug delivery systems are crucial components in TER, offering targeted, controlled, and sustained release of drugs. These systems can enhance tissue regeneration by releasing drugs, growth factors, and genes directly to disease site.^{203,204}

5.1. Bone tissue engineering and regeneration applications of smart nanomaterials

Bone is an intricate and dynamic tissue essential for structural support, protection of vital organs, and haematopoiesis. However, bones can be damaged due to various reasons such as disease (osteosarcoma, osteoarthritis, and bone metastasis cancer), trauma, congenital abnormalities, aging, etc. In one study, Liu *et al.*²⁰⁵ loaded bone morphogenetic protein-2 (BMP-2) into an adhesive liposome which were then incorporated into the hydrogel to develop antibacterial and self-healing multifunctional DDSs for injection into osteoporotic cracks and bone marrow cavity. The results showed better osteogenic differentiation and rapid bone remodeling of osteoporotic fractures.

5.1.1. Bone tissue engineering and regeneration applications of polymeric micelles



Polymeric micelles based nanocarrier systems are widely employed for targeted drug delivery in TER due to their great loading efficiency, controlled release, low CMC, enhanced stability, and improved solubility of hydrophobic drugs. Lima *et al.*²⁰⁶ delineated a sophisticated drug release system utilizing polymeric micelle-based nanocarriers specifically fabricated for the subdued release of anti-inflammatory drug dexamethasone (Dex) for arthritic disease (Fig. 24 A). This innovative approach leveraged the elevated activity of the glutathione reductase (GR) enzyme present in inflamed joints to create a system that is sensitive to GR enzyme activity, thereby enabling efficient and targeted delivery of Dex in the treatment of arthritic diseases. The micelle limited the exposure of non-target tissues to Dex, decreasing the risk of adverse effects.

In other study, Long *et al.*²⁰⁷ developed an innovative polymeric micelle system designed to respond to hypoxic conditions and target bone metastasis for the treatment of bone metastatic prostate cancer efficiently (Fig. 24 B). The system exploited the unique microenvironment created during bone metastasis, particularly the hypoxic conditions, to ensure targeted and efficient delivery of DOX medication. Alendronate was incorporated into the micelles to confer bone-targeting properties whereas azobenzene was used as a hypoxia-sensitive linker which undergoes structural changes in response to hypoxic conditions, triggering the release of the encapsulated drugs. *In vivo* study confirmed the selective accumulation of micelles in metastatic bone, hypoxia-triggered release of DOX at the metastatic site, suppression of tumour growth in bone, and inhibition of bone destruction by reduction of osteoclast activity and promotion of osteoblast activity.

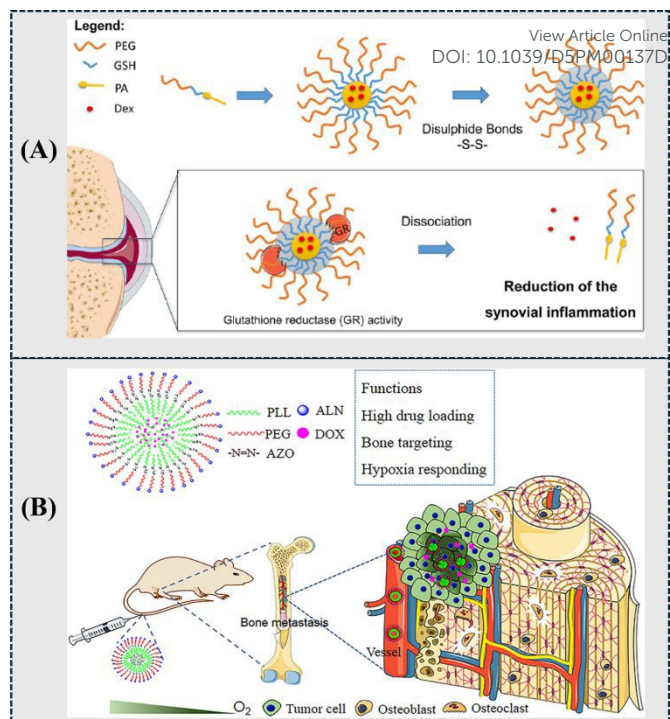


Fig. 24. (A) Schematic representation of the usage of glutathione reductase (GR)-sensitive polymeric micelles for arthritis treatment. Reprinted with permission from ref. 206. Copyright 2021, American Chemical Society; (B) Schematic illustration of applicability of hypoxia-responsive and bone tissue targeting polymeric micelles for targeted treatment of bone metastatic prostate cancer. Reprinted with permission from ref. 207. Copyright 2021, Elsevier.

5.1.2. Bone tissue engineering (BTE) and regeneration applications of polymeric nanomaterials

Polymeric NPs, specifically PLGA and chitosan, are increasingly being utilized in BTE for targeted drug delivery owing to their notable biodegradability, non-immunogenic, and ability to liberate medications directly to targeting sites. These NPs can be easily engineered to intensify bone regeneration and mend by imparting controlled growth factors, medications, and divergent bioactive molecules.^{208,209} Chitosan NPs have emerged as highly effective nanocarriers in BTE, primarily due to their intrinsic osteoinductive and antibacterial properties. These characteristics not only facilitate bone regeneration but also help mitigate the risk of infections, which is a significant challenge post-bone grafting.²¹⁰



5.1.3. Bone tissue engineering and regeneration applications of smart nanofibers

Nanofibers represent an advanced and versatile class of nanofibrous materials that are increasingly being explored for their applications in BTE and guided bone regeneration. These nanofibers can respond to various physical, chemical, and biological stimulus, making them highly suitable for creating dynamic and responsive environments conducive to bone healing and regeneration. One such example of smart nanofibers in BTE is a nano or micro fibrous composite consisting of polycaprolactone (PCL) and silk fibroin.²¹¹ This composite has demonstrated enhanced functionality in promoting bone regeneration and can be tailored by adjusting the nanofiber content within the scaffold. Additionally, hybrid scaffolds composed of nano or micro fibrous mats have shown increased cellular responses, particularly with MC3T3-E1 cells, compared to individual scaffolds.²¹² Electroconductive composite nanofibers represent a cutting-edge approach in BTE, offering a combination of electroactivity, biomimetic properties, and controlled growth factor delivery.²¹³ These scaffolds have demonstrated the ability to promote osteoinductivity, osteoconductivity, and biocompatibility, making them highly promising for enhancing the healing process in bone defects.²¹⁴ With ongoing advancements in material science and tissue engineering, the electroconductive nanofibers hold great potential for clinical translation and ameliorating patient outcomes in bone regeneration therapies.

5.2. Cartilage tissue engineering and regeneration applications of smart nanomaterials

Cartilage-targeting nanoplateforms have been extensively researched and developed, showing great promise in overcoming the dense type II collagen barriers in cartilage and serving as effective drug carriers. These nanoplateforms utilize various

materials and strategies to enhance their targeting, penetration, and therapeutic efficacy within the challenging environment of cartilage tissue.

Bajpayee *et al.*²¹⁵ demonstrated a novel approach for intra-articular (IA) treatment of osteoarthritis (OA) employing DEX-loaded avidin nanoplateform. The approach leveraged the small size and positive charge characteristics of avidin to achieve rapid and effective penetration into cartilage tissue. The positive charge of avidin improved its retention within the cartilage, ensuring sustained release of DEX and prolonged anti-inflammatory effects. Hu *et al.*²¹⁶ developed an advanced cartilage-targeting drug, termed CAP-PEG-PAMAM, employing a partly PEGylated polyamidoamine (PAMAM) dendrimer, for efficacious delivery of drugs to articular cartilage, addressing several challenges associated with cartilage-targeting drug delivery. The chondrocyte-affinity peptide (CAP) peptide specifically binds to chondrocytes, enhancing the targeting and uptake of the nanocarrier in cartilage tissue. The study revealed efficient delivery and rapid penetration of nanocarrier into the deep zones of cartilage, ensuring that therapeutic agents reach their target cells effectively.

Recently, Xue *et al.*²¹⁷ reported a twofold drug delivery system using MOF-furnished mesoporous polydopamine (MPDA) structure. The development of the system involved loading rapamycin (Rap) and bilirubin (Br) into the mesopores and shell of MOF, respectively. To target collagen II in cartilage, they conjugated a collagen II-directing peptide (WYRGRL) onto the nanocarrier, resulting in the RB@MPMW nanoplateform (Fig. 25 A). The results displayed back-to-back release of Br and Rap from the nanoplateform in presence of NIR light. Br's rapid release from the MOF shell showed outstanding ROS scavenging potency and anti-apoptotic effects, albeit reducing autophagy activity to some extent. The presence of NIR light caused the quick release



of Rap from the MOF based nanosystem and elevated activation of autophagy and protection of chondrocyte (Fig. 25 B).

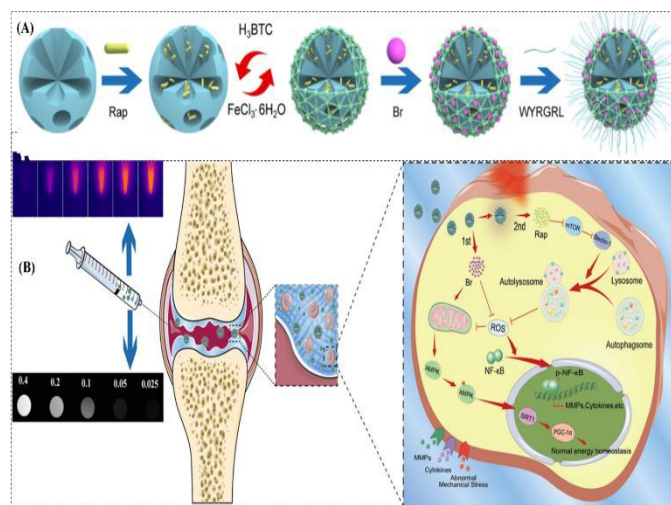


Fig. 25. Schematic illustration of (A) Fabrication of RB@MPMW nanoplateform; (B) Cartilage-targeting dual drug delivery mechanism as well as NIR laser response of the nanoplateform in osteoarthritis therapy. Reprinted with permission from ref. 217. Copyright 2021, Elsevier.

5.3. Tissue engineering and regeneration applications of smart nanomaterials-based 3D bioprinting

3D bioprinting has emerged as the utmost additive biomanufacturing technology, revolutionizing the fields of TER medicine. This advanced technology, boosted with outstanding bioinks and sophisticated bioprinters, enables the construction of functional tissues and organs, potentially eliminating the need for artificial organs. Moreover, integration of NMs into bioink platforms represents a significant advancement in this technology. Various research groups recently explored how NMs can enhance the properties and functionalities of bioinks, making them more suitable for creating complex tissue structures and promoting tissue regeneration.^{218,219} Recently, Rizwana *et al.*²¹⁹ made a notable stride in regenerative medicines by developing NMs-based multimodal bioink designed for the treatment of peripheral nerve injuries. This innovative bioink serves dual purposes: it acts as a carrier for cells and functions as a free radical scavenger (Fig. 26 A). The

bioink formulation consists of PVA and cerium oxide NPs (NC), employing a novel dual crosslinking method with citric acid and NaOH.

Digital light processing (DLP) printing technology has emerged as a significant tool in BTE, allowing fabrication of complex and highly precise polymeric scaffolds. It offers significant benefits in terms of material handling, cell viability, structural complexity, printing speed, and resolution, making it a powerful technique for fabricating complex tissue engineering scaffolds. Recently, Kumari *et al.*²²⁰ combined methacrylate-k-carrageenan (MA@k@CA) with bioactive SNPs (BSNPs) using DLP printing, achieving high precision and resolution in creating complex bone structures (Fig. 26 B-E). The incorporated BSNPs improved osteogenic properties (i.e., mechanical strength, viscosity, rheological properties, etc.) of hydrogel, promoting bone growth and regeneration. *In vitro* study was executed with pre-osteoblast loaded scaffolds of MA@k@CA-BSNP and results manifested fostering of cell proliferation, mass transfer, and osteogenesis by the DLP-fabricated porous structures, showing bone ingrowth. *In vivo* study of the hydrogel scaffold was conducted on Wistar rats and results manifested slow degradation of the MA@k@CA@BSNP hydrogels and good biocompatibility (no inflammation on subcutaneous tissue, kidney, liver, spleen, and heart tissues) over the study period.

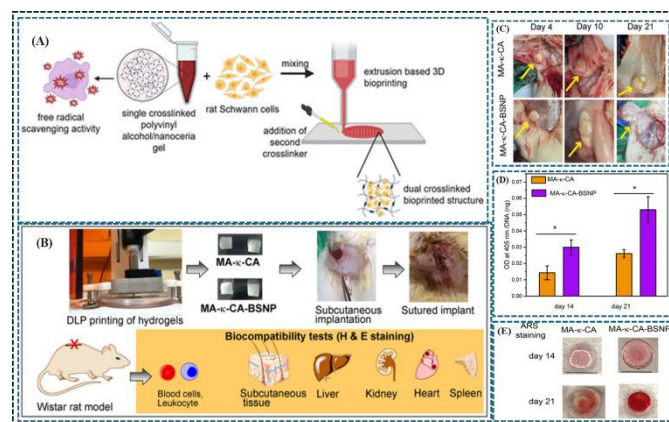


Fig. 26. Schematic representation of (A) Cerium oxide nanoparticles (nanoceria) based multimodal bioink serving as both a cell carrier as well as a free radical scavenger; (B) DLP printing of hydrogels; (C) Subcutaneous implantation; (D) Biocompatibility tests (H & E staining); (E) Wistar rat model.



well as free radical scavengers for the treatment of peripheral nerve injury. Reprinted with permission from ref. 219. Copyright 2023, American Chemical Society; (B) Schematics of *in vivo* biocompatibility of DLP-printed MA@k@CA@BSNP, and MA@k@CA hydrogels after subcutaneous implantation inside laboratory Wistar rats. No symptoms of skin inflammation, illness/mortality, and adverse effects on liver kidney, spleen, and heart were observed; (C) Digital images showing subcutaneously implanted MA@k@CA@BSNP, and MA@k@CA hydrogels on days 4, 10, and 21; (D) Assessment of osteogenic differentiation in DLP-printed-osteoblast-laden MA-k@CA@BSNP, and MA@k@CA hydrogels employing the alkaline phosphatase (ALP) activity assay. The assessment showed remarkable enhancement in ALP activity by the MA@k@CA@BSNP composite hydrogels compared to native MA-k-CA hydrogels; (E) Digital images demonstrating deposition of calcium in the Alizarin Red S stained MA@k@CA@BSNP composite hydrogels (deep brick orange-red colour) than native MA@k@CA hydrogels on days 14 and 21. Reprinted with permission from ref. 220. Copyright 2024, Royal Society of Chemistry.

5.4. Tissue engineering and regeneration applications of smart nanomaterials-based hybrid bioinks

NMs-based hybrid bioinks furnish a propitious approach to enhancing the performance of bioinks in 3D bioprinting. By exploiting the distinct properties of both natural and synthetic NMs, these hybrid bioinks provide improved biocompatibility, mechanical strength, and functionalization, making them highly suitable for advanced tissue engineering applications.

Zhang *et al.*²²¹ produced NMs-based bioink using GO/alginate/gelatine composite to construct 3D bone-mimicking scaffolds employing a 3D bioprinting technique. This bioink was laden with human mesenchymal stem cells (hMSCs). The findings reported that while higher GO concentrations (0.5GO, 1GO, and 2GO) generally improved the initial performance of bioinks, the 1GO concentration stroked the best balance, providing high scaffold fidelity, bioprintability, cell viability, mechanical strength, and osteogenic differentiation, making it the most promising concentration for BTE applications. The integration of graphene, CNTs, nanoclay, transition metal

dichalcogenides, polymeric NPs, magnetic and MOF NMs into polymeric hydrogels enhances their mechanical strength, biocompatibility, and functionality, providing advanced materials for 3D bioprinting and proliferating their applications in TER medicine.²²²⁻²²⁴

5.5. Soft tissue engineering and regeneration applications of smart nanomaterials

Smart NMs hold vast potential in soft tissue engineering and regeneration, offering innovative solutions for creating tissue scaffolds, enhancing cell growth, and delivering bioactive compounds precisely. These materials respond to distinct stimuli, balance with physiological conditions, and mimic natural tissue properties, which are all critical in soft tissue applications like skin, muscle, nerve, and cartilage regeneration.²²⁵

5.5.1. Muscle tissue engineering

The integration of various NMs and cells in the development of implantable 3D muscle tissue is a significant area of research in TER medicines. NMs based on CNTs, chitosan, fibrin, PEG, HA, collagen, alginate, decellularized extracellular matrix (dECM), hyaluronic acid (HA), Poly(oligo ethylene glycol) methacrylate/cellulose nanocrystal (POEGMA/CNC), Polycaprolactone (PCL), and keratin play an important role in the manufacture of implantable 3D muscle tissue.²²⁶ A variety of cells such as hMPCs (human muscle progenitor cells), HUVEC (human umbilical vein endothelial cells), and C2C12 (mouse myoblasts) are utilized in conjunction with the nanomaterials based bioinks.²²⁶

NM-infused bioinks present significant advancements in muscle tissue engineering by overcoming some of the key limitations of traditional bioinks. These limitations include challenges in balancing the printability of the bioink with crucial cellular requirements such as absorbability, adhesion, and support for cell growth and differentiation.²²⁷ Conventional bioinks often



struggle to achieve this balance, which can impede the effectiveness of tissue engineering efforts. The infusion of NMs into bioinks addresses these challenges by enhancing the mechanical properties and biocompatibility of the constructs. These nanomaterial-infused bioinks are particularly effective in crafting tissue constructs that closely mimic the natural muscle tissue.²²⁸ They offer improved cellular adhesion and absorption, better mechanical strength, and enhanced support to cell proliferation. This makes them highly suitable for engineering functional muscle tissues that can integrate well with the body's natural systems, thereby improving the potential for successful tissue regeneration and repair. Thus, the integration of NMs into bioinks for muscle TER improvements in various critical aspects, such as biocompatibility, cell viability, printability, and muscle regeneration. Researchers have observed that these bioinks, when combined with cells, not only support the creation of complex tissue structures but also promote the alignment of cells, which is essential for functional muscle tissue.^{226,228}

One of the most significant benefits of incorporating NMs into 3D bioprinted constructs is their ability to enhance myoblast cell differentiation, for instance C2C12 cells, into mature skeletal muscle cells.²²⁸ This process is typically challenging and often requires additional myogenic agents to achieve. However, with NM-infused bioinks, the differentiation occurs more naturally, eliminating the need for these extra agents and simplifying the tissue engineering process. One of the key innovations in 3D bioprinting for muscle tissue engineering is the incorporation of microchannel structures within the printed constructs. By optimizing the initial cell density and ensuring a more even distribution of nutrients, these microchannels help construct more conducive environment for tissue growth and maturation.²²⁹

5.5.2. Skin appendages and other tissue engineering/regeneration/vascularization

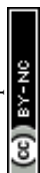
Skin appendages including sweat glands, hair follicles, and nails play crucial roles in sensation, thermoregulation, and skin homeostasis.^{230,231} Engineering or regenerating these structures along with their vascularization is an advanced field in regenerative medicine and tissue engineering. NMs based on CNTs, alginate, and gelatine have transformative potential in tissue engineering, especially for regenerating skin appendages and promoting vascularization, which are critical for the functionality and longevity of engineered tissues.²³² Combining gene therapy with skin appendage engineering to activate or repress certain pathways could yield more reliable appendage regeneration. Smart biomaterials that can dynamically respond to the needs of regenerating tissues (e.g., releasing growth factors in response to local cues) are being explored for skin and appendage regeneration.

The usage of NMs-based hybrid bioinks has opened exciting possibilities in the bioprinting and manufacturing of various tissues and organs inclusive of kidney, spleen, heart,²³³ liver,²³⁴ pancreas, porous tissues, and even 3D tumour models.²³⁵ for evaluating the efficacy of NMs. Nanocomposite and nanocolloidal hydrogels represent an exciting approach to recreating ECM-like environments due to their customizable properties, including tunable mechanical properties, nanoscale features, bioactive cues, fibre alignment, porosity, and surface roughness.²³⁶

6. Nanotoxicity assessment

Nanotoxicity assessment is a complex and evolving field that is indispensable for confirming the safety and application of NMs.²³⁷⁻²⁴² By combining advanced experimental techniques, computational models,²⁴³⁻²⁴⁵ and regulatory frameworks, researchers can better understand and mitigate the potential risks associated with NMs, ultimately leading to safer and more sustainable technologies.

6.1. *In vitro* toxicity assessment



Advances in personalized medicine and related technologies are further fuelling the demand for *in vitro* toxicology testing, as these methods can provide more relevant and specific insights into how NMs and other substances can affect the human cells.²⁴⁶ The market based on *in vitro* toxicity testing is expected to grow to USD 17.1 billion up to 2028, manifesting a total annual growth rate of 9.5% from 2023-2028.²⁴⁷ Guidelines for evaluating *in-vitro* nanotoxicity proposed by ISO/TC 229, ASTM, and OECD have been recapitulated in Table 6. *In vitro* assays employing divergent cell line models of various organs are widely used to assess the potency and toxicity of NPs. These cell lines are typically chosen based on the organs where NPs are most likely to accumulate such as lungs, kidney, brain, etc.^{248,249}

Giudice *et al.*²⁵⁰ reported the usage of immortalized cell lines to examine the effects of metal nanoparticles (MNPs) on the immune system. A549 cells were employed to assess how exposure to silica nanoparticles (SiNPs) triggers innate immune responses, including the production of inflammatory cytokines (Fig. 27 A). They provided valuable insights into how different metal nanoparticles can influence immune system functions. This is critical for assessing the safety and potential health impacts of nanoparticles, guiding their safe use in medical and industrial applications.

Clift and colleagues²⁵¹ studied the interactions between AuNPs and B lymphocytes. They treated human B lymphocytes with AuNPs of divergent shape and surface properties (Fig. 27 B). The coated AuNPs had minimal interaction with B lymphocytes compared to uncoated ones. Importantly, even at a high concentration of 20 µg/mL over 24 hours, none of the AuNPs affected cell viability. Furthermore, the coated nanospheres did not impact on the expression of activation markers or cause an increase in pro-inflammatory cytokine secretion by naive B lymphocytes. However, uncoated nanospheres and rod-shaped

AuNPs led to decreased IL-6 cytokine generation by activated B lymphocytes, indicating a functional impairment.

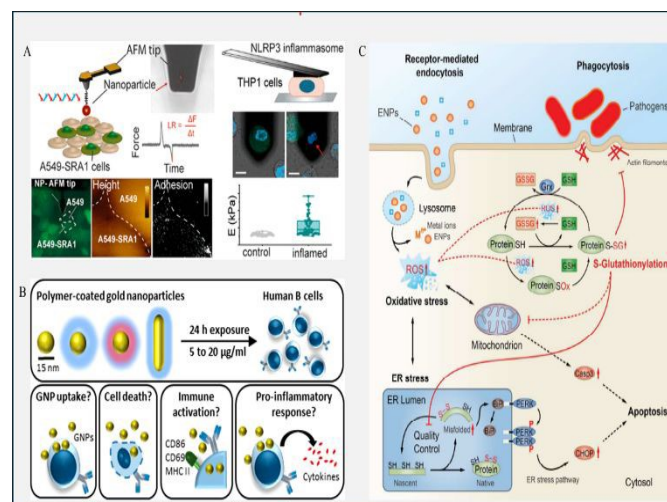


Fig. 27. Schematic illustration of the feasible applicability of immortalized cell lines to examine the effect of MNPs on the immune system. (A) Schematic representation of the interaction of SiNPs with SRA1 (scavenger receptor A1) on A549 cells and their subsequent effects on inflammasome activation, helping to elucidate the immune responses triggered by nanoparticle exposure. Reprinted with permission from ref. 250. Copyright 2022, American Chemical Society. (B) Schematic representation of how AuNPs with different surface coatings (PVA/PEG) and shapes (rods and spheres) affect B lymphocyte immune function. Polymer coated AuNPs interacted poorly with B lymphocytes compared to uncoated AuNPs. Reprinted with permission from ref. 251. Copyright 2019, American Chemical Society. (C) Illustration of participation of the suggested pathways and organelles in the initiation of oxidative stress or S-glutathionylation of proteins. It also highlights the potential influence on phagosome function, endoplasmic reticulum (ER) stress, and cell survival engendered by ENPs (engineered nanoparticles). Reprinted with permission from ref. 252. Copyright 2016, American Chemical Society.

Duan *et al.*²⁵² advanced the understanding of how ENPs (Engineered nanoparticles) affect macrophage functions through oxidative stress and SSG (S-glutathionylation protein) modifications (Fig. 27 C), offering valuable information for the development of safer NMs. Their study provided insights into protein signatures and pathways that serve as ROS sensors, facilitating cellular adaptation to ENPs, and identifying targets of ENP-induced oxidative stress that led to irreversible cell damage. Understanding these mechanisms can aid in designing safer ENPs that minimize adverse effects



on immune functions, which is crucial for their biomedical applications.

View Article Online
DOI: 10.1039/D5PM00137D

In vitro platforms play a decisive role in various aspects of biomedical research, including drug discovery and toxicity testing. However, despite their importance, these platforms have significant limitations, particularly in the assessment of pharmacokinetic (PK) and toxicokinetic (TK) parameters. The dynamic and complex nature of these processes in a whole organism cannot be fully replicated *in vitro*, which often leads to an incomplete understanding of a compound's behaviour in the body.

Table 6 Summary of *in vitro* toxicity of NMs

| Mode of Toxicity Assessment | Objective | Method/s | Remarks | Standard ID | Pros | Cons | Ref. |
|-----------------------------|------------------------------------------------------------------------------------------|----------------------------------------|----------------------------------------------------------------------------------------------------------------------------------------------------------------|--------------------|------------------------------------------------------------|--------------------------------------------------------------------------------------------|---------|
| Cytotoxicity | Study of metabolic Activity | MTT assay | Assessment of cytotoxicity of NPs employing human hepatocarcinoma cells and porcine kidney | ASTM E2526-08(201) | Simple and rapid | Insufficient sensitivity to detect number of viable cells and interference of dye with NPs | 253-255 |
| Cytotoxicity | | 3D cells | Assessing toxicity of NPs with the possibility of allocating high-throughput screening analysis | ISO/AWI TS 22455 | | | 256 |
| Cytotoxicity | To examine the toxicity of NMs and determine possible risks associated with human health | LDH and MTS assay | Measurement of the cytotoxicity of NPs | ISO 19007:2018 | Widely employed for characterizing NMs for medical devices | No detailed testing protocols | 254,256 |
| Cell uptake | To quantify absolute particle number or/ and surface per cell | Transmission electron microscopy (TEM) | To examine the uptake and intracellular outcome of NPs. Imparts signal of electron dense NPs and biological situation within one channel, which needs analysis | Nature Protocol | NPs tracking without linking to a probe. | Observer effects can significantly impact the accuracy of the interpretation. | 257,258 |



ARTICLE

Journal Name

| | | | | | | | |
|------------------------|----------------------------------------------------------------------------------------|--------------------------------------------------------------------------------------|--------------------------------------------------------------------------------------------------------------------------------------------------------------------------------------------------|----------------------|---------------------------------------------------------------------------------------------------------------------------------------------------------|------------------------------------------------------------------------------------------------------------------------------------------------------------------------------------------------------------------------------------|---------|
| | | | before quantification | | | View Article Online DOI: 10.1039/D5PM00137D | |
| Cell uptake | Quantification of NPs uptake | Flow cytometry | Quality Nano SOP | | Fluorescent NPs uptake measurement in individual cells and produce high quality content data with ease | To ensure accurate measurements and avoid interference from residual free or labile dye, careful characterization, and stability assessment of the starting dispersion of carbon nanomaterials in cell culture media is essential. | 259 |
| Cell uptake | Quick detection and characterization of the NPs internalized and trafficked organelles | | Production of quantitative data on NPs intracellular distribution, colocalization, and trafficking kinetics, employing a combination of advanced microscopy techniques and image analysis tools. | | Provide fast, high-throughput, and quantitative space- and time-resolved information on NPs numbers and their distribution across different organelles. | Imaging methods can be employed for more detailed information on intracellular outcomes | 260 |
| Hemolysis | To evaluate biocompatibility and hemolytic response/properties | <i>In vitro</i> blood biocompatibility Test | To assess NPs hemolysis Rate. | ASTM E25 24-08(201) | Simple | Limited to RBCs | 253 |
| Chemoattractant | To measure the chemoattractant capacity. | | <i>In vitro</i> measurement of chemoattractant capacity of NPs | ASTM WK60373 | | | 253,256 |
| Immunological response | To observe the host's immune reaction | Colony assay | To evaluate if NPs initiate the formation of mouse granulocyte-macrophage colonies. | ASTM E25 25-08(2013) | | Counting colonies that grow close together can indeed be challenging. | 253,256 |
| Endotoxin | Contamination by endotoxin | Limulus amoebocyte lysate test | For <i>in vitro</i> systems, Endotoxin test on NMs samples | EN ISO 29701:2010 | Applied to NMs studied for <i>in vitro</i> tests | | 256 |
| Oxidative stress | Removal of antioxidant capacity | Nanotechnologies -5- (and 6)-chloromethyl-2',7'-dichlorodihydrofluorescein diacetate | To evaluate if NPs induce ROS generation employing RAW 264.7 macrophage cell line | ISO/TS 19006:2016 | | | 254,256 |



As a result, *in-vivo* models, which appertain to utilization of live animals, remain the gold standard for laboratory examination to deduct toxicities.^{261,262} and other critical pharmacological properties. *In vivo* testing provides a comprehensive view of how a substance interacts with various biological systems, offering invaluable insights that are not possible to obtain through *in-vitro* methods alone.²⁶³ However, the use of *in-vivo* models raises ethical concerns and is subject to stringent regulatory and ethical guidelines.

6.2. *In vivo* toxicity assessment

The *in-vivo* toxicology market, which involves studying the effects of chemicals on living organisms, is projected to grow from USD 5.0 billion in 2020 to USD 6.6 billion by 2025.²⁶⁴ This represents a CAGR of 5.5% over the forecast period. The *in vivo* toxicology market is expected to experience steady growth, slightly slower than the rapid advancements and adoption seen in the *in vitro* market. This reflects a balanced approach in the industry, leveraging the strengths of both methodologies.

The selection of appropriate animal models for toxicological assessment is critical for obtaining relevant and reliable data. While no single model perfectly replicates human biology, a combination of traditional animal models, emerging technologies, and alternative methods can provide comprehensive insights into toxicological effects. Careful consideration of the study objectives, ethical implications, and the specific advantages and limitations of each model is essential for effective toxicological research.²⁶⁵

Nonmammalian models like *Caenorhabditis elegans* (*C. elegans*, a nematode) and *Drosophila melanogaster* (*D. melanogaster*, a fruit fly) are valuable tools in the field of nanotoxicology. They

provide important preliminary data on the safety and potential biological impacts of NMs, helping to identify hazards before advancing to more complex mammalian models. Their ability to reveal toxicity related to both the active components and the structural materials of nanocarriers is particularly beneficial in the development of safer nanomedicines. *In vivo* studies based on *C. elegans* revealed that polymeric NPs and unloaded solid lipid NPs exhibit higher toxicity, manifesting as increased mortality rates, reduced reproduction rates, and delayed development compared to tripolyphosphate/chitosan carriers.^{266,267} *D. melanogaster* is a validated model for monitoring genotoxicity endpoints and has been utilized to test the safety of polymeric and solid lipid-based nanocarriers. For example, a study based on *D. melanogaster* demonstrated that near-lethal doses of PLA NPs trigger oxidative stress as well as cell cycle arrest at G1.²⁶⁸ Additionally, aquatic models like *Danio rerio* (zebrafish), *Artemia salina*, and *Daphnia magna* have proven highly valuable for assessing the safety of polymeric NMs.²⁶⁹⁻²⁷¹ These alternate *in vivo* models serve as excellent tools for screening initial toxicity or as complementary steps. However, it's important to note that each nonmammalian model has its limitations compared to more complex models like rodents.



Table 7 Summary of *in vivo* toxicity of nanomaterials

| NPs | Type of NPs | Animal Model | Age (Weeks) | Gender | Remarks | Ref. |
|----------------------------------------------------------------------------------------|------------------|--------------------------------------------|-------------|--------|-----------------------------------------------------------------------------------------------------------------------------------------------------|------|
| AgNPs | Inorganic | Balb/c mice | 6-8 | Female | Caused toxicity based on cell-/organ-type-, particle-type- and dose-dependent manner. | 272 |
| AgNPs | Inorganic | Zebrafish (<i>Danio rerio</i>) | | | Caused toxicity based on size and concentration of AgNPs | 273 |
| Silica nanoparticles (SiNPs) | Inorganic | C57BL/6 mice | 6-8 | Female | SiNPs cause acute reproductive toxicity. | 274 |
| Bioinspired Ag and Se NPs | Inorganic | Swiss albino mice | Adult | Female | The bioinspired synthesized NPs did not cause a remarkable toxic effect at a higher therapeutic effect. | 275 |
| Ultrasmall superparamagnetic iron oxide nanoparticles (USPIONS) with/without ibuprofen | Inorganic | Balb/c mice | | Male | No systemic toxicity but unexpected anti-inflammatory effect of ibuprofen carrying USPIONS. | 276 |
| Zirconia nanoparticles (ZrO ₂ NPs) | Inorganic | Wistar rats | Adult | Male | The ZrO ₂ NPs caused hepatotoxicity. | 277 |
| Titanium dioxide nanoparticles (TiO ₂ NPs) with/without eugenol | Inorganic | Wistar rats | Adult | Male | TiO ₂ NPs cause oxidative damage to the kidney and liver. However, co-administration of NPs with eugenol mitigates the induced toxicity. | 278 |
| Poly(thioether-ester) (PTEe) nanoparticles | Polymeric | Swiss mice | | Male | No acute toxicity was caused. | 279 |
| β -cyclodextrin chitosan with/without epalrestat (EPL) | Polymeric | Albino rabbits | | | Caused acute oral toxicity. | 280 |
| Supramolecular polyamine phosphate nanoparticles (PANs) with/without PEG | Polymeric | BALB/cjrj | 10 | Female | Reduction in toxicity of PANs was observed due to pegylation. pegylation alter charge of PANs and increase their circulation half-time. | 281 |
| Silk nanoparticles | Polymeric | Mice | | | Systemic administration of silk nanosphere caused no toxicity. | 282 |
| Cyclodextrins (CDs) with/without docetaxel | Polymeric | Healthy rabbits | | Male | No toxic effects were reported on the major organs of the rabbits. | 283 |
| Polylactic acid-polyethylene glycol (PLAPEG) with/without encapsulated biosurfactant | Polymeric | Balb/c mice | 4-6 | Female | Biosurfactants loaded in PLA-PEG copolymeric NPs were observed nontoxic. | 284 |
| Chitosan-coated NPs | lignin Polymeric | Embryonic zebrafish (<i>Danio rerio</i>) | | | Compared to plain lignin NPs, engineered Ch-LNP formulations were observed to be more | 285 |



| | | | | | | | |
|-----------------------------------------------------------------------------|--------------------------|----------------------------------|-------|------|-------------------------------------------------------------------------------------------------------------------------------------------------------------------------------------------------------------------------------------------------------------------------------------------------------------------------------------------------------------------------------------------------------------------------------------------------------------------|--------------------------------|---------------------|
| Polyacrylic acid-coated cobalt ferrite core-shell magnetic NPs (PAA@CF-NPs) | | Sprague–Dawley rat | Adult | Male | toxic at higher concentrations. Injected PAA@CF-NPs appeared to be renal/hepatic biocompatible. Although, more examinations are required to evaluate their biodistribution, homeostatic conditions, and chronic toxicity. Small inflammatory changes were observed in normal parenchyma tissues of the spleen, kidney, and liver, while no acute damage was observed. PEG modified NPs exhibited better biocompatibility compared to bare and citrate-coated NPs. | DOI: 10.1039/D5PM00137D 286 | View Article Online |
| IONPs/haematite nanoparticles with/without PEG or citrate | Inorganic- and Polymeric | Albino rats | | | | 287 | |
| GONPs | Carbon-based | Nematodes-Caenorhabditis elegans | - | - | Long exposure to low doses of GONPs may cause issues in locomotion and reproduction as well as induction of oxidative stress. | 288 | |

Mice are widely employed in preclinical as well as nanotoxicity examinations since their genomes closely resemble the human genome. *In vivo* evaluation in these models typically involves examining apoptosis and inflammation in primary target organs such as the spleen, lung, kidney, heart, and brain, as well as other systems that may accumulate NPs. For example, Kupffer and hepatic sinusoids cells are crucial for liver functions in metabolism and detoxification, where NPs tend to concentrate. Relevant assessment models for drug nanocarriers should mimic the exposure route (injection, ingestion, inhalation, and transdermal delivery) and the intended applications to ensure accurate safety and efficacy evaluations.²⁶⁵

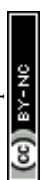
Different studies based on *in vivo* toxicity assessment of NMs have been incorporated in Table 7. Many of the incorporated studies have focused on

the assessment of the toxicity of the NPs with the purpose of employing them as future nanomedicine for cancer²⁸⁹ and other infections.^{290,291} Polymer coated nanoparticles reduced the associated toxicities and enhanced their systemic circulation time.^{258,259} The usage of nonmammalian models like *Daphnia magna*, *Danio rerio*, *Drosophila*, and *Caenorhabditis elegans* (a type of roundworm imparted insights into the effects of NPs on various aspects, including health, environmental impact, reproductive systems, and behavioural changes.^{273,285,288,292,293} Hence, providing valuable information about the potential risks associated with NPs exposure without using mammalian subjects.

6.3. *In silico* toxicity assessment

Nanoinformatics, a burgeoning field at the intersection of nanotechnology and informatics, employs various computational and predictive

Open Access Article. Published on 20 August 2025. Downloaded on 8/26/2025 5:13:41 PM.
This article is licensed under a Creative Commons Attribution-NonCommercial 3.0 Unported Licence.



RSC Pharmaceuticals Accepted Manuscript

modelling approaches to enhance the understanding and assessment of NMs' safety.^{294,295} The study aims to predict NMs properties, interaction of NMs with cells and biomolecules, transformation of NMs by divergent stimulus or biotransformation, and toxicity of byproducts of the transformed NMs as compared to their original forms.²⁹⁶ Various computational models and tools²⁹⁷ used to predict the toxicity of NMs used in biomedical/biological/environmental applications have been presented in Fig. 28.

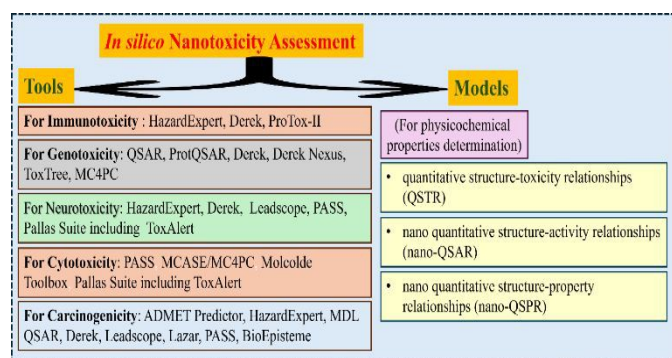


Fig. 28. Different computational models and tools used for nano/toxicological study.

The establishment of predictive models for the potential adverse effects of NPs relies on the encoding of their physicochemical properties as mathematical entities called descriptors²⁹⁸. These descriptors capture size, chemical composition, shape, and surface charge of the NPs. Artificial intelligence (AI), machine learning (ML), and deep learning (DL) methods play a critical role in generating predictive models based on these descriptors²⁹⁹. ML methods can significantly reduce the time and labour required for material testing by automating the analysis process. These methods enable the handling of large datasets and the screening of numerous materials simultaneously, facilitating the rapid identification of promising candidates. By analysing large volumes of data, AI and ML can uncover patterns and relationships that inform the design of new NMs with desired properties.³⁰⁰⁻³⁰² Singh *et al.*³⁰³ utilized a machine learning based approach to study how various

physicochemical descriptors (like zeta-potential, size, shape, concentration, polydispersity, and diffusion coefficients) of NMs influence their interactions with cell membranes and intracellular uptake at sublethal concentrations. Specifically, their ML algorithm identified the cell shape index and nuclear area as critical descriptors associated with alterations induced by NMs in the Madin-Darby canine kidney (MDCK) epithelial cell line model. This finding suggests that NMs capable of inducing changes in cell and nuclear shape at subtoxic levels may trigger epigenetic modifications that control epithelial to mesenchymal transition processes.

Quantitative structure-activity relationship (QSAR) and quantitative structure-toxicity relationship (QSTR) approaches have increasingly been recognized as valuable tools for safety and risk assessment in various fields, including nanotechnology.^{304,305} Some guidelines have been proposed to navigate the regulatory challenges associated with the development and application of QSAR/QSTR models.³⁰⁶ Modern 3D QSAR (3D-QSAR) and molecular docking techniques are particularly useful for predicting molecular characteristics as well as biological interactions in pharmaceuticals.³⁰⁷ Nonetheless, these 3D-QSAR and traditional molecular descriptors often fall short in capturing the unique properties of NPs. To address the specificity of NMs, quantitative structure nanotoxicity relationship (QNAR) models, also known as nano-QSAR models, have been developed.²⁹⁹ These models are designed to account for the unique descriptive properties of NMs, providing a more accurate prediction of their behaviour and interactions in biological and environmental systems.^{308,309} The NanoTox platform, developed under the GNU General Public License (<https://github.com/NanoTox>), is an open-source and freely available tool that provides access to nanotoxicology reports and offers a definite feature space for modelling NMs toxicity.³⁰² This



feature space incorporates both external and internal physicochemical properties of NMs, periodic table properties, and correlates these with cell type, cell line, and assay methods.

AuNPs have been considerably examined owing to their distinct characteristics and potent applicability in divergent fields inclusive of electronics, medicine, and biological sustainability.³¹⁰ However, understanding their potential toxic effects is crucial for their safe use. *In silico* profiling has been conducted on various AuNPs, leading to the design of geometrical nanodescriptors. These descriptors are essential for quantitative modelling and virtual screening of AuNPs. Quantitative nanostructure-activity relationship (QNAR) modelling has demonstrated high predictability for certain physicochemical characteristics, particularly hydrophobicity (log P) and zeta-potential. The QNAR models also show strong predictive power for simple biological activities, such as the uptake of AuNPs by human kidney epithelial cells (HEK293 cells) and lung cells (A549 cells). However, the accuracy of these models decreases for more complex bioactivities. For instance, moderate accuracy was observed for predicting the binding of AuNPs to the acetylcholinesterase enzyme and the induction of ROS in HEK293 cells.³¹¹ This indicates that while the models are useful for certain applications, they may need further refinement for more complex biological interactions. ROS (the byproducts of cellular oxidative metabolism, primarily produced by the mitochondria) generation is a critical endpoint in nanotoxicity assessments. Elevated levels of ROS disrupt cellular functions, damage proteins, nucleic acids, and lipids, and ultimately lead to apoptosis or necrosis.³¹² This underlines the importance of monitoring ROS production when assessing the toxicity of NPs, including metal and carbon-based NPs, as excessive ROS generation can have severe biological consequences.

CNTs, particularly single-walled CNTs (SWCNTs), are widely utilized in biomedical applications but are also known to pose some hazardous effects.³¹³ One of the notable toxic effects of SWCNTs is their ability to induce mitochondrial nanotoxicity, leading to bioenergetic dysfunction. Interestingly, this property can be exploited as a potential mechanism for cancer treatment, where disrupting cancer cell bioenergetics could be beneficial. Nanoinformatic tools that utilize quantitative structure-binding relationship (QSBR) models are being developed to better understand and predict the mitotropic behaviour of SWCNTs. These models use optimal structural nanodescriptors to predict how SWCNTs interact with mitochondria. By accurately modelling these interactions, QSBR models can help assess the risk or benefit relationships of SWCNTs in various applications, including their potential use in targeted cancer therapies.³¹⁴ This approach aims to balance the beneficial effects of SWCNTs in medical treatments with their potential risks, ensuring safer and more effective use of these NMs.

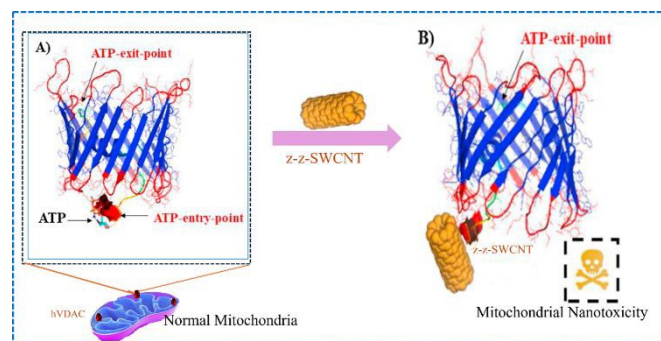


Fig. 29. Computational modelling showing mitochondrial channel nanotoxicity by the zigzag-SWCNT NMs; (A) Strong affinity of ATP molecules for the ATP-entry-points; (B) The z-z-SWCNT selectively weak/block the ATP-entry-point in the hVDAC1, potentially disrupting mitochondrial function by inhibiting ATP transport. Reprinted with permission from ref. 315. Copyright 2020, Elsevier.

González-Durruthy *et al.*³¹⁵ reported a significant advancement in the assessment of nanotoxicity and therapeutic potential of CNT-based NMs. They employed molecular docking and molecular dynamic (MD) simulations to investigate the interactions between SWCNTs and mitochondrial



channels, specifically focusing on the human mitochondrial voltage-dependent anion-selective channel (hVDAC1). The simulations demonstrated that zigzag-SWCNTs could selectively block the ATP-entry-point in hVDAC1 (Fig. 29), potentially disrupting mitochondrial function by inhibiting ATP transport. These findings validated the usage of *in-silico* strategies, such as molecular docking and MD simulations, to predict the interactions and potential toxic effects of NMs on cellular components.

MoS₂ NMs have gained attention for their capability in biological applications owing to their properties like carbon-based NMs. They are promising candidates for drug release applications toward microorganisms suitable for cancer theranostics. However, their applications are not without concerns. The findings from MD simulations and electrophysiology experiments have highlighted a potential concern regarding the interaction of MoS₂ nanoflakes with the voltage sensor domain of potassium channels.³¹⁶ This interaction could interfere with the proper functioning of these channels, which are critical for the electrical activity of cells, including nerve and muscle cells.

6.4. Mechanism of toxicity of nanomaterials

The mechanism of toxicity of nanomaterials in biomedical applications is complex and depends on various physicochemical properties such as size, surface charge, shape, composition, and surface functionalization.^{317,318} Understanding these mechanisms is critical to mitigate adverse biological effects and ensure safe clinical translation. The evaluation of mechanism of toxicity of nanomaterials in biological system involves different steps (Figure 30) as follows.

- (I) *Cellular uptake and bioavailability*: due to their small size nanomaterials enter cells directly by membrane penetration or indirectly via endocytosis (clathrin/caveolae-mediated, macropinocytosis, phagocytosis, etc.) (Figure 1₁). After cellular uptake, they

accumulate in organelles (e.g., mitochondria, lysosomes, etc.), interfere with cellular homeostasis, and trigger stress signalling pathways.³¹⁷

- (II) *Oxidative stress and ROS generation*: many nanomaterials (e.g., metal oxides like TiO₂, ZnO, etc.) catalyze the formation of ROS (Figure 30 IV₁, IV₂), leading to DNA damage, lipid peroxidation, protein denaturation/aggregation, and apoptosis/necrosis.³¹⁸
- (III) *Inflammatory Responses*: sometimes nanomaterials activate innate immune receptors like toll-like receptors (TLRs) and NOD-like receptor protein 3 (NLRP3) inflammasome (Figure 30 III₁), resulting in release of pro-inflammatory cytokines (e.g., IL-6, TNF- α , IL-1 β), recruitment of immune cells, and chronic inflammation/tissue damage.³¹⁹
- (IV) *Genotoxicity and DNA damage*: genotoxicity occurs via direct interaction of nanomaterials with DNA (e.g., intercalation, strand breaks, etc.), indirect damage through ROS, chromosomal aberrations and micronucleus formation (Figure 30 I₂). It leads to mutagenesis and carcinogenesis.³²⁰
- (V) *Protein corona formation*: when nanomaterials enter biological fluids, proteins adsorb to their surface and form "protein corona", that alters surface identity, cellular uptake profile, and immune recognition (Figure 30 III₂). This may lead to unexpected toxicity and immune activation.³²¹
- (VI) *Lysosomal dysfunction*: nanomaterials can accumulate in lysosomes (Figure 30 I₁), causing lysosomal membrane permeabilization, and release of cathepsins leading to cell death.³²²
- (VII) *Disruption of mitochondrial function*: nanomaterials damage mitochondrial functions (30 IV₁, IV₂) like impaired mitochondrial membrane potential, ATP



depletion, release of pro-apoptotic factors, and enhanced ROS generation.³²³

- (VIII) *Autophagy dysregulation*: nanomaterials can both induce and inhibit autophagy (Figure 30 III₁). Disruption of autophagy can exacerbate inflammation and neurotoxicity.³²⁴
- (IX) *Epigenetic alterations*: some nanomaterials have been shown to alter DNA methylation, histone modifications, and miRNA expressions (Figure 30 II₁, II₂). These changes can have long-term effects on gene expression and cell behaviour.³²⁵

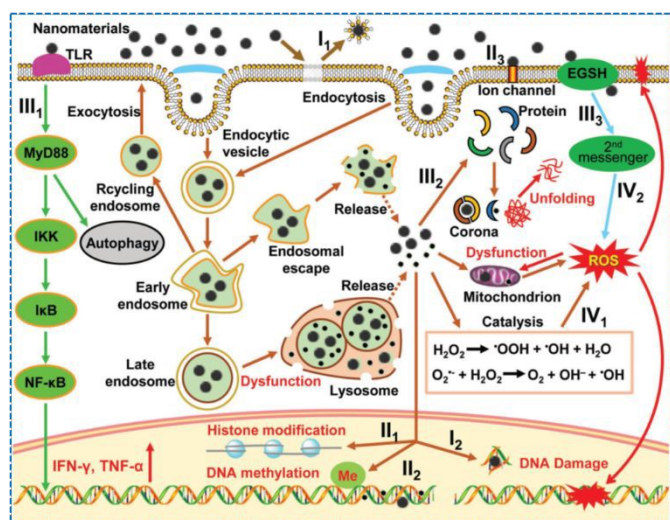


Fig 30. Different pathways for potential mechanisms of toxicity of nanomaterials in biological system. (I₁) Show direct physical destruction of biomembrane. (I₂) Show direct destruction of DNA. (II₁, II₂) show epigenetic effects induced by nanomaterials. (II₃) show nanomaterials induced blockage of ion channels. (III₁) Show interaction between nanomaterials and biomolecules leads to activation of inflammasome responses (e.g., TLRs) and autophagy. (III₂, III₃) Show interaction of nanomaterials with proteins leads to formation of corona that alters their functionality, cellular uptake immune responses. (IV₁) Direct generation of ROS from catalytic reactions. (IV₂) Show indirect production of ROS by the activation of ROS-related signaling pathways. Reprinted with permission from the ref.23. Copyright 2019, WILEY-VCH Verlag GmbH & Co. KGaA, Weinheim.

7. Clinical trials of smart nanomaterials

Clinical trials involving smart nanomaterials are advancing in various medical or biological fields, including diagnostic imaging, targeted drug delivery, and cancer therapy. These materials are

designed to respond to specific biological signals and/or environmental conditions, inclusive of temperature, magnetic fields, and pH, allowing for precise control over therapeutic actions. Smart nanomaterials like liposomes, dendrimers, and polymer-based NPs are being employed to encapsulate drugs and release them at targeted sites, minimizing side effects. These trials often focus on cancer treatments where drugs need to be released to tumour cells while sparing healthy cells.

Liposomes, as pioneering drug delivery systems, have remained prevalent due to their unique advantages. They offer flexibility in composition, are biocompatible, biodegradable, and have low immunogenicity.^{326,327} Structurally, liposomes are artificially constructed phospholipid vesicles that can be single or/and multilamellar and are typically between 50-100 nm in size. They contain a central aqueous core where hydrophilic drugs can be encapsulated, although hydrophobic drugs may also be incorporated within the lipid bilayer or chemically attached to the liposome surface. The key distinction between liposomes and micelles, despite both being composed of phospholipids, lies in their structures and applications. While liposomes have an aqueous core suitable for hydrophilic drugs, micelles have a hydrophobic core, making them more suited for encapsulating hydrophobic drugs. Both systems are utilized to achieve targeted delivery, thus minimizing systemic toxicity.³²⁸ Traditional liposomes, known as the "first generation," showed limitations in circulation time due to rapid clearance by the mononuclear phagocyte system, leading to an accumulation mainly in organs like the spleen and liver rather than in tumour tissues. To overcome this, new lipid formulations and modifications were developed, such as sterically stabilized liposomes containing sphingomyelin and choline or pegylated liposomes. These modifications led to extended circulation time, reduced uptake by the reticuloendothelial system (RES), and allowed



passive targeting to tumour tissues through the EPR effect.³²⁹ DoxilTM, a PEGylated liposomal formulation was first approved by the FDA in 1995 (80).³³⁰ Like DoxilTM, CaelyxTM also uses PEGylation and was approved in 1996 by European Medicines Agency (EMA). MyocetTM is a non-PEGylated liposomal formulation and was approved in 2000 by the EMA. All medications (DoxilTM, CaelyxTM, and MyocetTM) represent significant milestones in the field of nanopharmaceuticals, especially in oncology treatment, due to their ability to improve the safety and efficacy of doxorubicin. By encapsulating doxorubicin within liposomal nanocarriers, these formulations reduce the cardiotoxicity linked with the free drug and improve its targeting capabilities.^{330,331} DoxilTM and CaelyxTM have versatile indications across several cancer types due to their modified release profile and reduced toxicity. Both CaelyxTM and DoxilTM are used to treat ovarian cancer, particularly in patients whose disease has progressed after platinum-based chemotherapy. These formulations are also indicated for treating Kaposi's sarcoma in patients with AIDS, providing an option that targets the tumours with minimized systemic toxicity. CaelyxTM and MyocetTM are approved for treating metastatic breast cancer, addressing the need for less cardiotoxic options in this patient population.³²⁹

MepactTM (Mifamurtide) medication is a liposomal formulation containing muramyl tripeptide phosphatidylethanolamine, an immunomodulator. It works by activating monocytes and macrophages to enhance the immune response in paediatric and young adult patients for the treatment of bone cancer.³³² MarqiboTM medication is a nanoparticle formulation containing vincristine encapsulated in cholesterol- and sphingomyelin-based liposomes. Vincristine itself is a potent antineoplastic drug with a multitude of activity, particularly effective against haematological cancers. However, traditional vincristine administration is associated with side

effects such as neurotoxicity and/or peripheral neuropathy, which occur in a dose-dependent manner.^{333,334}

Protein-based nanoparticles (PNPs) are also advantageous in drug release systems owing to their biocompatibility and biodegradability. Unlike many synthetic NPs, PNPs can be formulated without organic solvents or toxic chemicals.^{335,336} OncasparTM is a PEGylated form of the asparaginase enzyme, employed in treating acute lymphoblastic leukaemia (ALL) in both adults and children. This formulation functions by depleting the blood levels of asparagine, an amino acid vital for the growth and division of tumour cells. Since these cancer cells cannot produce their own asparagine, its reduction leads to their death. Healthy cells, however, are less impacted as they can synthesize asparagine independently. The PEG modification helps reduce hypersensitivity, which is a common side effect in non-PEGylated asparaginase formulations. Moreover, PEGylation increases the enzyme's stability and duration in the bloodstream, allowing for less frequent dosing.^{337,338}

AbraxaneTM and PazenirTM are albumin-bound forms of paclitaxel (Taxol), which were approved by the FDA in 2005 and by the EMA in 2008. Paclitaxel, a pioneering member of the taxane family, is widely employed in cancer chemotherapy for its cytotoxic effects. It works by stabilizing microtubules, arresting cells in the G2/M phase of the cell cycle, which prevents them from forming a normal mitotic apparatus, leading to apoptosis. These formulations have shown efficacy toward solid tumours, inclusive of breast, lung, and pancreatic cancers.³³⁹

KadcylaTM (also known as Ado-Trastuzumab emtansine or T-DM1) is a pioneering antibody-drug conjugate that was the first of its kind approved by the FDA and the EMA in 2013. This innovative formulation combines trastuzumab, a humanized monoclonal antibody targeting the



HER2 receptor, with emtansine (DM-1), an antimicrotubular agent that interferes with cellular division.³⁴⁰ DM-1, once internalized, disrupts microtubule function, leading to cell cycle arrest and apoptosis in cancer cells.^{341,342}

As of now, in addition to Kadcyla™, a total of 11 other antibody-drug conjugates (ADCs) have received approval from the FDA and EMA.³³⁰ NanoTherm™ is a groundbreaking technology, specifically as the only metallic-based nanoparticle therapy for cancer to receive both EMA and FDA approvals.³⁴³ Developed by MagForce AG in Berlin, Germany, NanoTherm™ relies on iron oxide nanoparticles with an amino silane coating, designed to form a colloidal suspension of particles approximately 15 nm in size. These nanoparticles are injected directly into the tumour or its surrounding cavity and subsequently heated through an alternating magnetic field, allowing for localized hyperthermia. This heating either destroys cancer cells directly or sensitizes them to radiotherapy or chemotherapy, which can help prevent recurrence. The primary clinical indications for NanoTherm™ are prostate cancer and glioblastoma multiforme.³⁴⁴ While nanotechnology holds tremendous potential for advancing cancer therapies, several challenges such as toxicity and biocompatibility, targeting and specificity, clearance and degradation, manufacturing and scalability, regulatory and approval pathways, cost and accessibility, and personalization and patient-specific variability need to be tackled to make sure safe and effective clinical use.³⁴⁵⁻³⁵⁵

7.1. Key challenges in the clinical translation of smart nanomaterials

Despite successful laboratory demonstrations, clinical adoption of smart nanomaterials remains low due to a series of interconnected translational challenges, many of which are under-addressed in current literature.³⁵⁶ In this section, we discuss some of the critical challenges that need to be addressed.

1. Manufacturing scale-up and reproducibility

DOI: 10.1039/D5PM00137D

Scaling up synthesis of smart nanomaterials from lab-scale experiments to industrial-level manufacturing is highly challenging. The synthesis of these materials generally relies on multistep fabrication procedures, involving surface functionalization, ligand attachment, and core-shell layer engineering.³⁵⁷ These techniques are highly sensitive to reaction conditions. Batch-to-batch variations arises due to inconsistent shape, size, and surface chemistry. These variations particularly arise in black phosphorus and MXenes which degrade and oxidize readily during processing. To maintain functional stimuli-responsiveness (e.g., GSH and pH-sensitive drug release) under good manufacturing practice (GMP) conditions is a difficult task because industrial undertakings usually prioritize stability and simplicity over complexity. In addition, equipment employed at industrial scale may not replicate the fine-tuned parameters of small-scale synthesis. This leads to loss of biofunctionality and performance of smart nanomaterials.

2. Regulatory frameworks and approval pathways

Smart nanomaterials transcend conventional classifications of drugs, devices, and biologics, leading to a hybrid identity that introduces regulatory ambiguities and hinders their timely clinical translation.³⁵⁸ In addition to that regulatory bodies like the EMA and FDA lack established guidelines specific to stimuli-responsive systems. In continuation, these materials usually undergo dynamic transformations *in vivo* (e.g., change in charge, shape, etc.), complicating their toxicological analysis and long-term safety evaluation.

Moreover, the absence of standardized characterization protocols (e.g., for degradation kinetics, adaptive behaviour, stimulus-response,



etc.) make it difficult to produce and submit reproducible data for regulatory approval.

3. Long-term toxicity and biocompatibility

Preclinical studies typically assess short-term toxicity. However, for clinical applications, long-term biocompatibility and immunological responses are critical. Smart nanomaterials which switch their properties inside the body may produce unknown degradation products. These unknown products could accumulate and interact unpredictably with biological systems.³⁵⁹ Moreover, chronic toxicity, immunogenicity, organ-specific accumulation, and interference with cellular pathways are insufficiently studied. For example, black phosphorus degrades into phosphate ions. However, its impact on cellular calcium signaling and potential calcification is still under investigation.³⁶⁰ Likewise, graphene and metallic hybrid systems may accumulate in the liver, lymph node, and spleen, raising concerns about long-term clearance and systemic burden.³⁶¹

4. Economic and scalability barriers

Smart nanomaterials usually require complex, high-cost manufacturing operations, involving cleanroom environments, rare materials, and multistage purification steps. The financial practicability of scaling up these platforms for routine clinical usage is rarely discussed in academic research. Cost-efficacy is essential for acquisition in healthcare systems, particularly in low-resource settings.³⁶² If smart nanomaterials fail to deliver significantly improved outcomes at a reasonable cost, they risk being overlooked in favor of simpler and more traditional alternatives.

5. Stability, shelf-life, and storage issues

Many smart nanomaterials, especially 2D materials (e.g., MXenes, black phosphorus, etc.) and hydrogels, are intrinsically unstable.³⁶³ Their responsiveness to environmental signals is

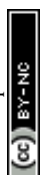
therapeutically advantageous but they are vulnerable to degradation during storage and transportation. Light, humidity, oxygen, and temperature can trigger premature degradation and loss of functionality. These factors complicate the logistics of packaging, sterilization, and storage under clinical settings.

8.0. Conclusions and future perspectives

Smart NMs hold transformative potential in wound healing, cancer theranostic, TER, and beyond, offering advanced solutions for targeted therapy and diagnostics. They have transfigured wound treatment through targeted and accelerated healing processes. NMs can deliver drugs directly to infected sites, promote tissue regeneration, and reduce infection. They enhance cell proliferation and differentiation, leading to ameliorated wound closure and reduced scarring.

NMs based wound healing future perspectives involve: (i) *personalized medicine*: development of smart NMs tailored to individual patients' needs, considering genetic and environmental factors; (ii) *advanced biocompatibility*: enhancing the biocompatibility of NMs to minimize immune response and adverse reactions; (iii) *integration with smart devices*: combining NMs with wearable devices for real-time monitoring and controlled release of therapeutics; (iv) *regenerative medicine*: exploring the potential of NMs in promoting stem cell remedy and tissue engineering for more complex wound healing applications. Future research should continue to focus on enhancing the biocompatibility and specificity of the smart NMs used in wound healing applications.

In cancer theranostic, smart NMs offer a dual approach of diagnosis and therapy, ameliorating effectiveness of drugs while inhibiting side effects. NMs can be manipulated to attack specified cancer



cells, deliver drugs, and provide imaging contrast, allowing for timely diagnosis and precise treatment.

The future perspectives of NMs-based cancer theranostic involve: (i) *development of multifunctional NMs*: development of NMs that combine multiple curative and diagnostic functions within a single platform is essential; (ii) *advanced targeting mechanisms*: enhancing targeting mechanisms for improving explicitness and reduce astray effects, possibly through advanced ligand-receptor interactions should be increased; (iii) *advanced non-invasive techniques*: refining non-invasive diagnostic techniques using NMs, such as liquid biopsies will boost the cancer theranostic. These techniques enhance diagnostic accuracy and therapeutic precision in cancer therapy; (iv) *advanced therapeutic monitoring*: real-time monitoring of treatment responses using NMs to adjust therapy dynamically. Smart NMs enable sophisticated, real-time, non-invasive monitoring of therapeutic responses in cancer therapy. By integrating diagnostic and therapeutic functions, these materials provide valuable insights into drug delivery, efficacy, and resistance. Future developments in this field aim to enhance the sensitivity, specificity, and multifunctionality of NMs, ultimately improving personalized cancer treatment and patient outcomes. The continuous advancement of nanotechnology will likely lead to more precise, efficient, and safer therapeutic monitoring strategies.

Nanotechnology offers a promising strategy for TER. Nanoscale scaffolds provide outstanding advantages over traditional therapies by closely mimicking native ECM. This creates an ideal environment for cell proliferation, adhesion, and differentiation. Key nanostructures, for example, nanotubes, nanofibers, polymeric nanoparticles, and nanocomposites, contribute to controlled degradation rates, enhanced mechanical strength, and improved bioactivity. They also have the capability to encapsulate small molecules, genetic

materials, and growth factors, protecting these agents and allowing for their sustained release at the injury site. 3D bioprinting holds considerable potential to meet the demand for biomimetic artificially regenerated tissues for transplantation in patients with damaged organs. The review also examines the use of hybrid bioinks made up of synthetic and natural NMs with various printers. However, the fabrication of inner tissues/organs may lead to biological safety and liability concerns, presenting another obstacle that needs to be addressed.

While smart NMs hold great promise, their potential toxicity remains a critical concern. Nanotoxicity studies have revealed that certain NMs can induce cytotoxicity, genotoxicity, and dysfunction of the heart, kidney, spleen, liver, etc. by accumulating in them. The toxicity of NMs is affected by both NMs shape, composition, size, coatings as well as the biological system with which they interact. Understanding and mitigating these effects are essential for safe clinical applications.

The future perspectives of nanotoxicity involve: (i) *comprehensive toxicity profiling*: development of standardized methods for comprehensive toxicity profiling of NMs is essential; (ii) *advanced green nanotechnology*: advancing green synthesis methods to produce environmentally benign and biocompatible NMs are the need of time to overcome the nanotoxicity; (iii) *robust regulatory frameworks*: establishment of robust regulatory frameworks and guidelines for the safe use of NMs in medical applications will help in reducing nanotoxicity; (iv) *long-term and comprehensive studies*: conducting long-term and comprehensive *in vivo* studies to understand the chronic effects and biodistribution of NMs would help in understanding and overcoming the nanotoxicity.

Hence, smart NMs represent a remarkable furtherance in biomedical applications, offering



innovative solutions for wound healing, cancer theranostic, tissue engineering and regeneration, and other medical challenges. However, their successful implementation requires careful consideration of their biocompatibility and potential toxic effects.

Taken together, smart nanomedicines based future research should focus on the following key areas: (i) standardization and scalability of synthesis protocols; (ii) comprehensive toxicological profiling; (iii) multifunctionality and stimuli-responsiveness in complex microenvironments; (iv) integration with digital health and theranostics; (v) overcoming regulatory and ethical barriers; (vi) application-specific innovations; (vii) real-world validation and clinical trials.

Hence, the future of smart nanomaterials in biomedicine lies in interdisciplinary convergence, regulatory reform, and patient-centric design. By integrating continued advances in materials science, systems biology, and digital health, smart nanomaterials are poised to revolutionize diagnostics, therapy, and regenerative medicine if safety, scalability, and societal acceptance are comprehensively addressed.

Author contributions

Manoj Kumar Goshisht: idea conceptualization, writing original draft, methodology, and editing, Ashu Goshisht: idea conceptualization, writing original draft, methodology, editing and reviewing. Animesh Bajpai: writing – original draft and reviewing. Abheshek Bajpai: writing – original draft and methodology.

Conflicts of interest

The authors declare that they have no known competing financial interests or personal relationships that could have appeared to influence the work reported in this paper.

Data availability

No primary research results, software or code have been included, and no new data were generated or analyzed as part of this review.

References

1. M. Yoshida and J. Lahann, *Smart Nanomaterials*, *ACS Nano* 2008, 2, 6, 1101–1107. <https://doi.org/10.1021/nn800332g>
2. B. K. Kashyap, V. V. Singh, M. K. Solanki, A. Kumar, J. Ruokolainen, K. K. Kesari, *Smart nanomaterials in cancer theranostics: challenges and opportunities*, *ACS Omega* 2023, 8, 16, 14290–14320. <https://doi.org/10.1021/acsomega.2c07840>.
3. A. K. Dąbrowska, F. Spano, S. Derler, C. Adlhart, N. D. Spencer and R. M. Rossi, *Skin Res. Technol.* 2018, 24, 165–174.
4. S. K. Nethi, S. Das, C. R. Patra and S. Mukherjee, *Biomater. Sci.* 2019, 7, 2652–2674.
5. S. F. Spampinato, G. I. Caruso, R. De Pasquale, M. A. Sortino and S. Merlo, *Pharmaceuticals (Basel)* 2020, 13, 60.
6. H. N. Wilkinson and M. J. Hardman, *Open Biol.* 2020, 10, 200223.
7. H. Singh, M. Dhanka, I. Yadav, S. Gautam, S. M. Bashir, N. C. Mishra, T. Arora, S. Hassan, *Tissue Engineering Part B: Reviews* 2024, 30, 230–253.
8. R. Mu, S. Campos de Souza, Z. Liao, L. Dong and C. Wang, *Adv. Drug Deliv. Rev.* 2022, 185, 114298.
9. C. K. Sen, G. M. Gordillo, S. Roy, R. Kirsner, L. Lambert, T. K. Hunt, F. Gottrup, G. C. Gurtner and M. T. Longaker, *Wound Repair Regen.* 2009, 17, 763–771.
10. M. Wang, X. Huang, H. Zheng, Y. Tang, K. Zeng, L. Shao and L. Li, *J. Control. Release* 2021, 337, 236–247.
11. M. M. Mihai, M. B. Dima, B. Dima and A. M. Holban, *Materials (Basel)* 2019, 12, 2176.
12. D. K. Chandra, R. L. Reis, S. C. Kundu, A. Kumar, and C. Mahapatra, *ACS Biomaterials Science & Engineering* 2024, DOI: 10.1021/acsbmaterials.4c00166.
13. H. Sung, J. Ferlay, R. L. Siegel, M. Laversanne, I. Soerjomataram, A. Jemal and F. Bary, *CA: Cancer J. Clin.* 2021, 71, 209–249.
14. F. Bray, J. Ferlay, I. Soerjomataram, R. L. Siegel, L. A. Torre and A. Jemal, *CA: Cancer J. Clin.* 2018, 68, 394–424.
15. Y. Hosomi, S. Morita, S. Sugawara, T. Kato, T. Fukuhara, A. Gemma, K. Takahashi, Y. Fujita, T. Harada, K. Minato, K. Takamura, K. Hagiwara, K. Kobayashi, T. Nukiwa and A. Inoue, *J. Clin. Oncol.* 2020, 38, 115–123.
16. R. Baghban1, L. Roshangar, R. Jahanban-Esfahlan, K. Seidi, A. Ebrahimi-Kalan, M. Jaymand, S. Kolahian, T. Javaheri and P. Zare, *Cell Commun. Signal* 2020, 18, 59.
17. P. K. Gupta, *J. Pharm. Sci.* 1990, 79, 949–962.



18. R. Tenchov, R. Bird, A. E. Curtze, and Q. Zhou, *ACS Nano* 2021, 15, 16982–17015.
19. M. J. Mitchell, M. M. Billingsley, R. M. Haley, M. E. Wechsler, N. A. Peppas, and R. Langer, *Nat. Rev. Drug Discov.* 2021, 20, 101–124.
20. J. Liu, Z. Liu, Y. Pang and H. Zhou, *J. Nanobiotechnol.* 2022, 20, 127.
21. Y. Herdiana, N. Wathoni, S. Shamsuddin, and M. Muchtaridi, *Heliyon* 2022, 8, e08674.
22. D. Peer, J. M. Karp, S. Hong, O. C. Farokhzad, R. Margalit and R. Langer, *Nat. Nanotechnol.* 2007, 2, 751–760.
23. L. Yan, F. Zhao, J. Wang, Y. Zu, Z. Gu, Y. Zhao, *Adv. Mater.* 2019, 31, 1805391. <https://doi.org/10.1002/adma.201805391>
24. P. C. Ray, H. Yu and P. P. Fu, Toxicity and Environmental Risks of Nanomaterials: Challenges and Future Needs, *J. Environ. Sci. Health, Part C: Environ. Carcinog. Ecotoxicol. Rev.* 2009, 27, 1–35
25. Mamata, A. Agarwal, A. Awasthi, K. Awasthi and A. Dutta, Antibacterial activities of GO–Ag nanocomposites with various loading concentrations of Ag nanoparticles. *Appl. Phys. A* 2023, 129, 838. <https://doi.org/10.1007/s00339-023-07115-w>
26. A. Agrawal, R. Sharma, A. Sharma, K. C. Gurjar, S. Kumar, S. Chatterjee, H. Pandey, K. Awasthi, A. Awasthi. Antibacterial and antibiofilm efficacy of green synthesized ZnO nanoparticles using *Saraca asoca* leaves. *Environ Sci Pollut Res Int.* 2023, 30, 86328–86337. doi: 10.1007/s11356-023-28524-7.
27. S. K. Sohaebuddin, P. T. Thevenot, D. Baker, J. W. Eaton and L. Tang, *Part. Fibre Toxicol.*, 2010, 7, 22.
28. V. A. Senapati, A. Kumar, G. S. Gupta, A. K. Pandey and A. Dhawan, *Food Chem. Toxicol.* 2015, 85, 61–70.
29. X. Yuan, W. Nie, Z. He, J. Yang, B. Shao, X. Ma, X. Zhang, Z. Bi, L. Sun, X. Liang, Y. Tie, Y. Liu, F. Mo, D. Xie, Y. Wei and X. Wei, *Theranostics* 2020, 10, 4589–4605.
30. V. Ramalingam, S. Revathidevi, T. Shanmuganayagam, L. Muthulakshmi and R. Rajaram, *RSC Adv.* 2016, 6, 20598–20608.
31. L. Zhang, L. Wu, Y. Mi and Y. Si, *Bull. Environ. Contam. Toxicol.* 2019, 103, 181–186.
32. T. H. Shin, C. Seo, D. Y. Lee, M. Ji, B. Manavalan, S. Basith, S. K. Chakkarapani, S. H. Kang, G. Lee, M. J. Paik and C. B. Park, *Arch. Toxicol.* 2019, 93, 1201–1212.
33. M. K. Goshisht, P. Kaur, M. S. Bakshi, *ACS Appl. Nano Mater.* 2024, 7, 14, 16949–16963, <https://doi.org/10.1021/acsnm.4c03061>.
34. F. Farjadian, S. Rezaeifard, M. Naeimi, S. Ghasemi, S. Mohammadi-Samani, M. E. Welland, L. Tayebi, *International journal of nanomedicine* 2019, 14, 6901–6915. <https://doi.org/10.2147/IJN.S214467>.
35. H. M. El-Husseiny, E. A. Mady, L. Hamabe, A. Abugomaa, K. Shimada, T. Yoshida, T. Tanaka, A. Yokoi, M. El-Badawy and R. Tanaka, *Materials Today Bio* 2022, 13, 2022, 100186, <https://doi.org/10.1016/j.mtbio.2021.100186>.
36. M. Moniruzzaman, S. D. Dutta, K.-T. Lim, J. Kim, *ACS Omega* 2022, 7, 42, 37388–37400, <https://doi.org/10.1021/acsomega.2c04130>.
37. M.S. Bakshi, *Acc. Mater. Res.* 2024, 5, 8, 1000–1012, <https://doi.org/10.1021/accountsmr.4c00151>.
38. M. Aflori, *Nanomaterials* 2021, 11, 396. <https://doi.org/10.3390/nano11020396>.
39. G.E. Yılmaz, I. Göktürk, M. Ovezova, F. Yılmaz, S. Kılıç, A. Denizli, *Hygiene.* 2023, 3, 269–290. <https://doi.org/10.3390/hygiene3030020>.
40. S. K. Mondal, S. Chakraborty, S. Manna and S. M. Mandal, *RSC Pharm.* 2024, 1, 388–402, <https://doi.org/10.1039/D4PM00032C>.
41. A. B. -Khiabani and M. Gasik, *Int. J. Mol. Sci.* 2022, 23, 3665. <https://doi.org/10.3390/ijms23073665>
42. K. M. Fahy, M. K. Eiken, K. V. Baumgartner, K. Q. Leung, S. E. Anderson, E. Berggren, E. Bouzos, L. R. Schmitt, P. Asuri, K. E. Wheeler, *ACS Omega* 2023, 8, 3, 3310–3318. <https://doi.org/10.1021/acsomega.2c06882>
43. M. K. Goshisht, R. Kaur, M.S. Bakshi, *Langmuir* 2025, 41, 12, 8214–8227. <https://doi.org/10.1021/acs.langmuir.4c05340>
44. A. Lamoot, A. Uvyn, S. Kasmi, B. G. De Geest, *Angew. Chem. Int. Ed.* 2021, 60, 6320. <https://doi.org/10.1002/anie.202015625>
45. J. Zhang, L. Mou, X. jiang, *Chem. Sci.*, 2020, 11, 923–936. <https://doi.org/10.1039/C9SC06497D>
46. X.-P. Li, D.-Y. Hou, J.-C. Wu, P. Zhang, Y.-Z. Wang, M.-Y. Lv, Y. Yi, W. Xu, *ACS Biomater. Sci. Eng.* 2024, 10, 9, 5474–5495. <https://doi.org/10.1021/acsbmaterials.4c00388>
47. M. Guo, Y. Yan, H. Zhang, H. Yan, Y. Cao, K. Liu, S. Wan, J. Huang and W. Yue, *J. Mater. Chem.*, 2008, 18, 5104–5112. <https://doi.org/10.1039/B810061F>
48. T. Fuoco, D. Pappalardo, A. Finne-Wistrand, *Macromolecules* 2017, 50, 18, 7052–7061. <https://doi.org/10.1021/acs.macromol.7b01318>
49. J. Wen, J. Xu, M. Hong, W. Li, T. Li, *Journal of Drug Delivery Science and Technology*, 105, 2025, 106638, <https://doi.org/10.1016/j.jddst.2025.106638>.
50. A. Joorabloo and T. Liu. *Journal of Controlled Release.* 2023, 356, 463–480.
51. E. Kolanthai, Y. Fu, U. Kumar, B. Babu, A. K. Venkatesan, K. W. Liechty and S. Seal, *Wiley Interdisciplinary Reviews: Nanomedicine and Nanobiotechnology* 2021, e1741.
52. M. K. Goshisht, L. Moudgil, M. Rani, P. Khullar, G. Singh, H. Kumar, N. Singh, G. Kaur, M. S. Bakshi, *J. Phys. Chem. C*, 2014, 118, 48, 28207–28219. <https://doi.org/10.1021/jp5078054>
53. X. Chen, D. Wu, Z. Chen, *MedComm.* 2024; 5, 8, e643. <https://doi.org/10.1002/mco2.643>



54. U. Havelikar, K.B. Ghorpade, A. Kumar, A. Patel, M. Singh, N. Banjare, and P. N. Gupta, *Discover Nano* 19, 165, 2024. <https://doi.org/10.1186/s11671-024-04118-1>
55. G. Gaucher, M.-H. Dufresne, V. P. Sant, N. Kang, D. Maysinger, J.-C. Leroux, *Journal of Controlled Release*, 109,1-3, 2005, 169-188, <https://doi.org/10.1016/j.jconrel.2005.09.034>.
56. A. Crintea, A.C. Motofelea, A. S. Şovrea, A.-M. Constantin, C.-B. Crivii, R. Carpa, A.G. Duţu, *Pharmaceutics*. 2023, 15,5,1406. <https://doi.org/10.3390/pharmaceutics15051406>
57. M. Vallet-Regí, F. Schüth, D. Lozano, M. Colilla, and M. Manzano, *Chem. Soc. Rev.*, 2022,51, 5365-5451. <https://doi.org/10.1039/D1CS00659B>
58. A. Vashist, G. P. Alvarez, V. A. Camargo, A. D. Raymond, A. Y. Arias, N. Kolishetti, A. Vashist, P. Manickam, S. Aggarwal, and M. Nair, *Biomater. Sci.*, 2024,12, 6006-6018, <https://doi.org/10.1039/D4BM00224E>
59. P. Makvandi, C.Y. Wang, E. N. Zare, A. Borzacchiello, L. N. Niu and F. R. Tay, *Adv. Funct. Mater.* 2020, 30, 1910021.
60. Y. Zheng, M. Wei, H. Wu, F. Li and D. Ling, *J Nanobiotechnology* 2022, 20, 328.
61. D. Franco, G. Calabrese, S.P. Guglielmino and S. Conoci, *Microorganisms* 2022, 10, 1778.
62. I. X. Yin, J. Zhang, I. S. Zhao, M. L. Mei, Q. Li and C. H. Chu, *Int. J. Nanomed.* 2020, 15, 2555–2562.
63. G. R. Tortella, O. Rubilar, N. Durán, M.C. Diez, M. Martínez, J. Parada and A. B. Seabra, *J. Hazard. Mater.* 2020, 390, 121974.
64. S. Sathiyaraj, G. Suriyakala, A. Dhanesh Gandhi, R. Babujanarthanam, K. S. Almaary, T. W. Chen and K. Kaviyarasu, *J. Infect. Public Health* 2021, 14, 1842–1847.
65. Sonia, A. Singh, Shivangi, R. Kukreti, S. Kukreti, M. Kaushik, *Biomater. Adv.* 2022, 134, 112678,
66. A. S. Abu Lila, B. Huwaimel, A. Alobaida, T. Hussain, Z. Rafi, K. Mehmood, M. H. Abdallah, T. A. Hagbani, S. M. D. Rizvi, A. Moin and A. F. Ahmed, *Materials (Basel)*, 2022, 15, 5709.
67. L. Wang, W. Zheng, S. Li, Q. Hou and X. Jiang, *Chem. Commun. (Camb)*, 2022, 58 7690-7693.
68. L. Qiu, C. Wang, M. Lan, Q. Guo, X. Du, S. Zhou, P. Cui, T. Hong, P. Jiang, J. Wang and J. Xia, *ACS Appl Bio Mater.*, 2021, 4, 3124-3132
69. Y. Hu, J. Shao, H. Dong, D. Yang, X. Dong, *ACS Materials Lett.* 2024, 6, 9, 4209–4229, <https://doi.org/10.1021/acsmaterialslett.4c01165>.
70. B. Singh, J. Kim, N. Shukla, J. Lee, K. Kim, M.-H. Park, *ACS Appl. Bio Mater.* 2023, 6, 6, 2314–2324, <https://doi.org/10.1021/acsubm.3c00178>
71. T. A. Singh, A. Sharma, N. Tejwan, N. Ghosh, J. Das and P. C. Sil, *Adv. Colloid Interface Sci.* 2021, 295, 102495.
72. A. Naskar, S. Lee and K. S. Kim, *RSC Adv.* 2020, 10, 1232–1242.
73. O. R. Abbasabadi, M. R. Farahpour, Z. G. Tabatabaei, *Int. J. Biol. Macromol.*, 2022, 217, 42-54.
74. H. Zhang, X. Zhang, Q. Cao, S. Wu, X. -Q. Wang, N. Peng, D. Zeng, J. Liao and H. Xu, *Biomater. Sci.* 2022, 10, 5888-5899.
75. M. K. Goshisht, *APMIS: acta pathologica, microbiologica, et immunologica Scandinavica*, 2025,133,7, e70050. <https://doi.org/10.1111/apm.70050>
76. R. Sharma, N. Gupta, V. Kumar, S. Pal, V. Kaundal, V. Sharma. *Int Surg J.* 2017, 4, 8, 2627–2631. doi:10.18203/2349-2902.isj20173401
77. D. Patel, R. Maisuria, J. Manza, D. Chaudhari, D. Dave, *Int Surg J.* 2019, 6, 2, 508–511. doi:10.18203/2349-2902.isj20190393.
78. Y. Tajdar, S. Singh, A. Raj, A. Raj, V. Bhushan, *Turk J Surg.*, 2024, 40, 1, 28–35. doi:10.47717/turkjsurg.2024.6168
79. Bheemya, A. I. Peter, V. Kalyanpur, *AJ Journal of Medical Sciences*, 2025, 2,1,11-16. doi:10.71325/ajjms.v2i1.25.5
80. G. Borkow, T. Roth, A. Kalinkovich, *Microbiol. Res.* 2022, 13, 366-376. <https://doi.org/10.3390/microbiolres13030029>
81. E. Melamed, J. Dabbah, T. Israel, I. Kan, M. S. Pinzur, T. Roth, and G. Borkow, *Advances in wound care*, 2025, <https://doi.org/10.1089/wound.2024.0273>
82. N. Chauhan, K. Saxena and U. Jain, *Biomedical Materials & Devices*, 2023, 1, 108–121.
83. D.K. Shanmugam, Y. Madhavan, A. Manimaran, G. S. Kalaraj, K. G. Mohanraj, N. Kandhasamy and K. K. Amirtharaj Mosas, *Gels*, 2023, 9, 22.
84. C. Xie, Y. Xu, Y. Liu, M. Chen, P. Du, Y. Zhang, X. Ma and S. Yang. *Chemical Engineering Journal* 2023, 477, 146997.
85. P. Bridgman, *J. Am. Chem. Soc.* 1914, 36,1344–1363.
86. M. Fojtů, X. Chia, Z. Sofer, M. Masařík and M. Pumera, *Adv. Funct. Mater.* 2017, 27, 1701955.
87. X. W. Huang, J. J. Wei, M. Y. Zhang, X. L. Zhang, X. F. Yin, C. H. Lu, J. B. Song, S. M. Bai and H. H. Yang, *ACS Appl. Mater. Interfaces* 2018, 10, 35495–35502.
88. S. Huang, S. Xu, Y. Hu, X. Zhao, L. Chang, Z. Chen and X. Mei, *Acta Biomater.* 2022, 137, 199-217.
89. B. Anasori, M. R. Lukatskaya, and Y. Gogotsi, *Nat. Rev. Mater.* 2017, 2, 16098.
90. V. M. Hong Ng, H. Huang, K. Zhou, P. S. Lee, W. Que, J. Z. Xu and L. B. Kong, *J. Mater. Chem. A* 2017, 5, 3039–3068.
91. K. Rasool, M. Helal, A. Ali, C. E. Ren, Y. Gogotsi and K. A. Mahmoud, *ACS Nano* 2016, 10, 3674-3684.
92. O. S. Lee, M. E. Madjet and K. A. Mahmoud, *Nano Lett.* 2021, 21, 8510–8517.
93. Y. Gao, Y. Dong, S. Yang, A. Mo, X. Zeng, Q. Chen and Q. Peng, *J. Colloid Interface Sci.* 2022, 617, 533–541.
94. C. Yu, S. Sui, X. Yu, W. Huang, Y. Wu, X. Zeng, Q. Chen, J. Wang and Q. Peng, *Colloids Surf. B. Biointerf.* 2022, 217, 112663.
95. G. P. Lim, C. F. Soon, N. L. Ma, M. Morsin, N. Nayan, M. K. Ahmad and K. S. Tee, *Environ. Res.* 2021, 201, 111592.
96. X. Zhao, A. Vashisth, E. Prehn, W. Sun, S. A. Shah, T. Habib, Y. Chen, Z. Tan, J. L. Lutkenhaus, M. Radovic and M. J. Green, *Matter* 2019, 1, 513–526.



97. H. Park, J.-U. Kim, S. Kim, N. S. Hwang, H. D. Kim, *Materials Today Bio* 2023, 23, 100881, <https://doi.org/10.1016/j.mtbio.2023.100881>.
98. X. Li, J. Shan, W. Zhang, S. Su, L. Yuwen and L. Wang, *Small* 2017, 13, 1602660.
99. S. Bharti, S. K. Tripathi, and K. Singh, *Analytical Biochemistry* 2024, 685, 115404
100. A. S. Sethulekshmi, A. Saritha, K. Joseph, A. S. Aprem and S. B. Sisupal, *J. Control. Release* 2022, 348, 158-185.
101. W. Yin, J. Yu, F. Lv, L. Yan, L. R. Zheng, Z. Gu and Y. Zhao, *ACS Nano* 2016, 10, 11000-11011.
102. F. Cao, E. Ju, Y. Zhang, Z. Wang, C. Liu, W. Li, Y. Huang, K. Dong, J. Ren and X. Qu, *ACS Nano* 2017, 11, 4651-4659.
103. W. Duan, K. Xu, S. Huang, Y. Gao, Y. Guo, Q. Shen, Q. Wei, W. Zheng, Q. Hu and J.-W. Shen. *International Journal of Pharmaceutics* 2024, 659, 124247.
104. A. Joorabloo and T. Liu, *J Nanobiotechnol* 2022, 20, 407.
105. A. T. Yayehrad, E. A. Siraj, M. Matsabisa and G. Birhanu. *Regenerative Therapy*, 2023, 24, 361-376.
106. L. Mao, L. Wang, M. Zhang, M. W. Ullah, L. Liu, W. Zhao, Y. Li, A. A. Q. Ahmed, H. Cheng, Z. Shi and G. Yang. *Adv. Healthcare Mater.* 2021, 10, 2100402.
107. B. Wang, D. Zhao, Y. Li, X. Zhou, Z. Hui, X. Lei, L. Qiu, Y. Bai, C. Wang, J. Xia, Y. Xuan, P. Jiang and J. Wang, *ACS Appl. Nano Mater.* 2023, 6, 8, 6891-6900.
108. S. C. Owen, D. P. Y. Chan and M.S. Shoichet, *Nano Today* 2012, 7, 53-65.
109. R. Solanki and D. Bhatia, Stimulus-Responsive Hydrogels for Targeted Cancer Therapy. *Gels* 2024, 10, 440. DOI: <https://doi.org/10.3390/gels10070440>.
110. N. Zhang, Z. Wang, and Y. Zhao, *Cytokine Growth Factor Rev.* 2020, 55, 80-85.
111. Y. H. A. Hussein and M. Youssry, *Materials* 2018, 11, 688.
112. O. Gutiérrez Coronado, C. Sandoval Salazar, J. L. Muñoz Carrillo, O. A. Gutiérrez Villalobos, M. d. I. L. Miranda Beltrán, A. D. Soriano Hernández, V. Beltrán Campos, P. T. Villalobos Gutiérrez, *Int. J. Mol. Sci.* 2025, 26, 2633. <https://doi.org/10.3390/ijms26062633>.
113. M. Puzzo, M. De Santo, C. Morelli, A. Leggio, L. Pasqua, *Small Sci.*, 2024, 4, 2400113. <https://doi.org/10.1002/ssm.202400113>.
114. P. Singh, S. pandit, V. R. S. S. Mokkapat, A. Garg, V. Ravikumar, I. Mijakovic, *Int. J. Mol. Sci.*, 2018, 19, 1979.
115. P. Singh, H. Singh, Y. J. Kim, R. Mathiyalagan, C. Wang and D. C. Yang, *Enzym. Microb. Technol.* 2016, 86, 75-83.
116. W. Xu, J. Qian, G. Hou, Y. Wang, J. Wang, T. Sun, L. Ji, A. Suo and Y. Yao, *Acta Biomaterialia* 2019, 83, 400-413. [10.1002/adhm.202100402](https://doi.org/10.1002/adhm.202100402)
117. M. Liu, W. Lai, M. Chen, P. Wang, J. Liu, X. Fang, Y. Yang and C. Wang, *Colloids and Surfaces A: Physicochemical and Engineering Aspects* 2023, 662, 131016. <https://doi.org/10.1021/acsanm.2c05467>
118. F. Soetaert, P. Korangath, D. Serantes, S. Fiering, R. Iykov, *Advanced Drug Delivery Reviews* 2020, 163-164, 65-83, <https://doi.org/10.1016/j.addr.2020.06.025>.
119. T. Vangijzegem, V. Lecomte, I. Ternad, L. Van Leuven, R.N. Muller, D. Stanicki, S. Laurent. *Pharmaceutics* 2023, 15(1), 236. <https://doi.org/10.3390/pharmaceutics15010236>
120. S. Chung, R. A. Revia and M. Zhang, *Nanoscale Horiz.* 2021, 6, 696-717, <https://doi.org/10.1039/D1NH00179E>
121. C. A. Quinto, P. Mohindra, S. Tong and G. Bao, *Nanoscale* 2015, 7, 12728-12736. <https://doi.org/10.1039/C5NR02718G>.
122. V. Sachdeva, A. Monga, R. Vashisht, D. Singh, A. Singh, N. Bedi, *Journal of Drug Delivery Science and Technology* 2022, 74, 103585, <https://doi.org/10.1016/j.jddst.2022.103585>.
123. M. V. Shestovskaya, A. L. Luss, O.A. Bezborodova, V. V. Makarov, A. A. Keskinov, *Pharmaceutics* 2023, 15(10), 2406. <https://doi.org/10.3390/pharmaceutics15102406>
124. Z. Zhao, M. Li, J. Zeng, L. Huo, K. Liu, R. Wei, K. Ni and J. Gao, *Bioact. Mater.* 2022, 12, 214-245.
125. P. Rani, J. U. Rahim, S. Patra, R. Gupta, M. Gulati, B. Kapoor, *Journal of Drug Delivery Science and Technology* 2024, 96, 105715.
126. X. Li, J. Niu, L. Deng, Y. Yu, L. Zhang, Q. Chen, J. Zhao, B. Wang and H. Gao, *Acta Biomaterialia* 2024, 173, 432-441. <https://doi.org/10.1016/j.actbio.2023.11.019>
127. D. Brühwiler, *Nanoscale* 2010, 2, 887-892.
128. F. Tang, L. Li and D. Chen, *Adv. Mater.* 2012, 24, 1504-1534.
129. Q. He, J. Zhang, J. Shi, Z. Zhu, L. Zhang, W. Bu. L. Guo and Y. Chen, *Biomaterials* 2010, 31, 1085-1092.
130. X. Liu, W. Chen, D. Zhao, X. Liu, Y. Wang, Y. Chen and X. Ma, *ACS Nano*, 2022, 16, 10354-10363.
131. Y. Cai, T. Deng, Y. Pan, and J. I. Zink, *Adv. Funct. Mater.* 2020, 30, 2002043.
132. S. Yang, L. Chen, X. Zhao, P. Sun, L. Fu, F. You, M. Xu, Z. You, G. Kai, C. He, *Chem. Eng. J.* 2019, 378, 122171.
133. Y. Wang, Q. Zhao, N. Han, L. Bai, J. Li, E. Che, L. Hu, Q. Zhang, T. Jiang, S. Wang, *Nanomed. Nanotechnol. Biol. Med.* 2015, 11, 313-327.
134. Y. Zhang, Z. Ye, R. He, Y. Li, B. Xiong, M. Yi, Y. Chen, J. Liu and B. Lu, *Colloids and Surfaces B: Biointerfaces* 2023, 224, 113201. <https://doi.org/10.1016/j.colsurfb.2023.113201>
135. P. Zrazhevskiy, M. Sena, and X. Gao, *Chem. Soc. Rev.* 2010, 39, 4326-4354.
136. M. F. Bertino, R. R. Gadipalli, L. A. Martin, L. E. Rich, A. Yamilov, B. R. Heckman, N. Leventis, S. Guha. J. Katsoudas, R. Divan. and D. C. Mancini, *Nanotechnology* 2007, 18, 315603.
137. A. R. C. Osypiw, S. Lee, S. -M. Jung, S. Leoni, P. M. Smowton, B. Hou, J. M. Kim and G. A. J. Amaratunga, *Materials Advances* 2022, 3, 6773-6790.
138. S. Sun, Q. Guan, Y. Liu, B. Wei, Y. Yang, and Z. Yu, *Chin. Chem. Lett.* 2019, 30, 1051-1054.



139. Y. Li, P. Zhang, W. Tang, K. J. McHugh, S. V. Kershaw, M. Jiao, X. Huang, S. kalytchuk, C. F. Perkinson, S. Yue, Y. Qiao, L. Zhu, L. Jing, M. Gao and B. Han, *ACS Nano* 2022, 16, 8076–8094.
140. L. Karthikeyan, P. A. Rasheed, Y. Haldorai, R. Vivek, *ACS Appl. Polym. Mater.* 2023, 5, 9, 7167–7179, <https://doi.org/10.1021/acsapm.3c01148>
141. T. G. Katmerlikaya, B. C. Ersen, A. Dag, B. Sancakli, P. S. O. Ozgen, E. K. Yalcin, B. Avci, *ACS Appl. Polym. Mater.* 2024, 6, 7, 4149–4163. <https://doi.org/10.1021/acsapm.4c00238>
142. M. He, L. Yu, Y. Yang, B. Zou, W. Ma, M. Yu, J. Lu, G. Xiong, Z. Yu and A. Li, *Chin. Chem. Lett.* 2020, 31, 3178–3182.
143. Z. Hong, X. Zan, T. Yu, Y. Hu, H. Gou, S. Zheng, X. Gao and P. Zhou, *Chin. Chem. Lett.* 2023, 34, 107603.
144. N. Kamaly, B. Yameen, J. Wu, and O. C. Farokhzad, *Chem. Rev.* 2016, 116, 2602–2663.
145. K. Chansaenpak, G. Y. Yong, A. Prajit, P. Hiranmartsuwan, S. Selvapaandian, B. Ouengwanarat, T. Khrootkaew, P. Pinyou, C. S. Kue and A. Kamkaew, *Nanoscale Adv.* 2024, 6, 406–417. <https://doi.org/10.1039/D3NA00718A>
146. A. P. Singh, A. Biswas, A. Shukla and P. Maiti, *Signal Transduct. Target. Ther.* 2019, 4, 33.
147. Z. Mhlwatika and B. A. Aderibigbe, *Molecules* 2018, 23, 2205.
148. S. García-Gallego, G. Franci, A. Falanga, R. Gómez, V. Folliero, S. Galdiero, F. J. de la Mata, and M. Galdiero, *Molecules* 2017, 22, 1581.
149. A. Santos, F. Veiga and A. Figueiras, *Materials* 2019, 13, 65.
150. J. Recio-Ruiz, R. Carloni, S. Ranganathan, L. Muñoz-Moreno, M. J. Carmena, M. F. Ottaviani, F. J. de la Mata and S. García-Gallego, *Chem. Mater.* 2013, 35, 2797–2807.
151. B. Srinageshwar, S. Peruzzaro, M. Andrews, K. Johnson, A. Hietpas, B. Clark, C. McGuire, E. Petersen, J. Kippe, A. Stewart, O. Lossia, A. Al-Gharaibeh, A. Antcliff, R. Culver, D. Swanson, G. Dunbar, A. Sharma, J. Rossignol, *Int. J. Mol. Sci.* 2017, 18, 628.
152. L. M. Kaminskas, B. D. Kelly, V. M. McLeod, G. Sberna, D. J. Owen, B. J. Boyd, C. J. H. Porter, *J. Control. Rel.* 2011, 152, 241–248.
153. C. -S. Lee, T. W. Kim, Y. Kang, Y. Ju, J. Ryu, H. Kong, Y. -S. Jang, D. E. Oh, S. J. Jang, H. Cho, S. Jeon, J. Kim, T. H. Kim, *Materials Today Chemistry* 2022, 26, 101083. <https://doi.org/10.1016/j.mtchem.2022.101083>
154. S. Perumal, R. Atchudan, W. Lee, *Polymers* 2022, 14, 2510.
155. Y. H. A. Hussein and M. Youssry, *Materials* 2018, 11, 688.
156. Z. Cong, F. Yang, L. Cao, H. Wen, T. Fu, S. Ma, C. Liu, L. Quan, Y. Liao, *Int. J. Nanomed.* 2018, 13, 8549.
157. Z. Yang, R. Cheng, C. Zhao, N. Sun, H. Luo, Y. Chen, Z. Liu, X. Li, J. Liu, Z. Tian, *Theranostics* 2018, 8, 4097–4115.
158. W. Gao, G. Ye, X. Duan, X. Yang, and V. C. Yang, *Int. J. Nanomed.* 2017, 12, 1047.
159. X. Li, X. Yang, Z. Lin, D. Wang, D. Mei, B. He, X. Wang, X. Wang, Q. Zhang, and W. Gao, *Eur. J. Pharm. Sci.* 2015, 76, 95–101.
160. H. Shan, W. Yin, L. Wen, A. Mao and M. Lang, *Eur. Polym. J.* 2023, 195, 112214.
161. M. He, Z. Zhang, Z. Jiao, M. Yan, P. Miao, Z. Wei, X. Leng, Y. Li, J. Fan, W. Sun, X. Peng, *Chinese Chemical Letters* 2023, 34, 107574. <https://doi.org/10.1016/j.cclet.2022.05.088>
162. S. Sun, R. Han, Y. Sun, W. Chen, L. Zhao, X. Guan, W. Zhang, *Colloids and Surfaces B: Biointerfaces.* 2024, 238, 113909.
163. A. Akbarzadeh, R. Rezaei-Sadabady, S. Davaran, S. W. Joo, N. Zarghami, Y. Hanifehpour, M. Samiei, M. Kouhi and K. Nejati-Koshki, *Nanoscale Res. Lett.* 2013, 8, 102.
164. K. Otake, T. Shimomura, T. Goto, T. Imura, T. Furuya, S. Yoda, Y. Takebayashi, H. Sakai and M. Abe, *Langmuir* 2006, 22, 2543–2550.
165. T. M. Allen and P. R. Cullis, *Adv. Drug Deliv. Rev.* 2013, 65, 36–48.
166. Q. Xiao, X. Li, C. Liu, Y. Yang, Y. Hou, Y. Wang, M. Su, and W. He, *Chin. Chem. Lett.* 2022, 33, 4191–4196.
167. B. Børresen, J. R. Henriksen, G. Clergeaud, J. S. Jørgensen, F. Melander, D. R. Elema, J. Szebeni, S. A. Engelholm, A. T. Kristensen, A. Kjær, T. L. Andresen and A. E. Hansen, *ACS Nano* 2018, 12, 11386–11398.
168. S. Lee, H. J. Kim, J. -H. Choi, H. J. Jang, H. B. Cho, H. -R. Kim, J. -I. Park, K. -S. Park, K. -H. Park, *Journal of Controlled Release* 2024, 368, 756–767. <https://doi.org/10.1016/j.jconrel.2024.03.027>
169. G. Yang, S. Kim, J. Y. Oh, D. Kim, S. Jin, E. Choi, J. -H. Ryu, *Journal of Colloid and Interface Science* 2023, 649, 1014–1022.
170. M. G. M. Ghazy and N. A. N. Hanafy, *International Journal of Biological Macromolecules* 2024, 260, 129338.
171. M. Sun, H. Hu, L. Sun and Z. Fan, *Chin. Chem. Lett.* 2020, 31, 1729–1736.
172. J. Iglesias, *Breast Cancer Res.* 2009, 11, S21.
173. M. J. Hawkins, P. Soon-Shiong and N. Desai, *Adv. Drug Deliv. Rev.* 2008, 60, 876–885.
174. A.T. Guduru, A. Mansuri, U. Singh, A. Kumar, D. Bhatia and S. V. Dalvi, *Biomaterials advances* 2024, 161, 213886, <https://doi.org/10.1016/j.bioadv.2024.213886>.
175. Y. Xu, Y. Liu, T. He, Y. Zhang, M. Wang, H. Yuan, M. Yang, *Colloids and Surfaces B: Biointerfaces* 2021, 207, 112020, <https://doi.org/10.1016/j.colsurfb.2021.112020>.
176. R. Meng, L. Zuo, X. Zhou, *Medical Hypotheses* 2024, 184, 111271. <https://doi.org/10.1016/j.mehy.2024.111271>
177. X. Zhen, P. Cheng and K. Pu, *Small* 2019, 15, 1804105.
178. M. K. Goshisht, N. Tripathi, G. K. Patra and M. Chaskar, *Chem. Sci.* 2023, 14, 5842–5871.
179. X. Wei, J. Gao, R. H. Fang, B. T. Luk, A. V. Kroll, D. Dehaini, J. Zhou, H. W. Kim, W. Gao, W. Lu and L. Zhang, *Biomaterials* 2016, 111, 116–123.



180. X. Liu, Z. Chu, B. Chen and Y. Ma, *Materials Today Bio* 2023, 22, 100765. [10.1016/j.mtbio.2023.100765](https://doi.org/10.1016/j.mtbio.2023.100765)
181. K. Brindhadevi, H. A. Garalleh, A. Alalawi, E. Al-Sarayreh and A. Pugazhendhi, *Biochemical Engineering Journal* 2023, 192, 108828.
182. A. Sharma, P. Vaswani and D. Bhatia, *Nanoscale Adv.* 2024, 6, 3714-3732. DOI: <https://doi.org/10.1039/D4NA00145A>.
183. M. F. Naief, S. N. Mohammed, H. J. Mayouf and A. M. Mohammed, *Journal of Organometallic Chemistry* 2023, 999, 122819.
184. H. Cabral, K. Miyata, K. Osada and K. Kataoka, *Chem. Rev.* 2018, 118, 6844-6892.
185. M. He, L. Yu, Y. Yang, B. Zou, W. Ma, M. Yu, J. Lu, G. Xiong, Z. Yu and A. Li, *Chin. Chem. Lett.* 2020, 31, 3178-3182.
186. Z. Hong, X. Zan, T. Yu, Y. Hu, H. Gou, S. Zheng, X. Gao and P. Zhou, *Chin. Chem. Lett.* 2023, 34, 107603.
187. L. Tang, J. Li, T. Pan, Y. Yin, Y. Mei, Q. Xiao, R. Wang, Z. Yan and W. Wang, *Theranostics* 2022, 12, 2290-2321. [10.7150/thno.69628](https://doi.org/10.7150/thno.69628)
188. B. Wu, M. Li, L. Wang, Z. Iqbal, K. Zhu, Y. Yang and Y. Li, *J. Mater. Chem. B*, 2021, 9, 4319-4328. <https://doi.org/10.1039/D1TB00396H>
189. M. Zhao, Z. Li, C. Yu, Q. Sun, K. Wang and Z. Xie, *Chemical Engineering Journal* 2024, 482, 149039. <https://doi.org/10.1016/j.cej.2024.149039>
190. J. Wang, S. Zhou, F. Lu, S. Wang, Q. Deng, *Food Chemistry* 2024, 451, 139451.
191. X. Zhang, J. Tang, C. Li, Y. Lu, L. Cheng, J. Liu, *Bioactive Materials* 2021, 6, 2, 472-489, <https://doi.org/10.1016/j.bioactmat.2020.08.024>.
192. L. Sun, Y. Han, Y. Zhao, J. Cui, Z. Bi, S. Liao, Z. Ma, F. Lou, C. Xiao, W. Feng, J. Liu, B. Cai, and D. Li, *Frontiers in pharmacology*, 2024, 15, 1396975. <https://doi.org/10.3389/fphar.2024.1396975>
193. C. Sun, L. Wen, J. Zeng, Y. Wang, Q. Sun, L. Deng, C. Zhao and Z. Li, *Biomaterials* 2016, 91, 81-89.
194. S. Geng, X. Zhang, T. Luo, M. Jiang, C. Chu, L. Wu, P. Gong and W. Zhou, *Journal of Controlled Release* 2023, 354, 889-901. <https://doi.org/10.1016/j.jconrel.2022.12.054>
195. U. T. Uthappa, M. Suneetha, S. M. Ji, H. -H. Jeong and S. S. Han, *Microporous and Mesoporous Materials* 2023, 362, 112795.
196. S. Senapati, A. K. Mahanta, S. Kumar, and P. Maiti, *Signal Transduct. Target. Ther.* 2018, 3, 7.
197. H. Zhang, X. Liu, Y. Wu, C. Guan, A. K. Cheetham, and J. Wang, *Chem. commun.* 2018, 54, 5268-5288.
198. X. Lin, H. Wu, J. Zhang, X. Chen and X. Gao, *Chemical Engineering Journal*, 2024, 480, 147865.
199. Y. Li, J. Zhou, L. Wang and Z. Xie, *ACS Appl. Mater. Interfaces* 2020, 12, 30213-30220.
200. M. Ji, H. Liu, X. Liang, M. Wei, D. Shi, J. Gou, T. Yin, H. He, X. Tang and Y. Zhang, *Chemical Engineering Journal* 2024, 485, 149640. <https://doi.org/10.1016/j.cej.2024.149640>
201. M. Wu, J. Yang, T. Ye, B. Wang, Y. Tang, X. Ying, *ACS Appl. Mater. Interfaces* 2023, 15, 25, 29939-29947, <https://doi.org/10.1021/acsami.3c03928>
202. C. Dai, Y. Chen, X. Jing, L. Xiang, D. Yang, H. Lin, Z. Liu, X. Han, R. Wu, *ACS Nano* 2017, 11, 12, 12696-12712, <https://doi.org/10.1021/acs.nano.7b07241>.
203. D. Prakashan, A. Kaushik, S. Gandhi, *Chemical Engineering Journal* 2024, 497, 154371, <https://doi.org/10.1016/j.cej.2024.154371>.
204. N. Singh, K.P. Srikanth, V. Gopal, M. Rajput, G. Manivasagam, K. G. Prashanth, K. Chatterjee, S. Suwas, *J. Mater. Chem. B* 2024, 12, 5982-5993. DOI: <https://doi.org/10.1039/D4TB00379A>.
205. L. Liu, Y. Xiang, Z. Wang, X. Yang, X. Yu, Y. Lu, L. Deng, W. Cui, *NPG Asia Mater.* 2019, 11, 81, DOI: <https://doi.org/10.1038/s41427-019-0185-z>.
206. A. C. Lima, R. L. Reis, H. Ferreira, and N. M. Neves, *ACS Biomater. Sci. Eng.* 2021, 7, 7, 3229-3241. [10.1021/acsbiomaterials.1c00412](https://doi.org/10.1021/acsbiomaterials.1c00412)
207. M. Long, X. Liu, X. Huang, M. Lu, X. Wu, L. Weng, Q. Chen, X. Wang, L. Zhu, Z. Chen, *Journal of Controlled Release* 2021, 334, 303-317. [10.1016/j.jconrel.2021.04.035](https://doi.org/10.1016/j.jconrel.2021.04.035)
208. T. Kulsirirat, K. Sathirakul, N. Kamei, and M. Takeda-Morishita, *Int. J. Pharm.* 2021, 602, 120618. DOI: <https://doi.org/10.1016/j.ijpharm.2021.120618>.
209. Z. Liu, K. Wang, X. Peng, L. Zhang, *European Polymer Journal* 2022, 166, 110979. DOI: <https://doi.org/10.1016/j.eurpolymj.2021.110979>.
210. X. Shi, B. Ma, H. Chen, W. Tan, S. Ma, G. Zhu, *Biosensors* 2022, 12 (10), 847.
211. W. H. Park, B. S. Kim, K. E. Park, H. K. You, J. Lee, and M. H. Kim, *Int. J. Nanomedicine* 2015, 10, 485-502.
212. S. Kwak, A. Haider, K. C. Gupta, S. Kim, and I. -K. Kang, *Nanoscale Res. Lett.* 2016, 11, 323. DOI: [10.1186/s11671-016-1532-4](https://doi.org/10.1186/s11671-016-1532-4).
213. H. Samadian, H. Mobasheri, M. Azami, and R. Faridi-Majidi, *Sci. Rep.* 2020, 10, 1-14.
214. T. Gong, T. Liu, L. Zhang, W. Ye, X. Guo, L. Wang, L. Quan and C. Pan, *ACS Biomater. Sci. Eng.*, 2018, 4, 240-247.
215. A. G. Bajpayee, R. E. De la Vega, M. Scheu, N. H. Varady, I. A. Yannatos, L. A. Brown, Y. Krishnan, T. J. Fitzsimons, P. Bhattacharya, E. H. Frank, A. J. Grodzinsky, R. M. Porter, *Eur. Cell. Mater.* 2017, 34, 341-364.
216. Q. Hu, Q. Chen, X. Yan, B. Ding, D. Chen, L. Cheng, *Nanomedicine* 2018, 13, 749-767.
217. S. Xue, X. Zhou, W. Sang, C. Wang, H. Lu, Y. Xu, Y. Zhong, L. Zhu, C. He and J. Ma, *Bioactive Materials* 2021, 6, 2372-2389. DOI: <https://doi.org/10.1016/j.bioactmat.2021.01.017>.



218. D. K. Chandra, R. L. Reis, S. C. Kundu, A. Kumar, and C. Mahapatra, *ACS Biomaterials Science & Engineering* 2024, 10, 4145–4174. DOI: 10.1021/acsbiomaterials.4c00166.
219. N. Rizwana, K. Maslekar, K Chatterjee, Y. Yao, V. Agarwal and M. Nune, *ACS Appl. Nano Mater.* 2024, 7, 18177–18188. <https://doi.org/10.1021/acsanm.3c02962>.
220. S. Kumari, P. Mondal, S. Tyeb and K. Chatterjee, *J. Mater. Chem. B*, 2024, 12, 1926, DOI: 10.1039/d3tb02179c. <https://doi.org/10.1039/D3TB02179C>
221. J. Zhang, H. Eyssoylu, X.-H Qin, M. Rubert, R. Müller, *Acta Biomaterialia* 2021, 121, 637–652, <https://doi.org/10.1016/j.actbio.2020.12.026>.
222. N. Marovič, I. Ban, U. Maver and T. Maver, *Nanotechnology Reviews* 2023, 12, 20220570, <https://doi.org/10.1515/ntrev-2022-0570>.
223. A. Chakraborty, A. Roy, S. P. Ravi and A. Paul, *Biomater. Sci.* 2021, 9, 6337–6354, DOI: <https://doi.org/10.1039/D1BM00605C>
224. S. Nasra, D. Bhatia and A. Kumar, *Advanced Healthcare Materials* 2024, 13, 2400679, <https://doi.org/10.1002/adhm.202400679>.
225. A. Halim, K.-Y Qu, X.-F. Zhang, N.-P. Huang, *ACS Biomater. Sci. Eng.* 2021, 7, 8, 3503–3529, <https://doi.org/10.1021/acsbiomaterials.1c00490>
226. P. Zhuang, J. An, C. K. Chua, L. P. Tan, *Materials & Design* 2020, 193, 108794, <https://doi.org/10.1016/j.matdes.2020.108794>
227. E. Fornetti, F. De Paolis, C. Fuoco, S. Bernardini, S. M. Giannitelli, A. Rainer, D. Seliktar, F. Magdinier, J. Baldi, R. Biagini, S. Cannata, S. Testa, C. Gargioli, *Biofabrication* 2023, 15 (2), 025009, [10.1088/1758-5090/acb573](https://doi.org/10.1088/1758-5090/acb573)
228. H. J. Jo, M. S. Kang, H. J. Heo, H. J. Jang, R. Park, S. W. Hong, Y. H. Kim, D.-W. Han, *Int. J. Biol. Macromol.* 2024, 265, 130696, [10.1016/j.ijbiomac.2024.130696](https://doi.org/10.1016/j.ijbiomac.2024.130696)
229. J. H. Kim, Y.-J. Seol, I. K. Ko, H.-W. Kang, Y. K. Lee, J. J. Yoo, A. Atala and S. J. Lee, *Sci Rep.* 2018, 8, 12307. <https://doi.org/10.1038/s41598-018-29968-5>.
230. M. Hosseini, K. R. Koehler, and A. Shafiee, *Advanced healthcare materials*, 2022, 11(22), e2201626. <https://doi.org/10.1002/adhm.202201626>
231. C. Mazio, I. Mavaro, A. Palladino, C. Casale, F. Urciuolo, A. Banfi, L. D'Angelo, P. A. Netti, P. de Girolamo, G. Imparato, C. Attanasio, *Materials Today Bio* 2024, 25, 100949, <https://doi.org/10.1016/j.mtbio.2024.100949>.
232. L. Li, S. Qin, J. Peng, A. Chen, Y. Nie, T. Liu, K. Song, *Int. J. Biol. Macromol.* 2020, 145, 262–271, [10.1016/j.ijbiomac.2019.12.174](https://doi.org/10.1016/j.ijbiomac.2019.12.174)
233. Y. J. Shin, R. T. Shafraneck, J. H. Tsui, J. Walcott, A. Nelson, and D. H. Kim, *Acta biomaterialia* 2021, 119, 75–88. <https://doi.org/10.1016/j.actbio.2020.11.006>
234. D. Kim, M. Kim, J. Lee, J. Jang, *Front Bioeng Biotechnol* 2022, 10, 764682, <https://doi.org/10.3389/fbioe.2022.764682>
235. Y. Chen, L. Xu, W. Li, W. Chen, Q. He, X. Zhang, J. Tang, Y. Wang, B. Liu, and J. Liu, *Biofabrication* 2022, 14(2), 10.1088/1758-5090/ac48e4.
236. S. Fleischer, and T. Dvir, *Current opinion in biotechnology* 2013, 24(4), 664–671. <https://doi.org/10.1016/j.copbio.2012.10.016>
237. N. Tripathi and M. K. Goshisht, *ACS Appl. Bio Mater.* 2022, 5, 1391–1463.
238. P. Khullar, M. K. Goshisht, L. Moudgil, G. Singh, D. Mandial, H. Kumar, G. K. Ahluwalia and M. S. Bakshi, *ACS Sustainable Chem. Eng.*, 2017, 5, 1082–1093.
239. M. K. Goshisht, L. Moudgil, P. Khullar, G Singh, A. Kaura, H. Kumar, G. Kaur and M. S. Bakshi, *ACS Sustainable Chem. Eng.* 2015, 3, 3175–3187,
240. A. Mahal, M. K. Goshisht, P. Khullar, H. Kumar, N. Singh, G. Kaur and M. S. Bakshi, *Phys.Chem. Chem. Phys.* 2014, 16, 14257–14270.
241. U. Song, K. S. Pyo, H. H. Song, S. Lee and J. Kim, *Emerging Contaminants* 2024, 10, 100293.
242. A. Sharmila, S. M. Roopan and C. I. Selvaraj, *Journal of Drug Delivery Science and Technology*, 2024, 96, 105731.
243. N. Tripathi, N. Tripathi, M. K. Goshisht, *Mol Divers.* 2022, 26, 629–645, <https://doi.org/10.1007/s11030-020-10176-1>
244. N. Tripathi and M. K. Goshisht, Aggregation of luminophores in supramolecular systems: From mechanism to applications, *CRC Press* 2020, 201–220, <https://doi.org/10.1201/9781003027706>
245. D.-D. Varsou, P. D. Kolokathis, M. Antoniou, N. K. Sidiropoulos, A. Tsoumanis, A. G. Papadiamantis, G. Melagraki, I. Lynch and A. Afantitis, *Computational and Structural Biotechnology Journal* 2024, 25, 47–60.
246. J. M. Hillegass, A. Shukla, S. A. Lathrop, M. B. MacPherson, N. K. Fukagawa and B. T. Mossman, *Wiley Interdisciplinary Reviews: Nanomedicine and Nanobiotechnology* 2010, 2, 219–231.
247. *In Vitro Toxicology Testing Market Size, Share & Trends by Product & Service (Assays (ELISA & Western Blot), Equipment, Consumable, Software), Toxicity Endpoints (ADME, Genotoxicity, Cytotoxicity), Technology, Method, Industry (Pharma, Cosmetics) - Global Forecast to 2028.* <https://www.marketsandmarkets.com/Thanks/subscribePurchaseNew.asp?id=209577065&id=1555905> (accessed June 03, 2024).
248. T. Wu and M. Tang, *J. Appl. Toxicol.* 2018, 38, 25–40.
249. B. Kong, J. H. Seog, L. M. Graham, S. B. Lee, *Nanomedicine (Lond)* 2011, 6, 929–941.
250. C. Lo Giudice, J. Yang, M. A. Poncin, L. Adumeau, M. Delguste, M. Koehler, K. Evers, A. C. Dumitru, K. A. Dawson and D. Alsteens, *ACS Nano* 2022, 16, 306–316. <https://doi.org/10.1021/acs.nano.1c06301>
251. S. Hočevár, A. Milošević, L. Rodriguez-Lorenzo, L. Ackermann-Hirschi, I. Mottas, A. Petri-Fink, B. Rothen-Rutishauser, C. Bourquin, M. J. D. Clift, *ACS Nano* 2019, 13 (6), 6790–6800. <https://doi.org/10.1021/acs.nano.9b01492>



252. J. Duan, V. K. Kodali, M. J. Gaffrey, J. Guo, R. K. Chu, D. G. Camp, R. D. Smith, B. D. Thrall, W. J. Qian, *ACS Nano* 2016, 10, 524-538. [10.1021/acs.nano.5b05524](https://doi.org/10.1021/acs.nano.5b05524)
253. S. Devasahayam, *Characterization and Biology of Nanomaterials for Drug Delivery: Nanoscience and Nanotechnology in Drug Delivery*; Elsevier 2018; pp 477-522.
254. S. Jesus, M. Schmutz, C. Som, G. Borchard, P. Wick, O. Borges, *Front. Bioeng. Biotechnol.* 2019, 7, 261.
255. M. G. Tirumala, P. Anchi, S. Raja, M. Rachamalla, C. Godugu, *Frontiers in Pharmacology* 2021, 12, 612659. DOI: 10.3389/fphar.2021.612659.
256. B. Halamoda-Kenzaoui, U. Holzwarth, G. Roebben, A. Bogni, and S. Bremer-Hoffmann, *WIREs Nanomedicine and Nanobiotechnology* 2019, 11, e1531.
257. B. Drasler, D. Vanhecke, L. Rodriguez-Lorenzo, A. Petri-Fink, B. Rothen-Rutishauser, *Nanomedicine* 2017, 12, 1095-1099.
258. M. Reifarth, S. Hoepfner, U. S. Schubert, *Adv. Mater.* 2018, 30, 1703704.
259. A. Salvati, I. Nelissen, A. Haase, C. Aberg, S. Moya, A. Jacobs, F. Alnasser, T. Bewersdorff, S. Deville, A. Luch, K. A. Dawson, *NanoImpact* 2018, 9, 42-50.
260. H. Garcia Romeu, S. Deville, A. Salvati, *Small*, 2021, 17, 34, 2100887.
261. E. Frohlich, *Artificial Cells, Nanomedicine and Biotechnology* 2018, 46, 1091-1107.
262. V. V. Chrishtop, A. Y. Prilepskii, V. G. Nikonorova, V. A. Mironov, *Toxicology* 2021, 462, 152952. DOI: 10.1016/j.tox.2021.152952.
263. Y. Kohl, M. Biehl, S. Spring, M. Hesler, V. Ogourtsov, M. Todorovic, J. Owen, E. Elje, K. Kopecka, O. H. Moriones, N. G. Bastús, P. Simon, T. Dubaj, E. Runden-Pran, V. Puentes, N. William, H. Briesen, S. Wagner, N. Kapur, E. Mariussen, A. Nelson, A. Gabelova, Dusinska, M. Gabelova, T. Velten, T. Knoll, *Small* 2021, 17, 2006012.
264. *Markets and Markets. In Vivo Toxicology Market - Global Forecast to 2025*. <https://www.marketsandmarkets.com/Market-Reports/in-vivo-toxicology-testing-market-105308811.html> (accessed 2024-06-06).
265. Y. Yang, Z. Qin, W. Zeng, T. Yang, Y. Cao, C. Mei, Y. Kuang, *Nanotechnol. Rev.* 2017, 6, 279-289.
266. S. -K. Jung, X. Qu, B. Aleman-Meza, T. Wang, C. Riepe, Z. Liu, Q. Li, W. Zhong, *Environ. Sci. Technol.* 2015, 49, 2477-2485.
267. M. T. Jacques, J. L. Oliveira, E. V. R. Campos, L. F. Fraceto, D. S. Ávila, *Ecotoxicol. Environ. Saf.* 2017, 139, 245-253.
268. B. Liu, E. M. Campo, T. Bossing, *PLoS One* 2014, 9, e88681.
269. G. Peng, Y. He, X. Wang, Y. Cheng, H. Zhang, K. Savolainen, L. Madler, S. Pokhrel, S. Lin, *ACS Nano* 2020, 14, 4166-4177.
270. S. Rajabi, A. Ramazani, M. Hamidi, T. Naji, *DARU J. Pharm. Sci.* 2015, 23, 20.
271. C. Hurel, C. Bignon, C. Said-Mohamed, S. Amigoni, T. Devers, F. Guittard, *Environ. Sci. Pollut. Res.* 2018, 25, 21216-21223.
272. B. H. Mao, Y. K. Luo, B. J. Wang, C. W. Chen, F. Y. Cheng, Y. H. Lee, S. J. Yan and Y. J. Wang, *Part. Fibre Toxicol.* 2022, 19, 6.
273. B. Cunningham, A. E. Engstrom, B. J. Harper, S. L. Harper, M. R. Mackiewicz, *Nanomaterials* 2021, 11, 1516.
274. J. Li, J. Tian, H. Yin, Y. Peng, S. Liu, S. Yao, L. Zhang, *Environ. Int.* 2021, 152, 106497.
275. A. K. Mittal and U. C. Banerjee, *Mater. Today Commun.* 2021, 26, 102001.
276. M. K. Uchiyama, C. B. Hebeda, S. Sandri, M. de Paula-Silva, M. Romano, R. M. Cardoso, S. H. Toma, K. Araki, S. H. P. Farsky, *Nanomedicine* 2021, 16, 741-758.
277. T. Sun, X. Liu, X. Zhan, L. Ou, R. Lai, *Process Saf. Environ. Prot.* 2021, 147, 134-145.
278. M. R. Wani, N. Maheshwari and G. Shadab, *Environ. Sci. Pollut. Res.* 2021, 28, 22664-22678.
279. P. E. Feuser, M. de M. Cardoso, N. C. Galvani, R. P. Zaccaron, L. M. Venturini, F. K. Rigo, R. A. Machado-de-Ávila, P. C. L. Silveira, C. Sayer and P. H. Hermes de Araújo, *J. Biomed. Mater. Res. Part B Appl. Biomater.* 2022, 110, 702-711.
280. Z. Alvi, M. Akhtar, N. U. Rahman, K. M. Hosny, A. M. Sindi, B. A. Khan, I. Nazir and H. Sadaquat, *Polymers (Basel)* 2021, 13, 4350.
281. P. Andreozzi, C. Simo, P. Moretti, J. M. Porcel, T. U. Lüdtk, M. d. I. A. Ramirez, L. Tamberi, M. Marradi, H. Amenitsch, J. Llop, M. G. Ortore and S. E. Moya, *Small* 2021, 17, 2102211.
282. T. Deptuch, A. Florczak, A. Lewandowska, E. Leporowska, K. Penderecka, A. Marszałek, A. Mackiewicz and H. Dams-Kozłowska, *Nanomedicine* 2021, 16, 1553-1565.
283. H. Sadaquat, M. Akhtar, M. Nazir, R. Ahmad, Z. Alvi and N. Akhtar, *Int. J. Pharm.* 2021, 598, 120363.
284. S. Rana, J. Singh, A. Wadhawan, A. Khanna, G. Singh and M. Chatterjee, *J. Pharm. Sci.* 2021, 110, 1727-1738.
285. J. S. Stine, B. J. Harper, C. G. Conner, O. D. Velez and S. L. Harper, *Nanomaterials* 2021, 11, 111.
286. K. V. Chandekar, M. Shkir, T. Alshahrani, E. H. Ibrahim, M. Kilany, Z. Ahmad, M. A. Manthrammel, S. AlFaify, B. Kateb and A. Kaushik, *Mater. Sci. Eng. C* 2021, 122, 111898.
287. K. Akhtar, N. A. Shad, M. M. Sajid, Y. Javed, F. Muhammad, B. Akhtar, M. Irfan Hussain, A. Sharif and W. A. Munawar, *Adv. Appl. Ceram.* 2021, 120, 287-299, 111898.
288. M. -H. Tsai, H. -R. Chao, J. -J. Jiang, Y. -H. Su, M. P. Cortez, L. L. Tayo, I. -C. Lu, H. Hsieh, C. -C. Lin, S. -L. Lin, W. N. W. Mansor, C. -K. Su, S. -T. Huang and W. -L. Hsu, *Aerosol Air Qual. Res.* 2021, 21, 200559.
289. A. Bakhtiar, A. S. Neah, K. Y. Ng and E. H. Chowdhury, *J. Pharm. Investig.* 2022, 52, 95-107.
290. A. Shah, I. Tauseef, M. A. Yameen, S. K. Haleem, S. Haq and S. Shoukat, *Microsc. Res. Technol.* 2022, 85, 181-192.



291. M. A. Heinrich, B. Martina and J. Prakash, *Nano Today* 2020, 35, 100961.
292. A. Sarkar, T. S. Mahendran, A. Meenakshisundaram, R. V. Christopher, P. Dan, V. Sundararajan, N. Jana, D. Venkatasubbu, S. Sheik Mohideen, *Chemosphere* 2021, 284, 131363.
293. E. J. S. Pinto, J. T. C. de. Araujo, R. M. d. A. Ferreira, R. N. P. Souto, L. A. Lima, P. G. de B. Silva, M. T. Garcia, A. de la Fuente, F. F. O. de. Sousa, *J. Drug Delivery Sci. Technol.* 2021, 63, 102513.
294. A. S. Barnard, B. Motevalli, A. J. Parker, J. M. Fischer, C. A. Feigl, G. Opletal, *Nanoscale* 2019, 11, 19190-19201. DOI: 10.1039/c9nr05912a.
295. M. Gonzalez-Durruthy, A. V. Werhli, V. Seus, K. S. Machado, A. Pazos, C. R. Munteanu, H. Gonzalez-Diaz and J. M. Monserrat, *Sci. Rep.* 2017, 7 (1), 1-19.
296. I. Lynch, A. Afantitis, D. Greco, M. Dusinska, M. A. Banares, G. Melagraki, *Nanomaterials* 2021, 11, 121.
297. S. K. Verma, A. Nandi, F. Z. Simnani, D. Singh, A. Sinha, S. S. Naser, J. Sahoo, S. S. Lenka, P. K. Panda, A. Dutt, N. K. Kaushik, D. Singh, M. Suar, *Materials & Design* 2023, 235, 112452, <https://doi.org/10.1016/j.matdes.2023.112452>.
298. H. I. Labouta, N. Asgarian, K. Rinker, D. T. Cramb, *ACS Nano* 2019, 13 (2), 1583-1594.
299. Y. Jia, X. Hou, Z. Wang, X. Hu, *ACS Sustainable Chemistry and Engineering* 2021, 9, 6130-6147. DOI: 10.1021/acssuschemeng.1c00483.
300. M. K. Goshisht, *ACS Omega* 2024, 9 (9), 9921-9945, 10.1021/acsomega.3c05913.
301. N. Tripathi, M. K. Goshisht, S. K. Sahu, C. Arora, *Mol Divers.* 2021, 25(3), 1643-1664. doi: 10.1007/s11030-021-10237-z.
302. N. A. Subramanian and A. Palaniappan, *ACS Omega* 2021, 6 (17), 11729-11739, DOI: 10.1021/acsomega.1c01076.
303. A. V. Singh, R. S. Maharjan, A. Kanase, K. Siewert, D. Rosenkranz, R. Singh, P. Laux, A. Luch, *ACS Appl. Mater. Interfaces* 2021, 13 (1), 1943-1955.
304. A. M. Nystrom, and B. Fadeel, *J. Controlled Release* 2012, 161, 403-408.
305. A. B. Raies and V. B. Bajic, *Wiley Interdiscip. Rev. Comput. Mol. Sci.* 2016, 6, 147-172.
306. N. Basant, S. Gupta, K. P. Singh, *Toxicol. Res. (Camb)*. 2016, 5 (4), 1029-1038.
307. M. Na, S. H. Nam, K. Moon and J. Kim, *Environ. Sci. Nano*, 2023, 10, 325. DOI: 10.1039/d2en00672c
308. D. Fourches, D. Pu, C. Tassa, R. Weissleder, S. Y. Shaw, R. J. Mumper and A. Tropsha, *ACS Nano* 2010, 4 (10), 5703-5712.
309. R. Concu, V. V. Kleandrova, A. Speck-Planche, M. N. D. S. Cordeiro, *Nanotoxicology* 2017, 11 (7), 891-906.
310. M. K. Goshisht, *Advanced Materials Proceedings* 2017, 2, 535-546, [10.5185/amp.2017/690](https://doi.org/10.5185/amp.2017/690)
311. X. Yan, A. Sedykh, W. Wang, X. Zhao, B. Yan and H. Zhu, *Nanoscale* 2019, 11 (17), 8352-8362. DOI: 10.1039/D5PM00137D
312. P. P. Fu, Q. Xia, H. M. Hwang, P. C. Ray and H. Yu, *Journal of Food and Drug Analysis* 2014, 22, 64-75. DOI: 10.1016/j.jfda.2014.01.005.
313. R. Alshehri, A. M. Ilyas, A. Hasan, A. Arnaout, F. Ahmed, and A. Memic, *J. Med. Chem.* 2016, 59, 8149-8167. DOI: 10.1021/acs.jmedchem.5b01770.
314. M. Gonzalez-Durruthy, A. V. Werhli, L. Cornetet, K. S. Machado, H. Gonzalez-Diaz, W. Wasiliesky, C. P. Ruas, M. A. Gelesky and J. M. Monserrat, *RSC Adv.* 2016, 6 (63), 58680-58693.
315. M. Gonzalez-Durruthy, A. K. Giri, I. Moreira, R. Concu, A. Melo, J. M. Ruso, M. N. D. S. Cordeiro, *Nano Today* 2020, 34, 100913. <https://doi.org/10.1016/j.nantod.2020.100913>
316. Z. Gu, L. D. Plant, X. Y. Meng, J. M. Perez-Aguilar, Z. Wang, M. Dong, D. E. Logothetis and R. Zhou, *ACS Nano* 2018, 12 (1), 705-717.
317. A. Albanese, P. S. Tang, and W. C. Chan, *Annual review of biomedical engineering*, 2012, 14, 1-16. <https://doi.org/10.1146/annurev-bioeng-071811-150124>
318. A. Manke, L. Wang, Y. Rojanasakul, *Biomed Res Int.* 2013, 2013, 942916. doi: 10.1155/2013/942916.
319. K. Pondman, S. L. Gac, U. Kishore, *Immunobiology*, 2023, 228, 2, 152317, <https://doi.org/10.1016/j.imbio.2022.152317>
320. M. Encinas-Gimenez, P. Martin-Duque, A. Martín-Pardillos, *Int. J. Mol. Sci.* 2024, 25, 1983. <https://doi.org/10.3390/ijms25041983>
321. Y. Sun, Y. Zhou, M. Rehman, Y.-F. Wang, S. Guo, *Chem Bio Eng.* 2024, 1, 9, 757-772. <https://doi.org/10.1021/cbe.4c00105>
322. Y. Feng, H. Fu, X. Zhang, S. Liu, X. Wei, *Ecotoxicology and Environmental Safety*, 2024, 286, 117215, <https://doi.org/10.1016/j.ecoenv.2024.117215>
323. S. K. Misra, J. M. Rosenholm, K. Pathak, *Molecules*, 2023, 28, 4701. <https://doi.org/10.3390/molecules28124701>
324. V. Alcolea-Rodriguez, V. I. Dumit, R. Ledwith, R. Portela, M. A. Bañares, A. Haase, *Nano Lett.* 2024, 24, 38, 11793-11799. <https://doi.org/10.1021/acs.nanolett.4c01573>
325. M. Aloisi, A. M, G. Poma, *Environments*, 2025, 12, 234. <https://doi.org/10.3390/environments12070234>
326. (326) F. Farjadian, A. Ghasemi, O. Gohari, A. Roointan, M. Karim, M. R. Hamblin, *Nanomedicine* 2019, 14, 93-126.
327. L. Cattel, M. Ceruti, F. Dosio, *J. Chemother.* 2004, 16, 94-97.
328. M. L. Immordino, P. Brusa, S. Arpicco, B. Stella, F. Dosio, L. Cattel, *J. Control. Release* 2003, 91, 417-429.
329. G. M. Jensen, D. F. Hodgson, *Adv. Drug Deliv. Re.* 2020, 154, 2-12.
330. DOXIL approved by FDA, *AIDS Patient Care* 1995, 9, 306. Available online: <https://pubmed.ncbi.nlm.nih.gov/11361446/> (accessed on 11 November 2024).



331. Y. A. Tereshkina, T. I. Torkhovskaya, E. G. Tikhonova, L. V. Kostryukova, M. A. Sanzhakov, E. I. Korotkevich, Y. Y. Khudoklinova, N. A. Orlova, E. F. Kolesanova, *J. Drug Target.* 2022, 30, 313-325.
332. L. Kager, U. Pötschger, S. Bielack, *Ther. Clin. Risk Manag.* 2010, 6, 279-286.
333. S. S. Legha, *Med. Toxicol.* 1986, 1, 421-427.
334. FDA Approves Liposomal Vincristine (Marqibo) for Rare Leukemia. Available online: <https://www.cancernetwork.com/view/fda-approves-liposomal-vincristine-marqibo-rare-leukemia> (accessed on 11 November 2024).
335. S. Hong, D. W. Choi, H. N. Kim, C. G. Park, W. Lee, H. H. Park, *Pharmaceutics* 2020, 12, 604.
336. J. T. Zhang, J. Ma, R. K. Kankala, Q. Yu, B. Wang, A. Z. Chen, *ACS Appl. Bio Mater.* 2021, 4, 4039-4048.
337. P. A. Dinndorf, J. Gootenberg, M. H. Cohen, P. Keegan, R. Pazdur, *Oncologist* 2007, 12, 991-998.
338. Y. A. Heo, Y. Y. Syed, S. J. Keam, *Drugs* 2019, 79, 767-777.
339. A. P. Singh, S. Sharma, D. K. Shah, *J. Pharmacokinet. Pharmacodyn* 2016, 43, 567-582.
340. J. M. Lambert, R. V. J. Chari, *J. Med. Chem.* 2014, 57, 6949-6964.
341. A. I. Fraguas-Sánchez, I. Lozza, A. I. Torres-Suárez, *Cancers*, 2022, 14, 1198.
342. S. J. Keam, *Drugs*, 2020, 80, 501-508.
343. K. Mahmoudi, A. Bouras, D. Bozec, R. Ivkov, C. Hadjipanayis, *Int. J. Hyperth.* 2018, 34, 1316-1328.
344. P. Rivera Gil, D. Hühn, L. L. del Mercato, D. Sasse, W. J. Parak, *Pharmacol. Res.*, 2010, 62, 115-125.
345. D. Bobo, K. J. Robinson, J. Islam, K. J. Thurecht, S. R. Corrie, *Pharm. Res.* 2016, 33, 2373-2387.
346. T. M. Allen, P. R. Cullis, *Adv. Drug Deliv. Rev.* 2013, 65, 36-48.
347. K. L. Aillon, Y. Xie, N. El-Gendy, C. J. Berkland, M. L. Forrest, *Adv. Drug Deliv. Rev.* 2009, 61, 457-466.
348. M. K. Goshisht, G. K. Patra, A. Mahal, A. K. Singh, Shobha, M. Parshad, *Inorganica Chimica Acta* 2025, 574, 122403, <https://doi.org/10.1016/j.ica.2024.122403>.
349. M. A. Dobrovolskaia, S. E. McNeil, *Nat. Nanotechnol* 2007, 2, 469-478.
350. A. E. Nel, L. Mädler, D. Velegol, T. Xia, E. M. Hoek, P. Somasundaran, F. Klaessig, V. Castranova, M. Thompson, *Nat. Mater.* 2009, 8, 543-557.
351. C. Fornaguera, M. J. García-Celma, *J. Pers. Med.* 2017, 7, 12.
352. J. K. Vasir, V. Labhasetwar, *Adv. Drug Deliv. Rev.* 2007, 59, 718-728.
353. D. C. Drummond, O. Meyer, K. Hong, D. B. Kirpotin, D. Papahadjopoulos, *Pharmacol. Rev.* 1999, 51, 691-743.
354. N. Desai, *AAPS J.* 2012, 14, 282-295.
355. R. van der Meel, E. Sulheim, Y. Shi, F. Kiessling, W. J. M. Mulder, T. Lammers, *Nat. Nanotechnol.* 2019, 14, 1007-1017.
356. M. Samadzadeh, A. Khosravi, A. Zarepour, G. J. Soufi, A. Hekmatnia, A. Zafarabi, and S. Iravani, *RSC Adv.*, 2025, 15, 24696-24725. <https://doi.org/10.1039/D5RA03927D>
357. M. M. Mahmud, N. Pandey, J. A. Winkles, G. F. Woodworth, A. J. Kim, *Nano Today*, 2024, 56, 102314, <https://doi.org/10.1016/j.nantod.2024.102314>.
358. S. Gujjar, S. Kukal, P. Jayabal, N. Balaji, S. Sainger, S. Roy, S. Rallapalli, R. Mahadevappa, S. Minocha, S. Kumar, S. Mathapati, *Nano Trends*, 2025, 11, 100127. <https://doi.org/10.1016/j.nwnano.2025.100127>.
359. X. Ma, Y. Tian, R. Yang, H. Wang, L. W. Allahou, J. Chang, G. Williams, J. C. Knowles, A. Poma, *J Nanobiotechnol* 2024, 22, 715. <https://doi.org/10.1186/s12951-024-02901-x>.
360. A. Bigham, M. Serrano-Ruiz, M. Caporali, I. Fasolino, M. Peruzzini, L. Ambrosio, and M. G. Raucci, *Chem. Soc. Rev.*, 2025, 54, 827-897, <https://doi.org/10.1039/D4CS00007B>.
361. H. Lin, T. Buerki-Thurnherr, J. Kaur, P. Wick, M. Pelin *et al.* *ACS Nano*, 2024, 18, 8, 6038-6094. <https://doi.org/10.1021/acsnano.3c09699>
362. C. A. d. Assis, L. G. Greca, M. Ago, M. Y. Balakshin, H. Jameel, R. Gonzalez and O. J. Rojas, *ACS Sustainable Chem. Eng.* 2018, 6, 9, 11853-11868. <https://doi.org/10.1021/acssuschemeng.8b02151>.
363. J. Kleyhans, M. Sathekge, T. Ebenhan, *Materials*, 2021, 14, 4784. <https://doi.org/10.3390/ma14174784>.



Recent advances in biomedical applications of smart nanomaterials: A comprehensive review

Manoj Kumar Goshisht,^{*a,b} Ashu Goshisht,^{*c} Animesh Bajpai,^d and Abhishek Bajpai^e

Data availability

No primary research results, software or code have been included, and no new data were generated or analyzed as part of this review.

